COMPRESSION TESTING OF TRADITIONAL TIMBER FRAMING TRUSS JOINERY

By

MATTHEW MCGINNIS
Bachelor of Science, Civil Engineering, University of New Hampshire, 2017

THESIS

Submitted to the University of New Hampshire
in Partial Fulfillment of
the Requirements for the Degree of

Master of Science
In
Civil and Environmental Engineering

December 2022

This thesis has been examined and approved in partial fulfillment of the requirements for the degree of Master of Science in Civil and Environmental Engineering by:

Thesis Advisor, Dr. Ray Cook
Associate Professor of Civil and Environmental Engineering

Dr. Erin Bell
Professor of Civil and Environmental Engineering

Dr. Robert Henry
Associate Professor Emeritus of Civil and Environmental Engineering

on 11/10/2022

Approval signatures are on file with the University of New Hampshire Graduate School.

ACKNOWLEDGEMENTS

Three entities helped make this project possible through their support and funding: The University of New Hampshire (UNH) Civil and Environmental Engineering Department, The Timber Frame Engineering Council (TFEC), a council of The Timber Framers Guild (TFG), and Vermont Timber Works (VTW).

Thank you to all at UNH who worked with, advised, and supported this project:

- Dr. Ray Cook, who allowed and advised me to pursue this niche, unique project with complete support throughout all stages.
- Dr. Erin Bell and Dr. Robert Henry for participating on this committee and humoring me with the numerous after-class and pop-in questions pertaining to this project.
- Noah MacAdam, who worked extensively with me to set up the UNH high bay so this project could be safely completed and taught me the multitudes of data collection software and hardware needed to complete this project.
- Dominic Emory, who worked with the destructed trusses to detail the interior failure mechanisms, some images of which were included in this Thesis.

I would like to extend my appreciation to the TFEC, and through them, the TFG, for their inspiration for this project and their financial support, without which this project would not have been possible. I would especially like to thank Mark Gillis, who was my main contact with the TFEC throughout this project and was a big support in dispersing the survey and procuring funding.

I am grateful for VTW, who donated the time, labor, materials, experience, and all other aspects of the shipping and fabrication of the truss specimens used in this project, without which

this project would not have been possible. Thank you to Doug Friant, Dan Kelleher, Richard Labrecque, Amos Delay, and the rest of the VTW crew for collaborating with me to develop a work/school/life balance which enabled me to continue to forward my career as a timber frame engineer with VTW while completing my Master of Science degree. Thank you for the patience and support throughout this project.

I want to thank my family for their support of this project and my corresponding schedule. Mom, Dad, Ben, Kath; thank you all for providing encouragement for me to achieve this degree and spaces to live with you over the past couple of years. Thank you also for humoring my detailed discussions of timber joinery throughout our family weekends.

Lastly, but certainly not least, I would like to thank Dr. Melissa Gloekler for her unwavering support and patience throughout this project. Thank you for always being there to listen to my rambles and providing great insight for my limitless questions regarding the scientific process and technical writing. You were a great inspiration for me to go back to school to attain this degree.

TABLE OF CONTENTS

LIST OF TABLES

LIST OF FIGURES

ABSTRACT

Timber Framing is one of the earliest forms of construction, utilizing large cross-section timbers that connect to one another with interlocking joinery. These joinery styles were developed over millennium through trial and error, so there is limited research on the failure modes, structural capacities, and factors of safety associated with current design practices. This research project fills a knowledge gap, identified by the Timber Frame Engineering Council (TFEC) of Alstead, NH, regarding the joinery design of traditional birdsmouth (angled bearing) connections and how the connections act under compressive loads.

The three most popular truss peak joints (two angled compression members, single tension member) and truss heel joints (single angled compression member, single tension member) were determined through a survey designed by the author and distributed through the TFEC. A king post truss was chosen to simultaneously load the truss peak and truss heel in compression by applying a load to the truss king post, loading it in tension and forcing compression into the truss top chords. Thirteen truss specimens (nine unique and four replicates) were loaded to failure in The University of New Hampshire reaction frame. The specimens were designed with different joint types but with consistent geometry and materials to limit variability between the specimens. Each specimen was fabricated by the same team at Vermont Timber Works of North Springfield, VT.

The performances of the different joinery styles were compared using multiple factors: ease of fabrication (determined from survey), measured and calculated responses (determined from vertical applied load data and vertical deflection data), and failure modes with corresponding loads (determined using Digital Image Correlation analysis of each joint). All thirteen trials carried maximum imposed loads that exceeded their calculated design load by a factor of 2.0 or greater.

All four predicted failure modes from the current code practices were observed (block shear, peg yielding, shoulder bearing failure, and mortise and tenon bearing failure), as well as additional serviceability failure modes that did not affect the specimen's structural integrity. Block shear was the only observed failure that prevented a specimen from carrying additional load, which occurred in nine of thirteen specimens.

The optimum joints performed the best regarding the measured and calculated responses (e.g., maximum sustained load, maximum stiffness) and had the highest load carrying capacities, with corresponding factors of safety, for their respective joint types (truss peak or truss heel). The best performing peak option was found to have a full-width, continuously sloping shoulder, a centered tenon with bearing face perpendicular to the king post (vertical member), and was joined with one 1" peg per side. The best performing heel option was found to have a full-width shoulder with bearing face perpendicular to the top chord (angled member), no tenon, and was joined for constructive purposes with one ¼" timber screw centered on the truss width.

1 Introduction

1.1 Project Overview

Timber Framing is one of the earliest forms of construction, utilizing large cross-section timbers that connect to one another with interlocking joinery (i.e., mortise and tenon joinery). The techniques of constructing with large timbers, especially how they are joined, have evolved through trial and error and have been passed down from master to apprentice over millennium. Due to this long history and practice, timber framing is unlike other modern construction methods and materials, which have their origins in scientific testing and structured design following the industrial revolution (Foliente, 2000).

This research project fills a knowledge gap identified by the Timber Frame Engineering Council (TFEC), which is a council composed of engineers and interested members in the Timber Framers Guild (299 Pratt Road, Alstead, NH). The knowledge gap concerns the joinery design of traditional birdsmouth (angled bearing) connections and how the connections act under compressive loads (Figure 1-1 (a) and (b)).

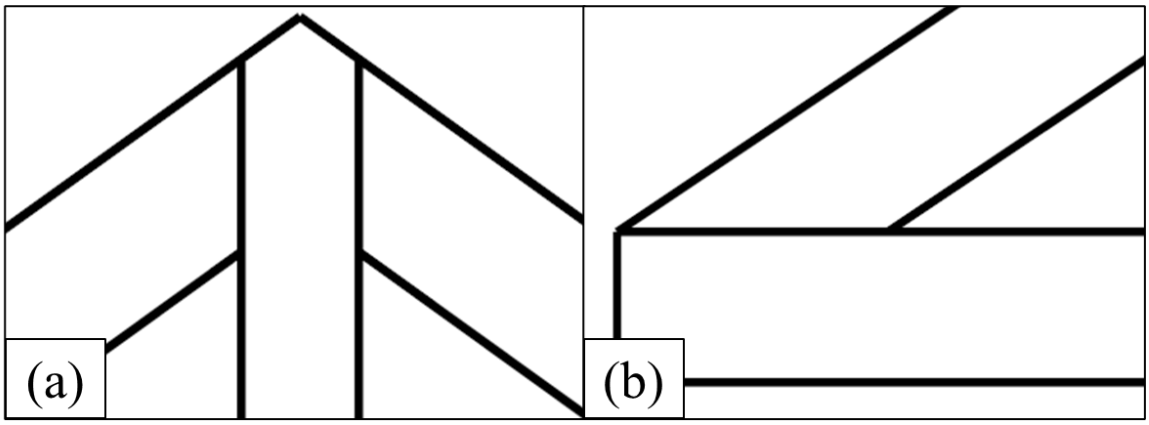

Figure 1-1: (a) Truss Peak - three-member angled bearing connection with two members in compression, (b) Truss Heel - two-member angled bearing connection with one member in compression.

Angled bearing connections are commonly seen in timber trusses or lateral resistance framing (i.e., diagonal braces), and rely on joined timbers (two or more) that fit together to transfer

compressive loads between them in bearing. The connections utilize bearing shoulder joinery, mortise and tenon joinery, or a combination of both, and the joints take a myriad of forms depending on the loading situation, geometry, designer, carpenter, tradition, and culture. A shoulder is defined as a full-width cut in one member that fits into the opposite cut-out of another member (Figure 1-2a). A tenon is defined as a projecting element from one member that fits into a mortise (a pocket or cut-out) in another member (Figure 1-2b). These joinery methods are prevalent in the industry, but despite their widespread use, research regarding the failure modes and ultimate capacities is limited.

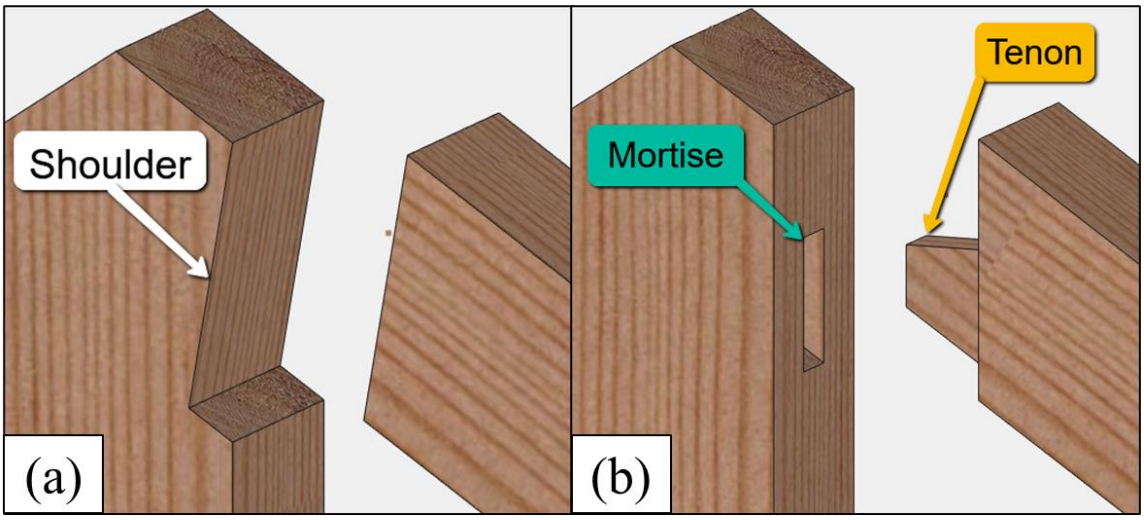

Figure 1-2: (a) Shoulder angled bearing joint, (b) Mortise and tenon angled bearing joint.

A king post truss was chosen to analyze a three-member joint (i.e., truss peak) and two-member joint (i.e., truss heel) simultaneously (Figure 1-3). The truss was designed to equally load the truss peak and truss heel joints in compression only. The truss geometry, materials, and loading procedures were also designed to be consistent for each truss, with the only variation being the joint configurations for the truss peaks and truss heels.

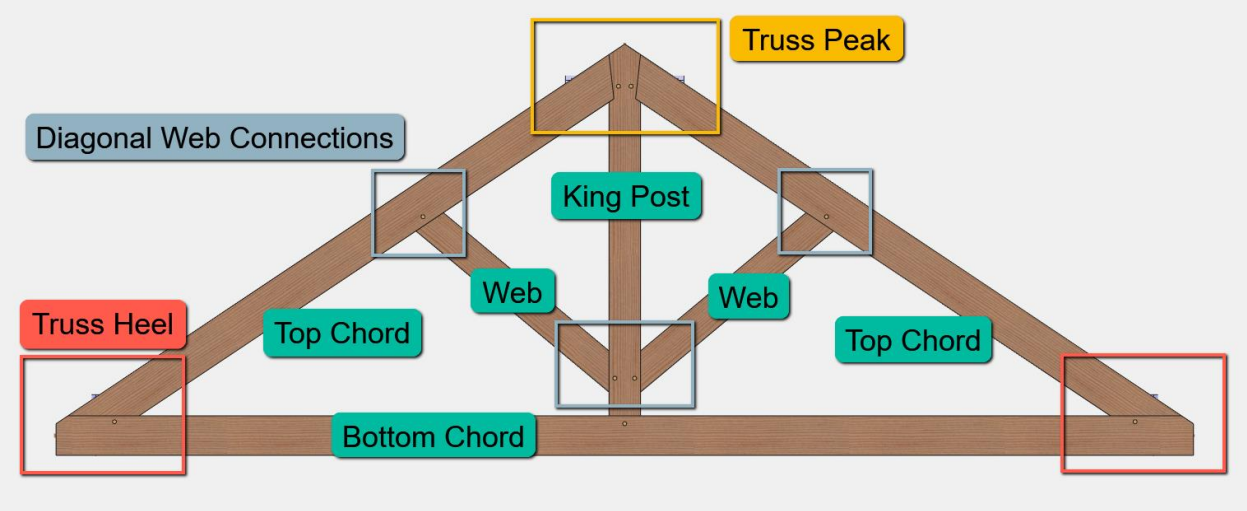

Figure 1-3: King post truss nomenclature.

This project emphasized replicating real-world conditions of the timber framing community as close as possible. Common practices (e.g., draw boring of pegs: where the peg drilling in the tenon is set back 1/32" relative to the mortise member drilling to "draw" the timbers together, and back-cutting of tenons: where the length of the tenon is limited to prevent tenons on opposite sides of a member [three-member connection only] from bearing against each other) were followed to replicate the joinery fabrication and style of the industry. The preferred common practices, materials, and joinery designs were determined through a survey designed for this project and distributed through the TFEC. The responses from the survey resulted in surfaced Douglas Fir timbers (i.e., sanded-four-sides (S4S), where the actual dimensions are ½" under nominal dimensions), White Oak pegs, and hand-cut timbers being used for this Thesis. The survey results were also used to determine the three most popular truss peak joints and truss heel joints (Section 2.1.5 and Appendix A). Thirteen truss specimens were designed by the author and fabricated by Vermont Timber Works during the winter of 2021 (Figure 1-4). Each truss was designed and fabricated with consistent materials and methods, with the only intentional variability coming from the different joint designs (truss peak and truss heel).

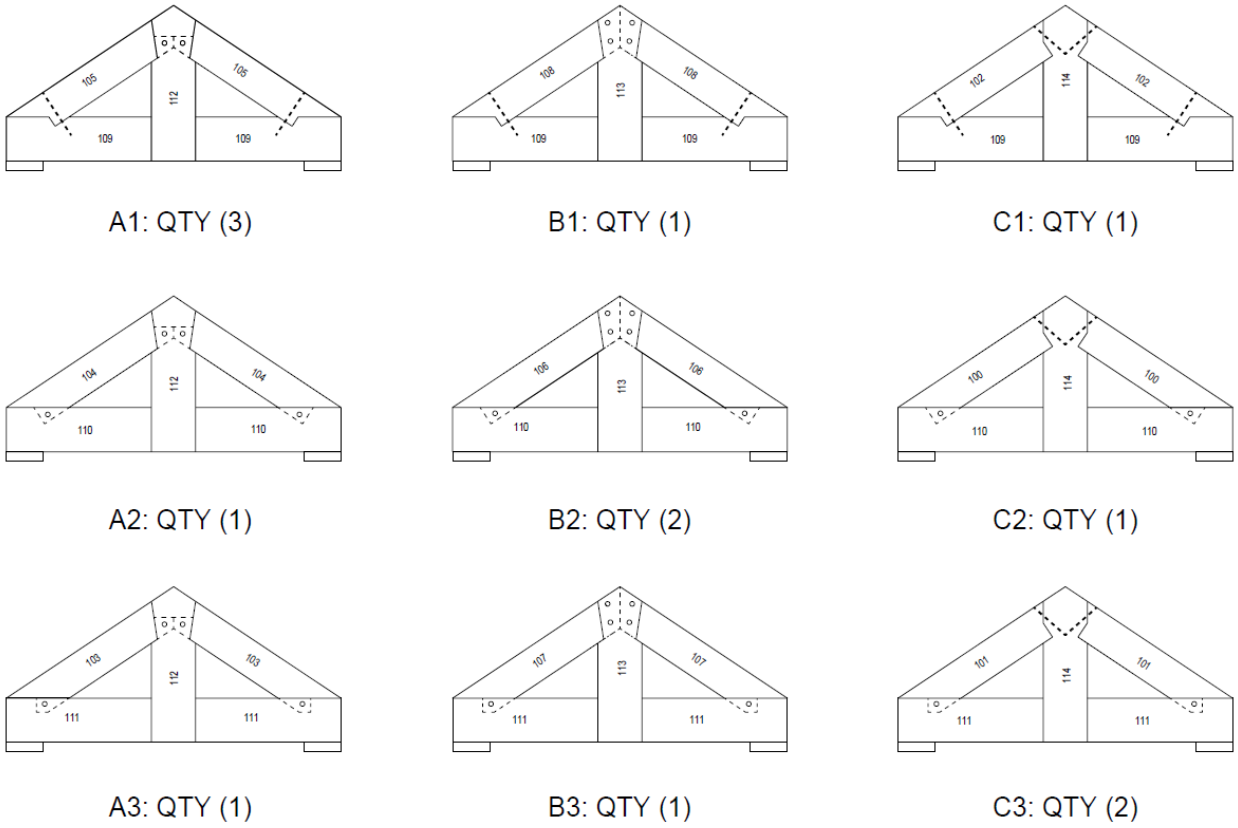

Figure 1-4: 2D elevations of the nine unique truss designs.

The specimens had their material properties measured and were structurally tested to failure in the University of New Hampshire's (UNH) high bay during the Spring and Summer of 2021. Each truss was subject to the same testing procedures, numerical measurements, and observational procedures to best determine failure modes and corresponding loads.

The joints and truss specimens were compared in numerous ways: the ease of fabrication for each joinery style was determined from the survey results (Appendix A), the full specimens were compared using the measured and calculated responses, determined from the vertical load and the vertical deflection data, and individual joints and replicates were compared using the observed joinery failures, observed using Digital Image Correlation images and generated strain maps (Section 2.4.5). The concurrent loads at failure were compared against the allowable design loads, calculated with modern building codes, for each joint type to determine factors of safety for

each failure. The optimum joint style for the Truss Peak and Truss Heel was determined using a decision matrix, combining the relative performances of each joint for each basis of comparison (Section 4.3.1).

1.2 Thesis Objectives

The primary objective of this project was to determine an optimum joinery style for the truss heel connection (i.e., single compression member) and truss peak connection (i.e., two compression members). The optimum joinery style for each configuration was determined with a decision matrix, including comparisons of each joint style using multiple factors: ease of fabrication, measured and calculated responses, average sustained load at structural failure (if applicable), and minimum block shear failure load (if applicable).

The secondary objective of this project was to identify and categorize the unique joint failure modes (e.g., block shear) to develop factors of safety. The observed failure modes and loads were compared to the expected failure modes and loads, calculated from current practices in the industry, and factors of safety for each failure mode were determined.

1.3 Background Information and Literature Review

Timber is one of the oldest building materials in the world. It can withstand both tension and compressive forces, allowing timbers to be used as beam elements and develop spans in structures unlike other earlier building materials (e.g., waddle-and-dab, brick, adobe). The first structures to utilize timber used it either as simple beams (i.e., as roof members to support earthen roofs in dug dwellings), or as columns (i.e., woven huts or posts in earthen lodges). These structures have been dated as early as c. 9000 BC (Foliente, 2000).

The art of timber framing has its roots in simpler construction forms (i.e., stave construction: utilizing vertical timbers around the perimeter of the building, and log-cabin

construction: utilizing horizontally stacked timbers). The size of these structures were limited by the available timber lengths and used significant amounts of material for the size of the structure (Bramwell, 1976). Timber framing as a building practice expanded upon these structural designs, using hewn timbers joined together to create larger, stronger structures that used less material. Timber framing dominated building practices throughout Europe and the Far East (i.e., Japan) from c. 6500-2500 BC until the industrial revolution in the late 1800s (Foliente, 2000). The first archaeologically dated mortise and tenon joints were found to be c. 200 BC in both Europe and the Far East, and the earliest timber frame structures that are still standing were constructed c. 600 AD (Benson, 1980).

Modern building codes require engineered solutions based on scientific research; hence the field of timber framing has been working to develop standards and design values for traditional joinery methods. This area of research has been growing in the past three decades but is still sparse relative to other building materials developed during the industrial revolution (e.g., steel and reinforced concrete). Brungraber (1985) is often cited for pioneering modern research methods regarding traditional Timber Framing practices. His dissertation focused on physical tests and finite-element computer modeling of full-scale timber frames (i.e., bents) under racking and gravity loads. He also analyzed a double-pegged mortise and tenon (M&T) joint in bending and shear to establish baseline values of the M&T joint stiffness for use in a Finite Element Analysis (FEA) program. Multiple research projects followed the framework used by Brungraber to further analyze the behavior of timber structures, but with a focus on peg behavior, full-frame modeling, and tension capacity of M&T joinery. Schmidt and MacKay (1997), Schmidt and Daniels (1999), and Miller and Schmidt (2004) all worked to develop design values for timber pegs for use in the modeling and analysis of M&T tension joinery (e.g., bending capacity, dowel bearing capacity,

shear strength). Until this research, the American Wood Council - National Design Specification used dowel connection equations based on the European Yield Model, which was only valid for timbers fastened with steel dowels (Schmidt and MacKay, 1997). They additionally detailed requirements for the placement of pegs in mortise and tenon joinery (e.g., edge distance, spacing, end distance), and established factors of safety for traditional timber framing tension joinery. Following his research, Miller (2009) produced a Technical Bulletin for the Timber Frame Engineering Council (TFEC) on the capacity of timber pegs, which is the current standard for designing with timber pegs.

Compared to the research regarding full-frame behavior and tension specific joinery, the research for compression testing of traditional M&T joinery is limited, especially in the United States. The TFEC identified this research gap in 2019 regarding the joinery design of traditional birdsmouth (angled bearing) connections and how the connections act under compressive loads, which was the origin of this thesis project.

Most studies involving timber joinery in compression include mechanical fasteners (e.g., metal side plates, dowel connections, etc.) resolving some or all the load transfer between members. Few peer-reviewed studies have investigated traditional heavy-timber bearing connections (Villar et al., 2007), but of those studies, the most common heavy-timber bearing connection evaluated is a “birdsmouth joint,” (i.e., single step joint, reverse-step joint) (Figure 1-5).

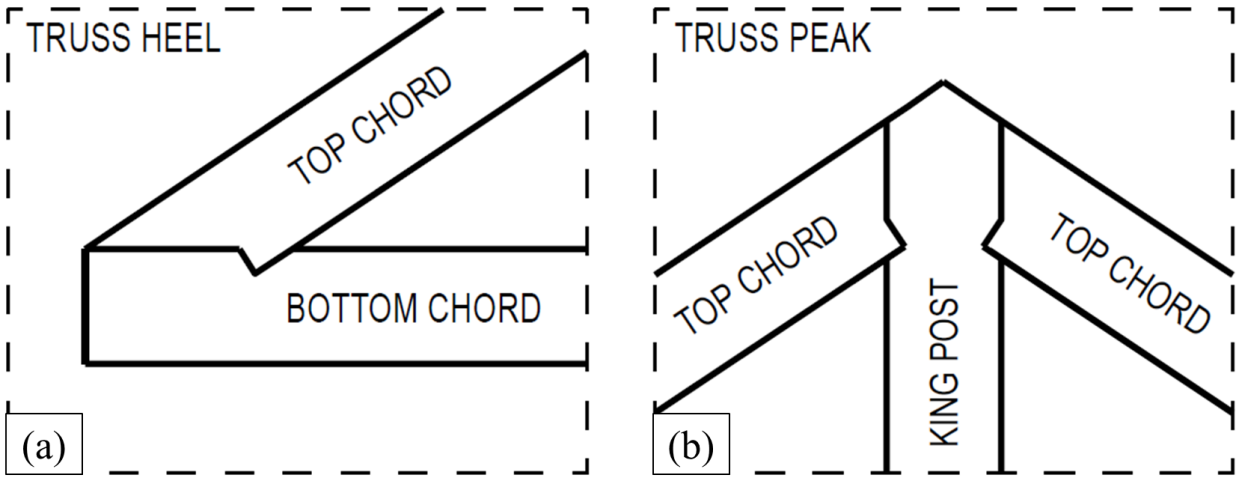

Figure 1-5: (a) Birdsmouth bearing joint at truss heel, (b) Birdsmouth bearing joint at truss peak.

Villar-García et al. (2018) modeled and tested a birdsmouth heel joint ("reverse-step heel joint") in Spruce glulam timbers. The bottom chord was supported by a roller support and pinned longitudinally to resolve tension forces. The top chord was angled at 30 degrees from the horizontal (approximately a 7/12 pitch) and loaded uniformly by a hydraulic actuator until failure. All six trials experienced block shear failure of the bottom chord, with ultimate failure loads approximately 50% above the design values for their configuration (i.e., Factor of Safety of approximately 1.5). Their analytical models show a significant shear stress magnification at the bottom of the notch, which decreases to zero shear stress at the end of the bottom chord. The block shear failure, identified as a semi-brittle failure, occurred once the shear strength of the bottom chord was exceeded at the notch surface, and the shear crack propagated through the end of the bottom chord in rapid progression. Their future research recommendations were to vary the species type and geometric parameters to verify the factor of safety adequacy and identify additional failure modes. Villar-García et al. (2018) also recommended using Digital Image Correlation (DIC) to better measure the surface strains (shear and bearing) at the notch surface, rather than traditional strain gauge rosettes.

DIC is a strain measurement technique that compares photographs or videos of distinct patterns on a test specimen throughout its loading procedure. The photos or videos are run through software using a specific computer vision algorithm to measure surface displacement and calculate surface strain of the specimen (McCormick and Lord, 2010). DIC has recently been applied to timber research projects. Villarino et al. (2020) utilized DIC to non-invasively and non-destructively determine the modulus of elasticity in compression (MOE_C) and compressive strength parallel to grain (F_C) of the Aleppo Pine. They found that DIC can reliability determine MOE_C values in the compression test, detect surface faults (anomalies), and can predict specimen failure prior to the specimen failing. Li et al. (2022) used 3D DIC to study surface strain, flexural direction, and expected failure locations of axially loaded circular columns. They found relative errors below 5% for the DIC data compared to traditional strain gauges, which met their testing requirements and verified the use of DIC to measure surface strain of circular timber columns.

Branco et. al. (2018) completed an "Analytical Campaign" to determine design parameters and expected failure modes for three truss heel designs: Single Step Joint (SSJ), Double Step Joint (DSJ), and Single Step Joint with Tenon-Mortise (SSJ-TM). The SSJ is similar to a birdsmouth shoulder design, but the bearing surface is on the forward face of the compression member, requiring the tension member to extend past the compression member. The DSJ and SSJ-TM are variations of the SSJ, where the DSJ has two stepped bearing surfaces, and the SSJ-TM has a single stepped bearing surface in addition to a central mortise and tenon joint (Figure 1-6). These joint types are generally used for diagonal web or brace connections due to the additional length of the tension member required.

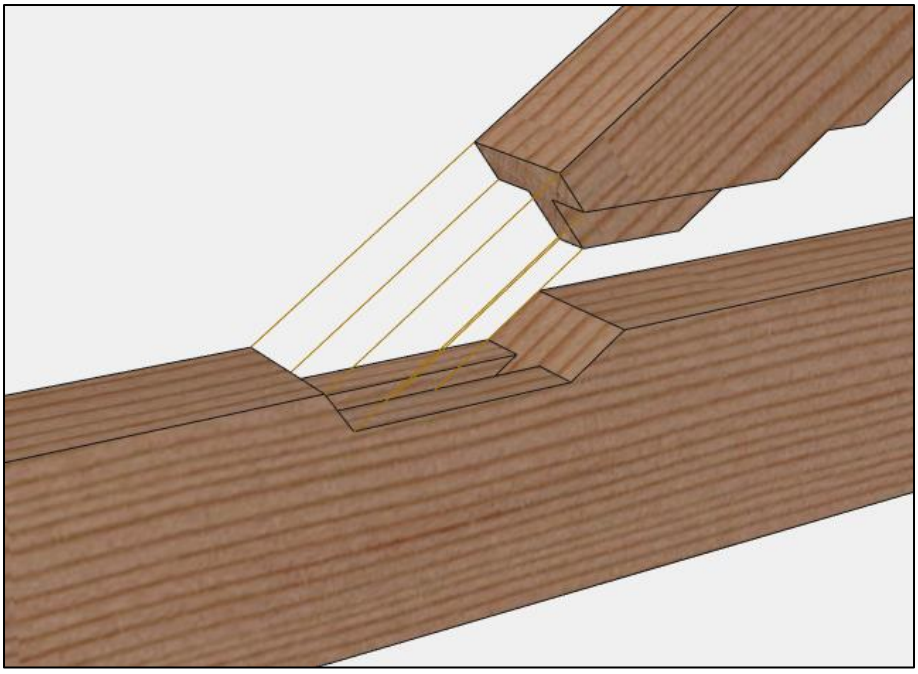

Figure 1-6: Single Step Joint with Tenon-Mortise.

For all three joints, Branco et. al. (2018) identified possible failure modes as bearing failures (i.e., crushing of either top chord or bottom chord fibers) or block shear failures of the bottom chord. They validated their SSJ model using previous data (Verbist et al., 2017), but were unable to do so for the DSJ and SSJ-TM models because of the lack of published data. Verbist et al. (2017) tested the SSJ with three angles of the SSJ shoulder (perpendicular to the top chord, perpendicular to the bottom chord, and the bisecting angle), and three rafter pitch angles, 30, 45, and 60 degrees. The lower rafter angles experienced shear stress concentrations and block shear failures like Villar-García et al. (2018), but the higher rafter angle joints either experienced bearing failures followed by block shear failures, or only bearing failures.

A single study was found for experimental angled bearing tests with mortise and tenon joinery. Feio et al. (2014) experimentally tested an SSJ-TM heel joint in Chestnut timbers at 35 degrees (approximately a 9/12 pitch). Their objective was to quantify the capacity of the traditional bearing joint and determine the adequacy of non-destructive and semi-destructive techniques used

in the field to determine in-situ performance (i.e., strength capacity). Their testing procedure had a nine-to-twelve-minute testing window, and they mostly observed bearing (i.e., crushing) failures of the tension member cheeks. Failure was defined when the system reached a strain limit of 2%.

Compared to truss heel joinery (i.e., single compression member), there is less information, design manuals, or peer-reviewed research on truss peak joinery (i.e., two or more compression members). Only historical collections of joinery designs (Jacoby, 1913) or reviews of historical accounts (Lewandoski et al., 2004) of truss peak joinery were found. No sources quantifying design integrity (i.e., physical research or modeling) of the truss peak joint were found.

This research project aimed to fill the research gap identified by the TFEC and build off previous projects to expand the knowledge of primary failure modes for varying geometric joints of the truss heel connections and truss peak connections. The failure modes and concurrent loads were used to calculate factors of safety for the various joinery methods not previously tested relative to the allowable design loads calculated using modern design codes.

2 Materials and Methods

2.1 Survey of Joinery Techniques and Practices

2.1.1 Survey Description

A survey was required to help focus this thesis due to the significant variety of framing methods and opinions in the timber framing field. The survey was designed and written by the author using Qualtrics Survey Software (Qualtrics, 333 W. River Park Drive Provo, UT) and distributed through the Timber Framing Engineering Council (TFEC) in September 2020. The survey was comprised of five sections: background information, truss peak, truss heel, diagonal web connections, and project recommendations. The background information questions were designed to determine common practices in the field of timber framing (e.g., peg material, size, and shape; preferred timber species and finish; common fabrication techniques). The truss peak, truss heel, and diagonal web questions were focused on determining usage and design of shoulders or mortise and tenon joinery. Common examples of truss peak joinery, truss heel joinery, and diagonal web joinery were provided in the survey to determine preferred joinery methods for the various configurations. Twenty-five professionals in the timber framing industry responded to the survey. The diagonal web connection responses were found to be similar to those of the truss heel connections. This information changes the focus of this research project to only analyze truss peak joinery (i.e., three member – two compression members and one tension member) and truss heel joinery (i.e., two member – one compression member, one tension member with support on the opposing side).

2.1.2 Survey Background Information

The background information of the survey covered preferred materials and general timber framing practices. Douglas Fir was recorded as the most popular timber species used in timber

framing, as it has high strength-to-weight properties and can be sourced in long lengths. The most popular peg size and material was 1" diameter, machine-turned White Oak. The respondents prefer to work with sanded four sides (S4S) material (i.e., each side is planed to remove the rough exterior from the mill) for the consistency of the sizes and aesthetic value. Lastly, most respondents use hand-cut joinery practices. These data points formed the baseline for the materials of the truss specimens used in this project. The trusses used in this project were fabricated with: Douglas Fir #1, S4S timbers, 1" machine-turned White Oak pegs, and were fabricated by hand by Vermont Timber Works (16 Fairbanks Road, North Springfield, VT).

2.1.3 Truss Peak Joinery

The truss peak joinery section of the survey was divided into two sections: questions about shoulder usage and questions about mortise and tenon usage. The responses regarding the shoulder usage provided relatively clear preferences in fabrication techniques, while the mortise and tenon responses were varied.

Every respondent to the survey utilizes some shoulder design for the peak connection. 16 of 23 respondents preferred the continuously sloping shoulder (Figure 2-1a). This shoulder is commonly used in conjunction with various tenon designs due to the steep angle of the shoulder that often cannot provide a sufficient friction-to-normal force ratio to resist the vertical force component of the truss peak connection. It is common practice to not rely on friction to prevent slippage of joints due to the unpredictable and sudden nature of friction failures. If the shoulder in question is designed to rely on friction, the angle of the joint (i.e., inverse angle of the compression member plus the angle of the shoulder) should be between 83-90 degrees relative to the compression member (TFEC 1-21) (Figure 2-2). For an 8/12 pitch roof, the inverse angle of the top chord is 56.3 degrees, so a relative shoulder slope of greater than 26.7 degrees would be

required. For a full depth shoulder, this is generally an impossible angle to meet and maintain sufficient material in the king post.

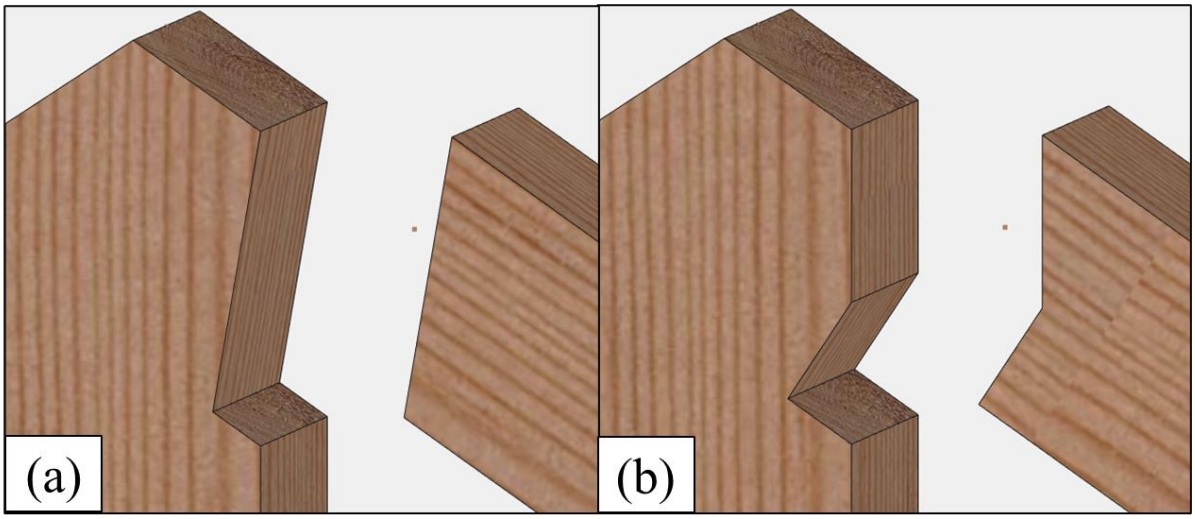

Figure 2-1: (a) Continuously Sloping Shoulder at truss peak, (b) Birdsmouth Shoulder at truss peak

7 of 23 respondents preferred the birdsmouth shoulder design (Figure 2-1b). This shoulder design rarely has an accompanying tenon, as the geometry of the shoulder is commonly designed to resolve the horizontal and vertical force component through direct bearing, negating the requirement of a tenon to resolve the vertical force component. The continuously sloping shoulder was voted easiest to fabricate and most structurally sound.

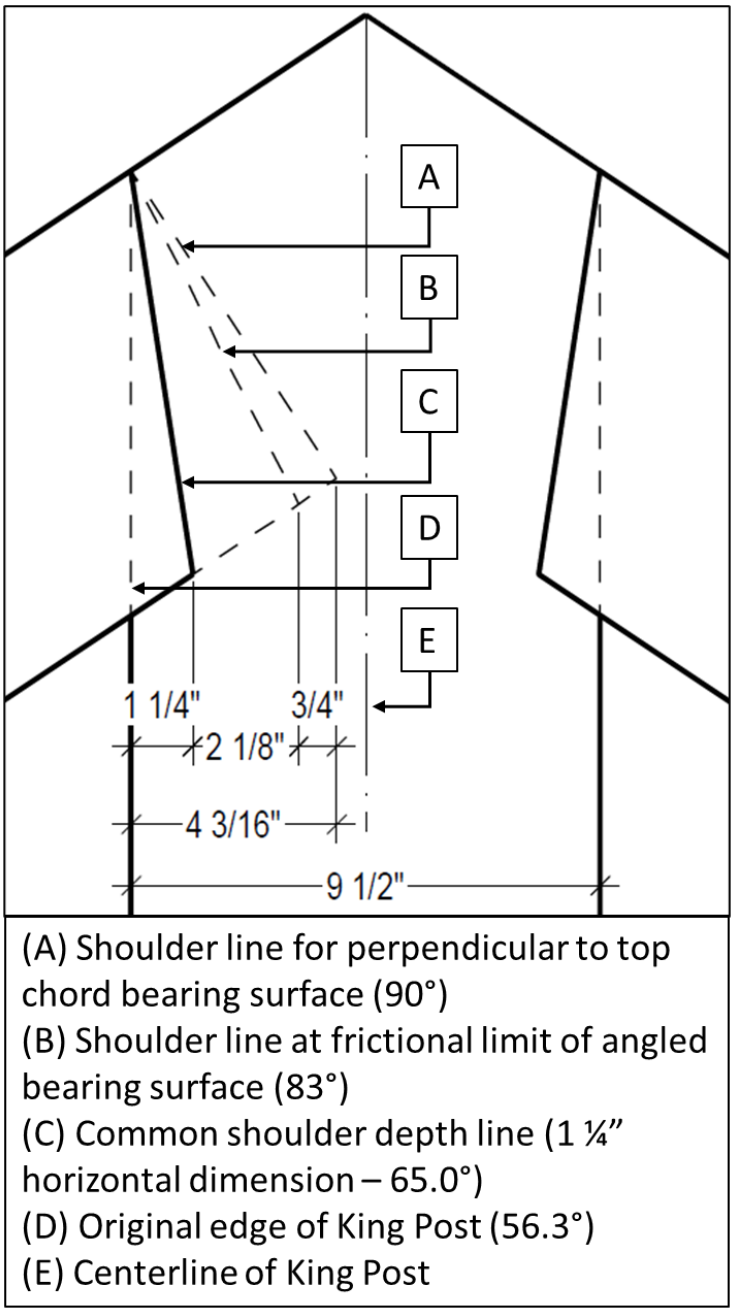

Figure 2-2: Truss peak shoulder angles required for friction surface usage.

The survey results do not indicate a clearly preferred tenon style: 6 of 23 respondents use a tenon perpendicular to king post (Figure 2-3a); 6 of 23 respondents use no tenon or a short "nub-tenon" (i.e., a shorter version of the tenon perpendicular to king post, generally 1" deep); 6 of 23 respondents use a full-height tenon (Figure 2-3b); 4 of 23 respondents use a tenon perpendicular

to top chord (Figure 2-3c); and 1 of 23 respondents did not provide an adequate response. The full-height tenon was voted easiest option to fabricate, whereas tenon perpendicular to king post was voted most structurally sound.

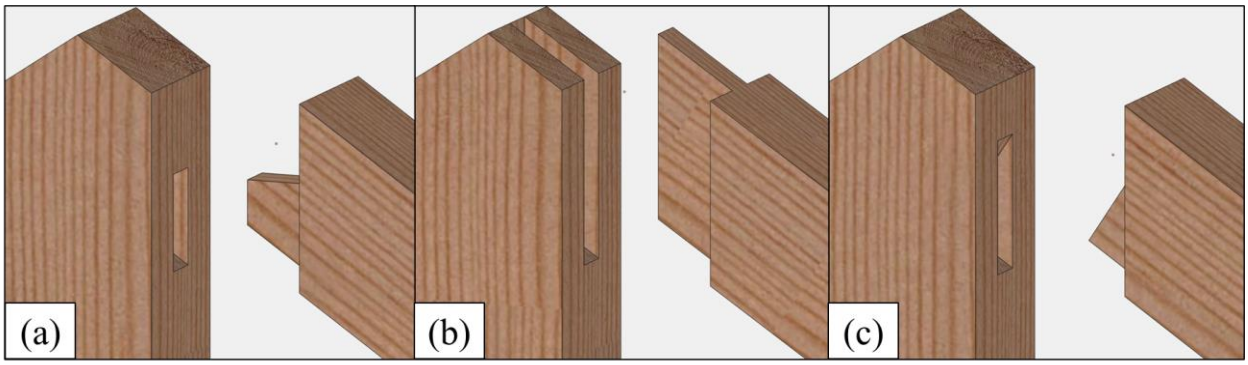

Figure 2-3: (a) Tenon perpendicular to king post, (b) Full depth tenon, (c) Tenon perpendicular to top chord.

Most respondents use a tenon depth of half of the king post depth, with a ½" gap (i.e., ¼" back-cut of each tenon) between the two tenons meeting in the middle of the king post. This gap is intended to prevent direct tenon-on-tenon bearing and is wide enough such that the gap will remain even if the king post experiences additional drying shrinkage in service (Figure 2-4). A 2" wide tenon thickness was written in most, but others use 1/3 to 1/4 of the king post width as their starting point or base the tenon width entirely on the circumstances and loading requirements.

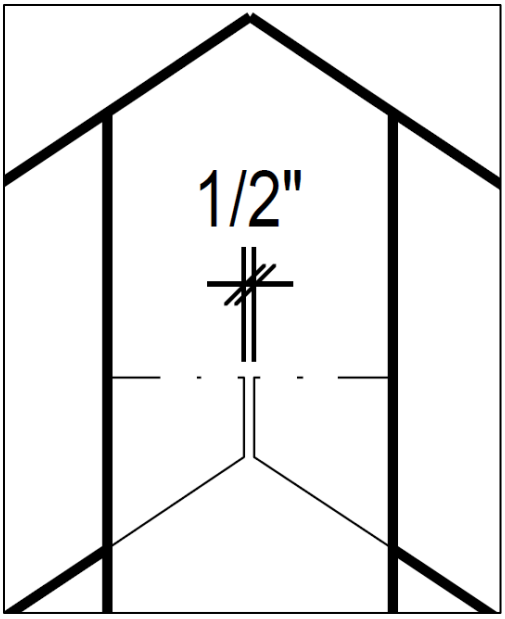

Figure 2-4: Typical 1/2" back-cut between top chord tenons.

Nearly all respondents stated that they add supplemental steel reinforcement for this joint. Timber screws perpendicular to the top chord and all-thread rods drilled horizontally through the peak connection were voted the two most popular methods (Figure 2-5A), with similar responses recorded for the for the heel connection (Figure 2-5B).

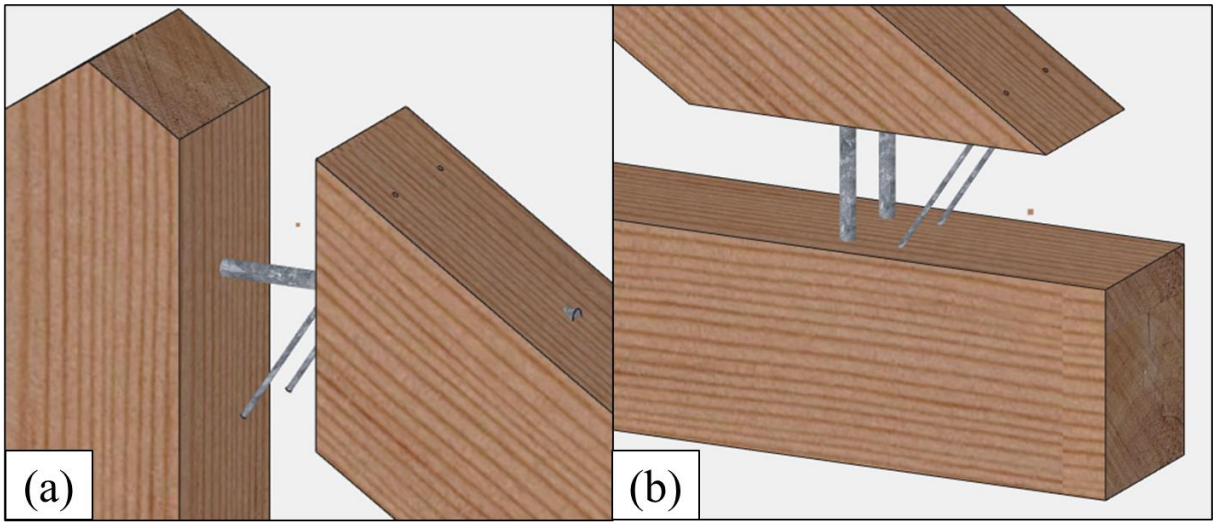

Figure 2-5: (a) All-thread and timber screws at truss peak, (b) All-thread and timber screws at truss heel.

2.1.4 Truss Heel Joinery

The truss heel joinery survey questions asked the recipients their design preferences for shoulders and tenons for this connection, where the top chord bears on the bottom chord, and the bottom chord is supported vertically on the opposite side.

16 of 22 respondents prefer the “birdsmouth” shoulder design for the truss heel connection (Figure 2-6). The remainder of the shoulder designs received, at most, 2 of 22 responses, so their designs were not included in this research project. The birdsmouth shoulder was voted the easiest to fabricate and the most structurally sound. A 2” depth was the most common write in value for the starting depth of the birdsmouth shoulder design for this joint. However, most respondents stated they design the depth of the shoulder for the required bearing area and to keep enough net section in the bottom chord to resist vertical shear failure (i.e., they have no common depth).

Figure 2-6: Birdsmouth shoulder at truss heel.

The tenon heel survey responses were similar to the truss peak survey responses, but there was not a singular preferred joinery style. 10 of 22 respondents use the tenon bearing surface

perpendicular to the bottom chord (Figure 2-7a). 6 of 22 respondents use the tenon bearing surface perpendicular to the top chord (Figure 2-7b). The remaining responses use either no tenon (4 of 22) or full-depth tenons (2 of 22). The tenon bearing surface perpendicular to the bottom chord was voted easiest to fabricate, while the tenon bearing surface perpendicular to the top chord was voted most structurally sound.

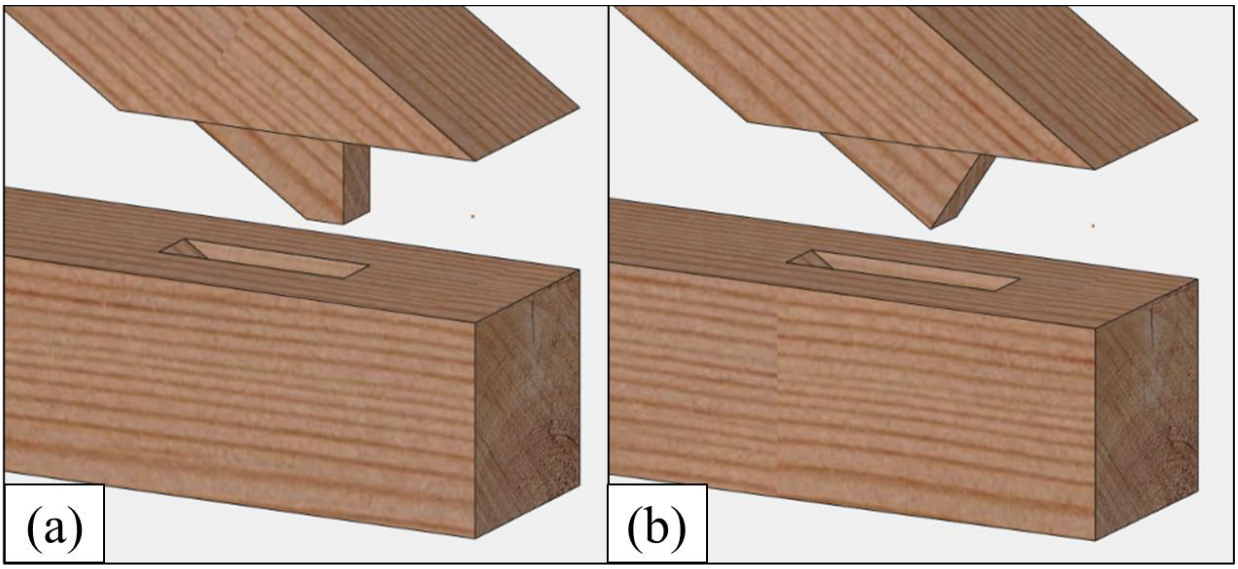

Figure 2-7: (a) Tenon perpendicular to the bottom chord, (b) Tenon perpendicular to the top chord

2.1.5 Timber Truss Joinery Selection

It would be beyond the practical scope of this project to test every available option, especially when replicate trials are considered. Therefore, the survey responses were used to choose the three most preferred truss peak joints and truss heel joints to test. The six joint options were incorporated into the design of nine unique (thirteen total) trusses used for this Thesis (Section 2.2).

The selected joinery designs used for this experiment are listed below. All tenons were designed to be 2” wide and are centered on the cross section of the timbers. All shoulders are cut

the full width of each member (5 ½”). Shop drawings showing exact specifications of the final joinery designs and other truss details are included in (Appendix B).

Truss-Peak:

Truss Peak Style A (Figure 2-8):

- 1 ¼” deep continuously sloped shoulder.
- 2” wide tenon, bearing face perpendicular to king post.
- Top chords joined to king post with (1) 1” peg per side.

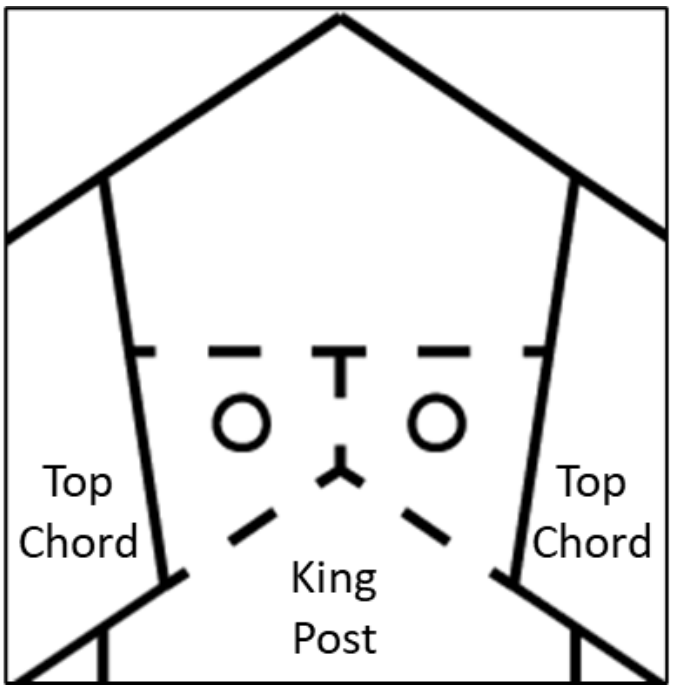

Figure 2-8: Truss Peak Style A.

Truss Peak Style B (Figure 2-9):

- 1 ¼” deep continuously sloped shoulder.
- 2” wide tenon, cut at full height of mortise (open top king post mortise).
- Top chords joined to king post with (2) 1” pegs per side.

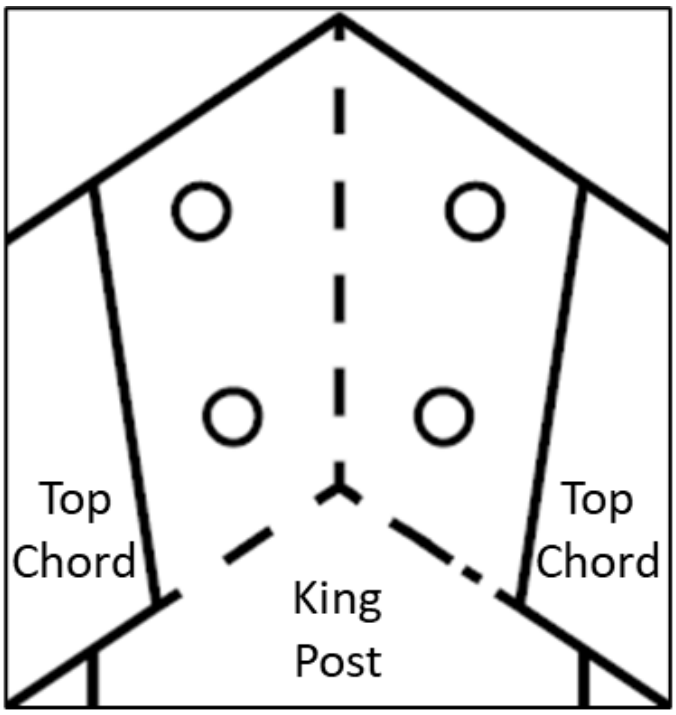

Figure 2-9: Truss Peak Style B.

Truss Peak Style C (Figure 2-10):

- 1 ½” deep birdsmouth shoulder.
- No tenon.
- Top chords joined to king post with (1) ¼”x7” Log Hog ® timber screw (manufactured by Fasten Master, 153 Bowles Road, Agawam, MA) per side.

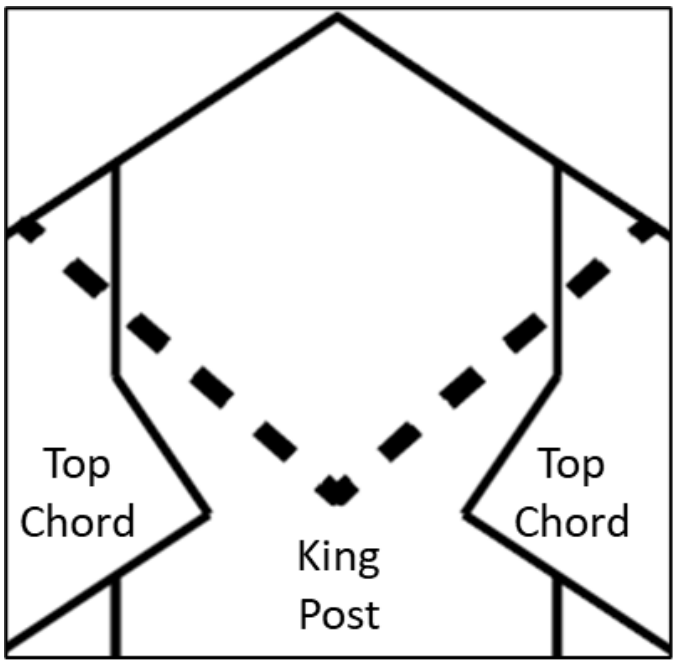

Figure 2-10: Truss Peak Style C.

Truss Heel:

Truss Heel Style 1 (Figure 2-11):

- 2” deep birdsmouth shoulder.
- No tenon.
- Top chords joined to bottom chord with (1) ¼”x7” Log Hog timber screw per side.

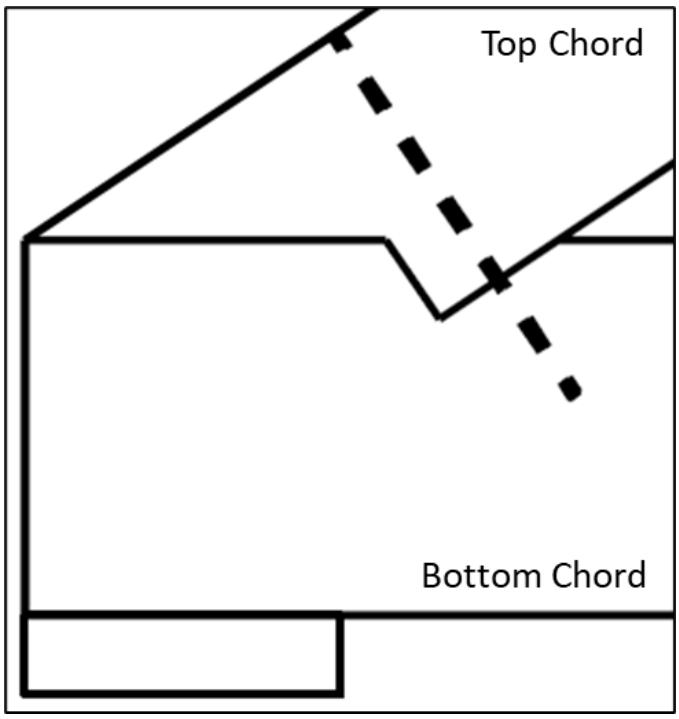

Figure 2-11: Truss Heel Style 1.

Truss Heel Style 2 (Figure 2-12):

- No shoulder.
- 2” wide, 4” deep tenon, bearing surface perpendicular to top chord.
- Top chords joined to bottom chord with (1) 1” peg per side.

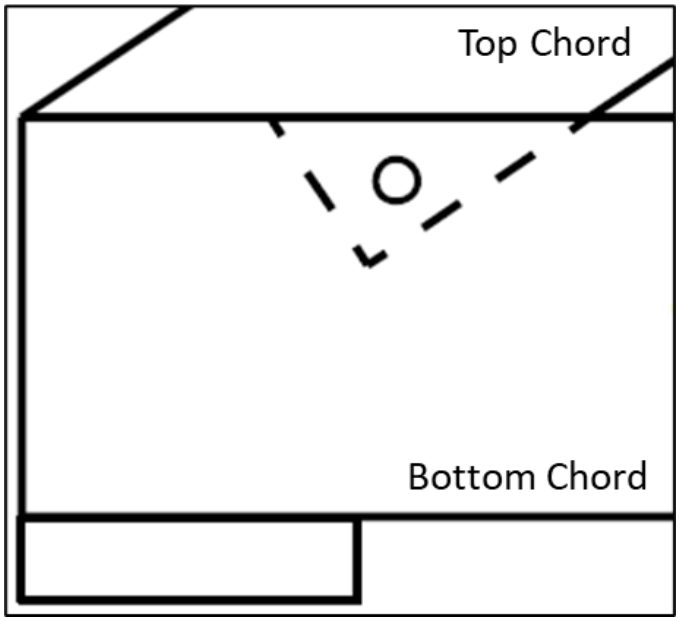

Figure 2-12: Truss Heel Style 2.

Truss Heel Style 3 (Figure 2-13):

- No shoulder.
- 2” wide, 4” deep tenon, bearing surface perpendicular to bottom chord.
- Top chords joined to bottom chord with (1) 1” peg per side.

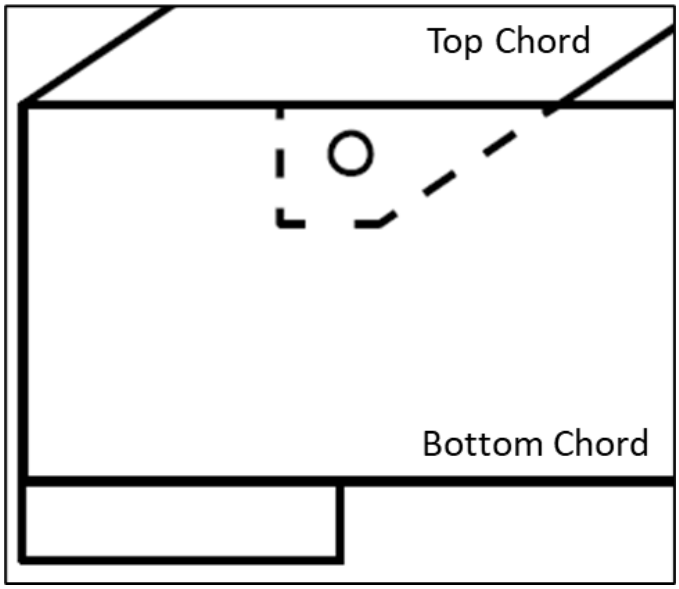

Figure 2-13: Truss Heel Style 3.

2.2 Timber Truss Design

2.2.1 Timber Truss Material Selection

The timbers chosen for this project conform to the West Coast Lumber Inspection Bureau and Western Wood Products Association requirements for No. 1 Douglas Fir-Larch timbers. Six-inch wide (nominal) material was chosen for each specimen. The trusses were originally designed to use eight-inch nominal material, but their estimated failure loads would likely have exceeded safe allowable loads for the available testing equipment and data acquisition hardware at UNH. Nominal six-inch material is generally the smallest available timber that can be used with traditional timber framing joinery methods and designs.

The 1,088 board feet of timber was purchased from Northwest Specialty Timber, Inc. of Sherwood, Oregon. The timbers were milled in green condition (i.e., not fully dried) to S4S heavy-timber specifications, which means their actual sizes are ½" under the nominal sizes; a S4S 6x8 (nominal) has true dimensions of 5 ½"x7 ½" (NDS, 2018). The timbers are all boxed-heart timbers, meaning the cross section contains the central pith of the tree. The top chords (6x8s) are classified as Post and Timber material, and the king posts and bottom chords (6x10s) are classified as Beams and Stringer material due to their respective cross section geometry (NDS, 2018).

The timber peg material used was 1" diameter, clear, straight-grain White Oak, machine turned dowel stock purchased from H.A. Stiles of Westbrook, Maine.

2.2.2 Timber Truss Description

Various configurations were considered as to how best to load the specimens for real-world applicability. Separate testing setups for the truss heel and truss peak joinery designs were originally considered, but these options proved difficult to design, load, and analyze. A truss that could load the peak and heel simultaneously was decided to be the best option for ease of loading, analysis, and best applicability to real-world loading conditions. To fit within the instrument and laboratory limitations, trusses were designed with full-sized joinery but shortened member lengths.

A king post truss was chosen for its simplicity, cost-effectiveness, ease of loading, and observation of the locations of interest (truss peak and truss heel). King post trusses utilize two angled top chords (i.e., principal rafters), a vertical king post, and a bottom chord (i.e., tie beam) (Figure 2-14). The top chords are joined to the king post at the truss peak, and the top chords are joined to the bottom chord at the truss heel. Unlike most king post trusses, the king post for this experiment is not connected to the bottom chord with a mortise and tenon joint. Instead, the bottom chords are interrupted to let the king post slide past the bottom chord, allowing free vertical

movement of the king post. The bottom chords were tied together with steel gusset/tension plates bolted to the interrupted ends of the bottom chords to transfer the bottom chord tension around the king post.

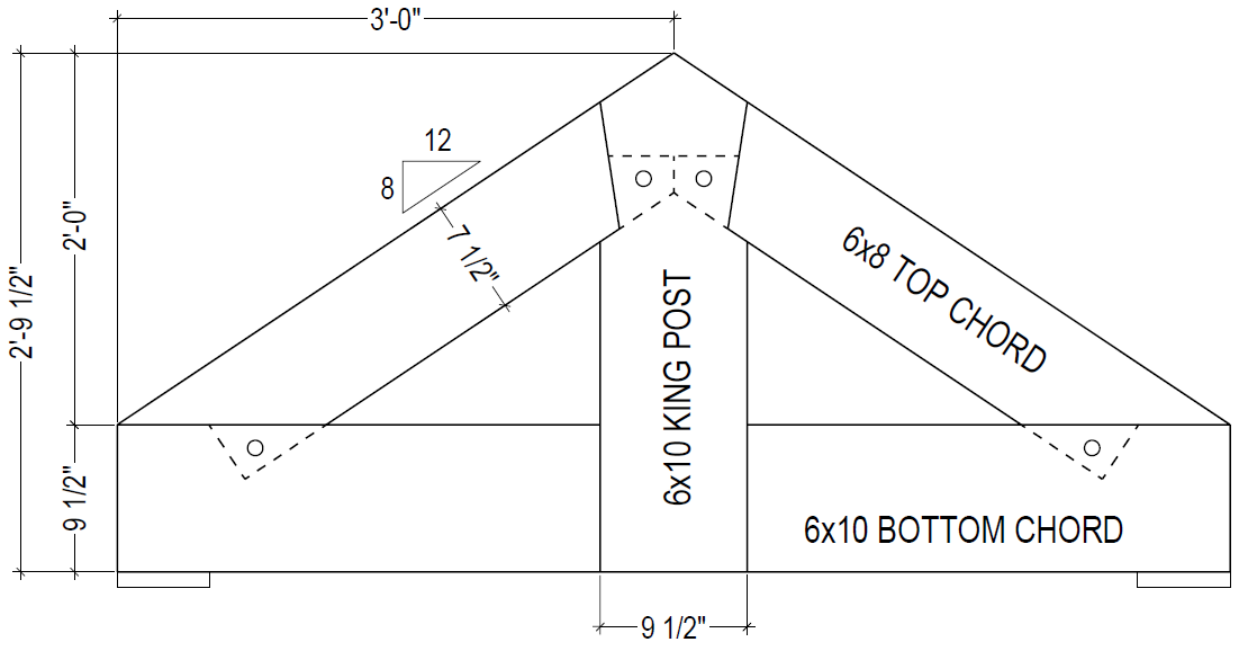

Figure 2-14: Sample 2D design of king post truss used for project with dimensions.

The pitch of the top chords of the trusses was chosen as 8/12 pitch (8" of rise per 12" of run, or 33.7º), which is a common roof pitch used in heavy timber construction and a central value of common roof pitches (typically ranging from 4/12 to 12/12). The species of the timbers and peg material are the same for each member of each truss as determined from the survey. The dimensions and fabrication methods of each truss were as similar as possible with hand-cut timbers. Naturally occurring variability of the timber specimens (e.g., density, grain, knots) was expected, and could not be practically controlled.

2.2.3 Timber Truss Loading Mechanism

The testing apparatus used was the UNH High Bay reaction (Figure 2-15). The steel reaction frame consists of two pairs of parallel I-Beams that are bolted to the foundation of the

high bay. Four steel angles, oriented vertically, are bolted to the parallel I-Beams. The four steel angles support a horizontal I-Beam that can be adjusted vertically to accommodate testing specimens of various heights. The clear horizontal spacing of the testing apparatus is approximately 6’ 8” and can accommodate test specimens up to 10’ tall.

Figure 2-15: Testing frame available at UNH.

A 150-ton hydraulic ram (model RC-150-DA-6, RAM-PAC, Hader Industries Inc - New Berlin, Wisconsin, USA) was used to apply load to the frames. The ram is bolted to the horizontal beam, oriented vertically, and exerts its force downwards towards the foundation. The ram does not generate loading or force data, so a load cell is required between the ram and the steel crib bolted to the truss. The load cell used (model 1232AF-100k, Interface, Scottsdale, AZ, USA) had a 100-kip capacity and could only measure linear, uniaxial force. Any unintentional lateral force

could cause moment (i.e., uneven or asymmetric loading) in the load cell, which could affect the measurements. To address this issue, a self-aligning spherical seating device (model 2840-113, Instron, High Wycombe, Buckinghamshire, United Kingdom) was placed between the ram and the load cell. The self-seating device had a spherical head which allowed free rotation of the joint above the load cell, resulting in purely axial load being applied to the load cell. The self-seating device had a 1000 kN (approximately 200 kip) dynamic loading capacity (Figure 2-16).

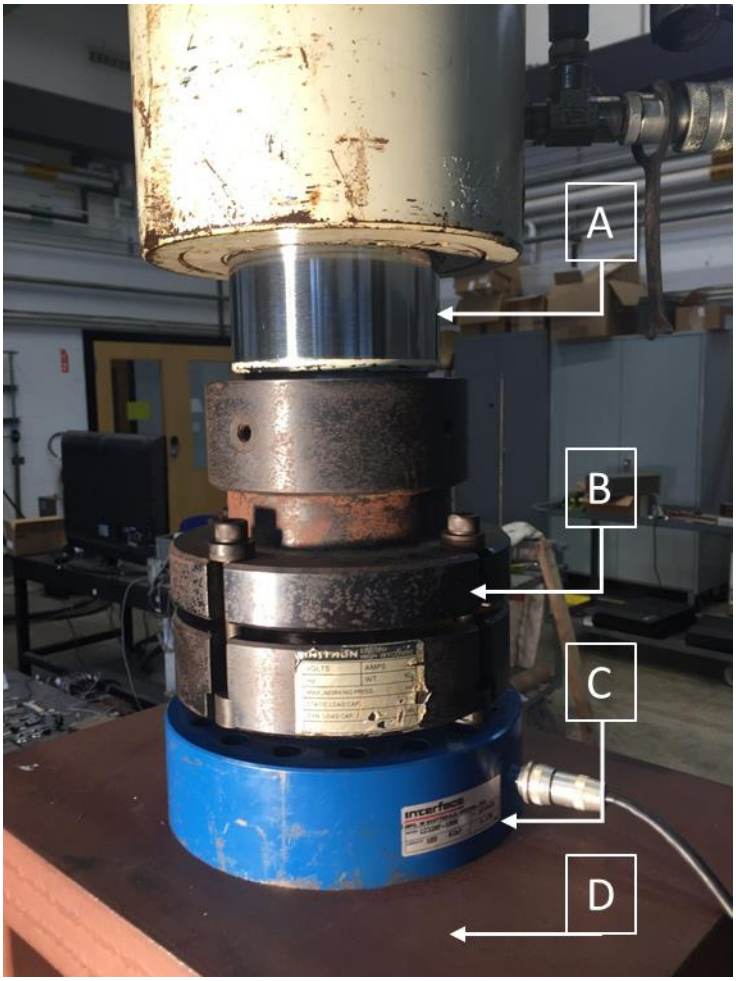

Figure 2-16: Loading equipment for applied load to truss (top to bottom): (A) hydraulic ram (white and silver), (B) spherical self-seating device (black), (C) load cell (blue), (D) steel testing frame (maroon).

A steel frame was designed by the author to allow observation of the truss peak while transferring the vertical load from the ram above the truss peak into the king post through steel side plates and bolt bearing (Figure 2-17).

Figure 2-17: Steel loading frame and gusset plates shown on example Truss A1 specimen.

The two bottom chord halves were connected through steel side plates (i.e., gusset plates) on each side to transfer the tension between the bottom chords while allowing free vertical movement of the king post. The steel used in the steel testing crib and gusset plate material was designed to stay in its linear elastic range for the expected breaking loads of the timber trusses, as the steel crib had to be reused 13 times. The plate steel used in the steel testing crib and gusset plate material conform to ASTM A36 (Gr. 36 ksi). The Steel HSS sections conform to ASTM A500 Gr. B (Gr. 46 ksi). The welds for the steel crib are all ¼" Fillet welds using Shielded Metal Arc Welds with E70 ksi electrodes. The testing frame was fabricated by Rick's Vermont Steel Craft of Rockingham, Vermont. The bolts used to connect the steel crib are all 1" diameter and

conform to ASTM A325 for heavy hex bolts and are hot-dipped galvanized. The nuts conform to ASTM A563.

The design of steel testing frame delivered a point load to the king post beneath the truss peak. This loading condition forced tension into the king post, which was resolved by compression in the top chords, tension in the bottom chords, and equal vertical reactions on each side. The goal of this truss design, where the king post could slip past the bottom chord, was to develop an ideal truss where the truss members and corresponding joints only experience axial loads (Figure 2-18).

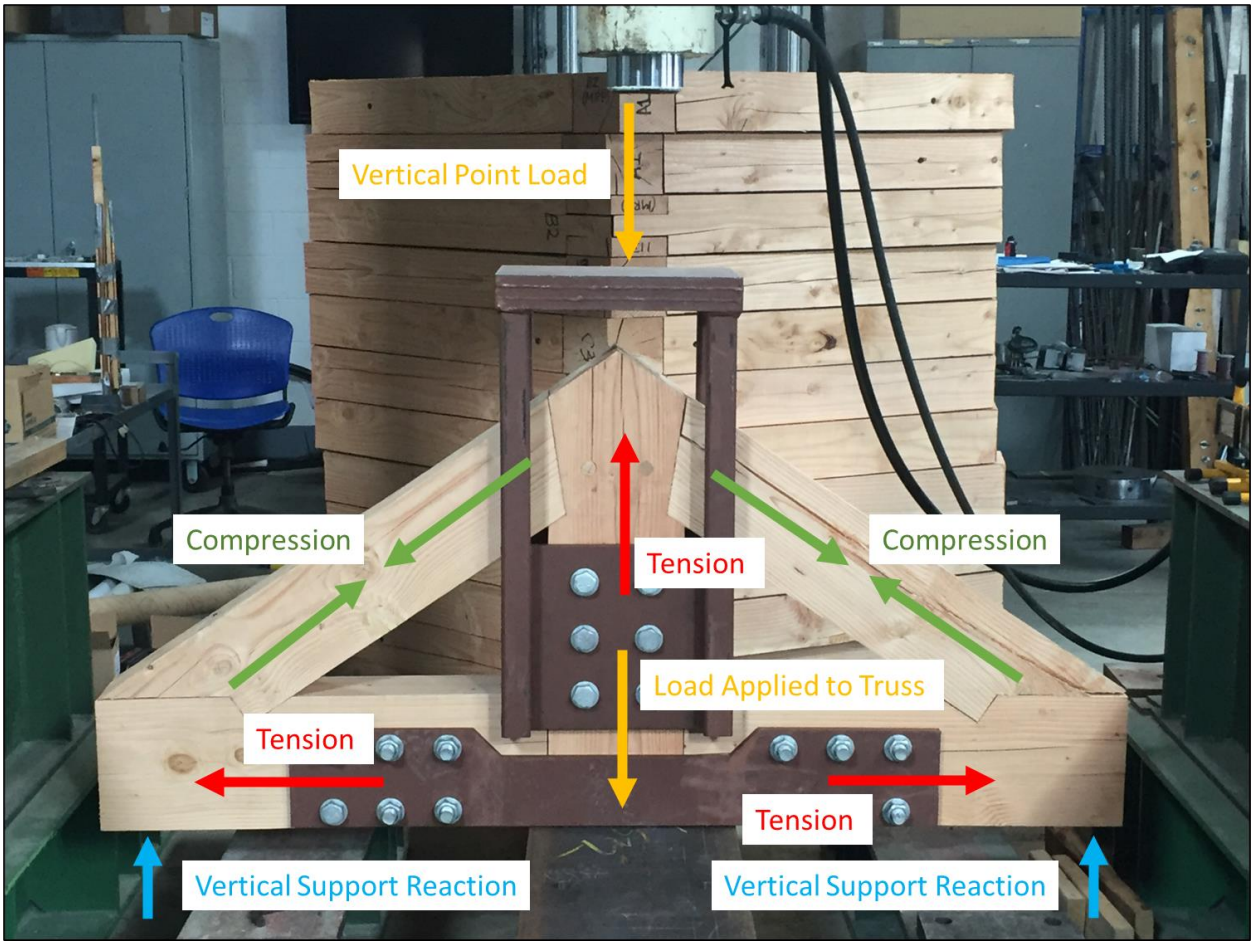

Figure 2-18: Designed load path of a sample truss.

The timber trusses were supported by roller supports on each end of the bottom chord. This reaction system provided a vertical reaction at the supports but allowed rotation and horizontal displacement of the bottom chords (Figure 2-19).

Figure 2-19: Truss heel support condition, showing roller support.

2.3 Allowable/Design Loads of Joinery Designs

The allowable loads for each joinery type were calculated using standard engineering practice and the latest applicable codes: The American Wood Council – National Design Specifications 2018 ed. (NDS, 2018) and the Timber Frame Engineering Council – Standard for Design of Timber Frame Structures and Commentary 2019 ed. (TFEC 1-19). The most conservative value between the NDS – 18 and the TFEC 1-19 was used for the allowable load calculations.

The standard practice for calculating the joint allowable loads was to calculate the allowable compressive load in the top chord (TC) and convert to the allowable point load applied to the truss at the king post (KP) using the truss geometry. The trusses used in this project have a TC pitch of 8/12 (33.7 degrees from horizontal). The geometry of the truss was calculated in-part using the Pythagorean Theorem:

$$C^2 = A^2 + B^2$$

$$C = \sqrt{A^2 + B^2}$$

Where:

$A =$ Horizontal dimension of the slope.

$B =$ Vertical dimension of the slope.

$C =$ Hypotenuse of roof pitch.

Therefore:

$$C = \sqrt{12^2 + 8^2} = 14.42$$

The truss vertical reactions, TC compression ratio, and bottom chord (BC) tension ratio were calculated using a nominal point load to the truss KP and the geometry of the truss:

$$R = \frac{1}{2} * P$$

$$C_{TC} = P * \left(2 * \left(\frac{8}{14.42}\right)\right) = 0.901 * P$$

$$T_{BC} = C_{TC} * \frac{12}{14.42} = (0.901 * P) * \frac{12}{14.42} = 0.75 * P$$

Where:

$P =$ Point load applied to truss king post, lbs.

$R =$ Truss reaction on each side, lbs.

C_{TC} = Relative compression in the TC, lbs.

T_{BC} = Relative tension in the BC, lbs.

Four possible failure modes were identified for all six joinery types: bearing failure of a mortise and tenon joint, bearing failure of a shoulder joint, block shear failure of the tension member, and peg yielding. The various failure limits were dependent on the joint-specific geometry and expected failure paths. The expected failure modes and corresponding loads for each unique joinery type were compiled according to the allowable TC compression (Table 2-1) and the allowable point load applied to the KP (Table 2-2).

All allowable loads were calculated using a load duration factor (C_D) of 1.6. This factor corresponds to an expected load time of 10 minutes and is generally used in practice for wind loading requirements (NDS, 2018). The design duration of each test was approximately ten minutes to match the duration factor and work with the project testing timeline. Full calculations regarding the allowable loading capacity of each joinery style are included in Appendix C.

Table 2-1: Predicted failure modes and allowable loads in compression of the TC for each joinery type.

Allowable Top Chord Compression (lbs)		Mortise and Tenon Bearing	Shoulder Bearing	Block Shear of Tension Member	Peg Yielding	Limiting Compression Load
Truss Peak Style	A	11090	-	11370	-	11090
	B	-	-	-	3030	3030
	C	-	11230	12130	-	11240
Truss Heel Style	1	-	13600	9450	-	9450
	2	10020	-	10840	-	10020
	3	10390	-	9810	-	9810

Table 2-2: Predicted failure modes and allowable loads applied to KP for each joinery type.

Allowable Point Load Applied to King Post (lbs)		Mortise and Tenon Bearing	Shoulder Bearing	Block Shear of Tension Member	Peg Yielding	Limiting Point Load
Truss Peak Style	A	12,310	-	12,620	-	12,310
	B	-	-	-	3,020	3,020
	C	-	12,470	13,470	-	12,470
Truss Heel Style	1	-	15,090	10,480	-	10,480
	2	11,120	-	11,700	-	11,120
	3	11,530	-	10,880	-	10,880

The expected failure load for each truss was based upon the joint configurations and relative capacities that they contained (Table 2-3).

Table 2-3: Calculated allowable loads for each truss design.

Trial Number	Truss Style	Allowable Top Chord Compression (lbs)		Allowable Point Load Applied to King Post (lbs)		Design load applied to the king post (lbs)
		Heel	Peak	Heel	Peak	
Preliminary Trial	A1	9,450	11,090	10,480	12,310	10,480
Trial 1	B3	9,810	3,020	10,880	3,020	3,020
Trial 2	C3	9,810	11,230	10,880	12,470	10,880
Trial 3	A1	9,450	11,090	10,480	12,310	10,480
Trial 4	C3	9,810	11,230	10,880	12,470	10,880
Trial 5	B2	10,020	3,020	11,120	3,020	3,020
Trial 6	C1	9,450	11,230	10,480	12,470	10,480
Trial 7	A1	9,450	11,090	10,480	12,310	10,480
Trial 8	C2	10,020	11,230	11,120	12,470	11,120
Trial 9	B1	9,450	3,020	10,480	3,020	3,020
Trial 10	A3	9,810	11,090	10,880	12,310	10,880
Trial 11	A2	10,020	11,090	11,120	12,310	11,120
Trial 12	B2	10,020	3,020	11,120	3,020	3,020
Average:		9,730	8,650	10,800	9,500	8,380
St. Dev:		251	3,910	281	4,490	3,720

2.4 Testing Set up and Testing Procedure

2.4.1 Specimen Preparation

Prior to testing, each truss specimen required preparation to prepare for data collection. The side that had the least number of natural defects was chosen for the side to apply the Digital Image Correlation (DIC) base paint and dot pattern. Each heel connection and peak connection were first sanded smooth with a belt sander using 80 grit paper, and any protruding pegs were sanded flush with the surrounding timber. A base cost of white KILZ Premium 3 Interior/Exterior Primer (Masterchem Industries LLC, 1801 E. St. Andrew Place, Santa Ana, CA) was applied to the sanded surface using a foam brush. The thick matte base coat was used to help fill in any small cracks, checks, or splits naturally occurring in the material and provide a non-reflective surface for the DIC photographs. Checks wider than ~1/16" were not able to be filled and were left in their natural state with paint on both sides. The white base coat was allowed to dry for 24 hours before applying a DIC specific pattern.

A specialized DIC dot roller was used to apply a uniform speckle pattern on the white base coat. The dot roller used was included in the VIC Speckle Pattern Application Kit from Correlated Solutions (Correlated Solutions Inc., 121 Dutchman Blvd. Irmo, SC). The goal of the roller mechanism was to attain ~50% coverage of the material surface with a random, high-contrast design (Correlated Solutions, n.d.). A standard black ink pad (Jet Black Ranger™ by Archival, 15 Park Road, Tinton Falls, NJ) was used for the roller ink.

The first two trials (Preliminary Trial 0 and Trial #1) used a 0.026" dot size and GoPro cameras (model: Hero 5, GOPRO, 3025 Clearview Way, San Mateo, CA), as recommended per the manufacturer recommendations for the camera resolution and testing area (Correlated Solutions, n.d.). This dot size and roller configuration resulted in errors when processing the data

in VIC-2D-6, an analysis program produced by Correlated Solutions. The issue was identified in post-processing of the data. The JPEG compression algorithm of the GOPRO cameras caused interference in the VIC-2D-6 program, which caused the strain results to have vertical or horizontal striations of the data (i.e., aliasing) (Figure 2-20).

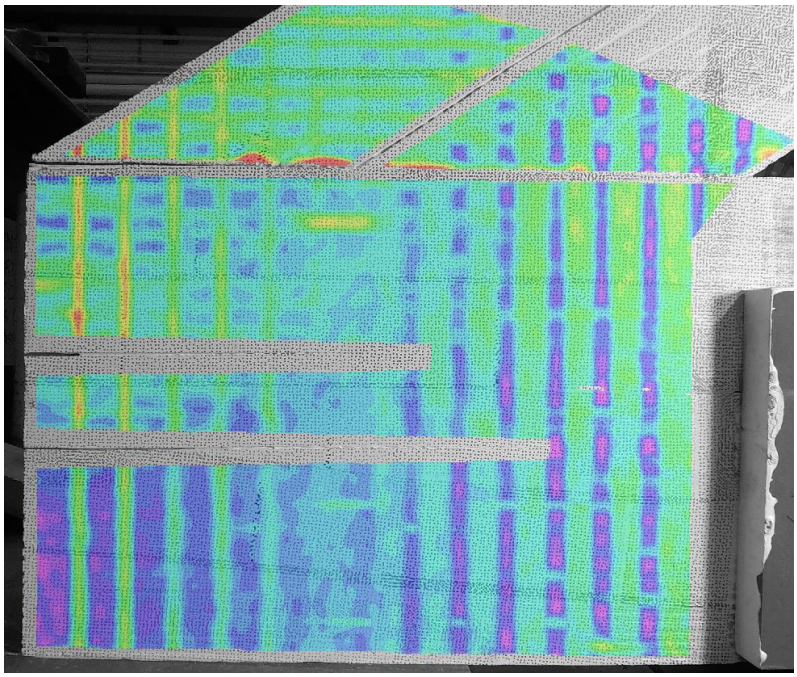

Figure 2-20: Aliasing of the DIC results for Heel 1 of Trial 1.

Three recommendations were provided by Ian Adkins of Correlated Solutions to resolve the issue: increase the dot size one step, do two passes of the dot roller with the second pass at 45 degrees to the longitudinal axis of the original roller pass, and use different cameras to record uncompressed photos (Figure 2-21). Therefore, Trial #2 through Trial #12 used the 0.05" dot size roller with two overlapping passes and Point Gray Research cameras (model GRAS-20S4M-C, FLIR Systems, Inc. 27700 SW Parkway Ave., Wilsonville, OR). The changes to the DIC application and measurements helped prevent aliasing and provided sufficient DIC data to analyze the joint strains for the remainder of the truss trials.

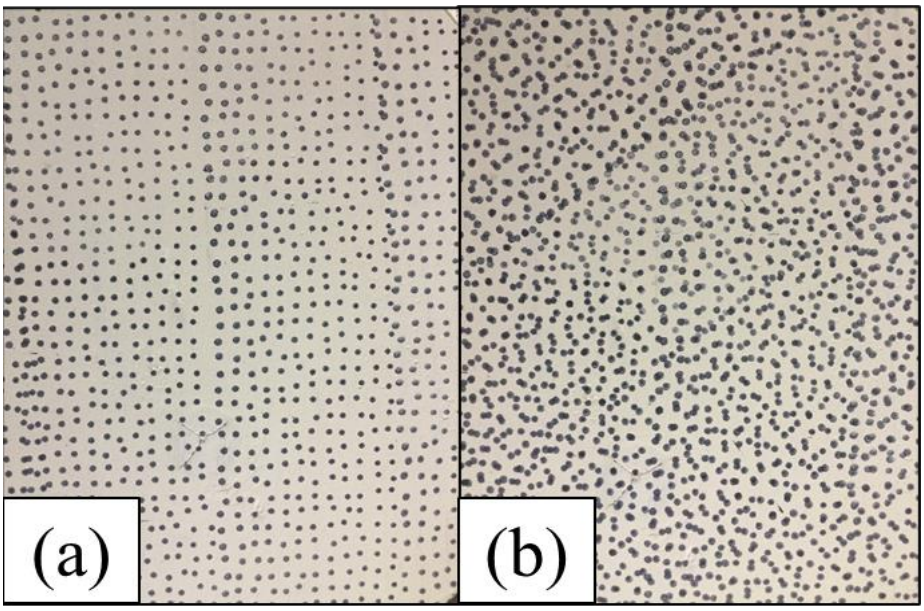

Figure 2-21: (a) 0.05" Dot pattern applied once, (b) second pass of 0.05" dot pattern applied at 45 degrees relative to first pass.

2.4.2 Pre-Test Measurements

Multiple measurements were recorded for each truss prior to the destructive testing. The pre-test measurements were done in two sections: all trusses were weighed, and the moisture content of every member was measured on a single day to establish baseline comparisons. Each truss was reweighed directly prior to the destructive test to determine the change in moisture content and the true parameters on the testing day.

On May 18, 2021, each truss was weighed on a Health-o-Meter three-hundred-pound scale (model HDR743DQ3-41 H252JYE, Sunbeam Products, Jarden Consumer Solutions, Boca Raton, FL). Additionally, each member of each truss (total of five members per truss) was measured at three locations (middle of member on face grain, third points of member on side grain) with a wood moisture meter (model MMC 210, Wagner, 326 Pine Grove Road, Rogue River, Oregon). The moisture readings were averaged to get an average moisture content reading for each truss member, and an average overall moisture content for each truss. The humidity and temperature of

the high bay was recorded with a digital thermometer at the time of each measurement recording and at the beginning of each testing trial (Model WT-137U, La Crosse Technology, 2809 Losey Blvd S La Crosse, WI).

To determine an average density of each truss, the volume of each truss was calculated using the shop drawing specifications. The volume, an assumed constant for every truss, was compared to the total weight of each truss. The tenons of each member were assumed to fully fill their respective mortise pockets, as it would have been difficult to determine the actual airspace surrounding each tenon, and the removal of additional mortise material was assumed to be negligible. The peg material (if applicable) and the log hog material (if applicable) density and volume discrepancies were assumed to be negligible to the volume and total weight of the truss and were assumed constant between design options. The volume was determined to be 50.5 board feet (bdft – a board foot is a traditional measurement in the timber industry that is 1/12 of a cubic foot, i.e., 1 $bdft = 12''x12''x1''$) per truss. Therefore, the volume of each truss was 4.21 cubic feet irrespective of the differences in joinery methods.

2.4.3 Test Set Up

The trusses were moved into position beneath the hydraulic ram using an overhead crane. The truss was centered beneath the hydraulic ram in both directions, and the heel supports were adjusted so each heel location was supported by the steel plate/roller for nine inches from the end of each bottom chord timber to replicate in-practice loading conditions. Two chain tension ties were attached to the front and back of the steel testing frame as a safety device to restrain the truss in case of lateral buckling (Figure 2-22).

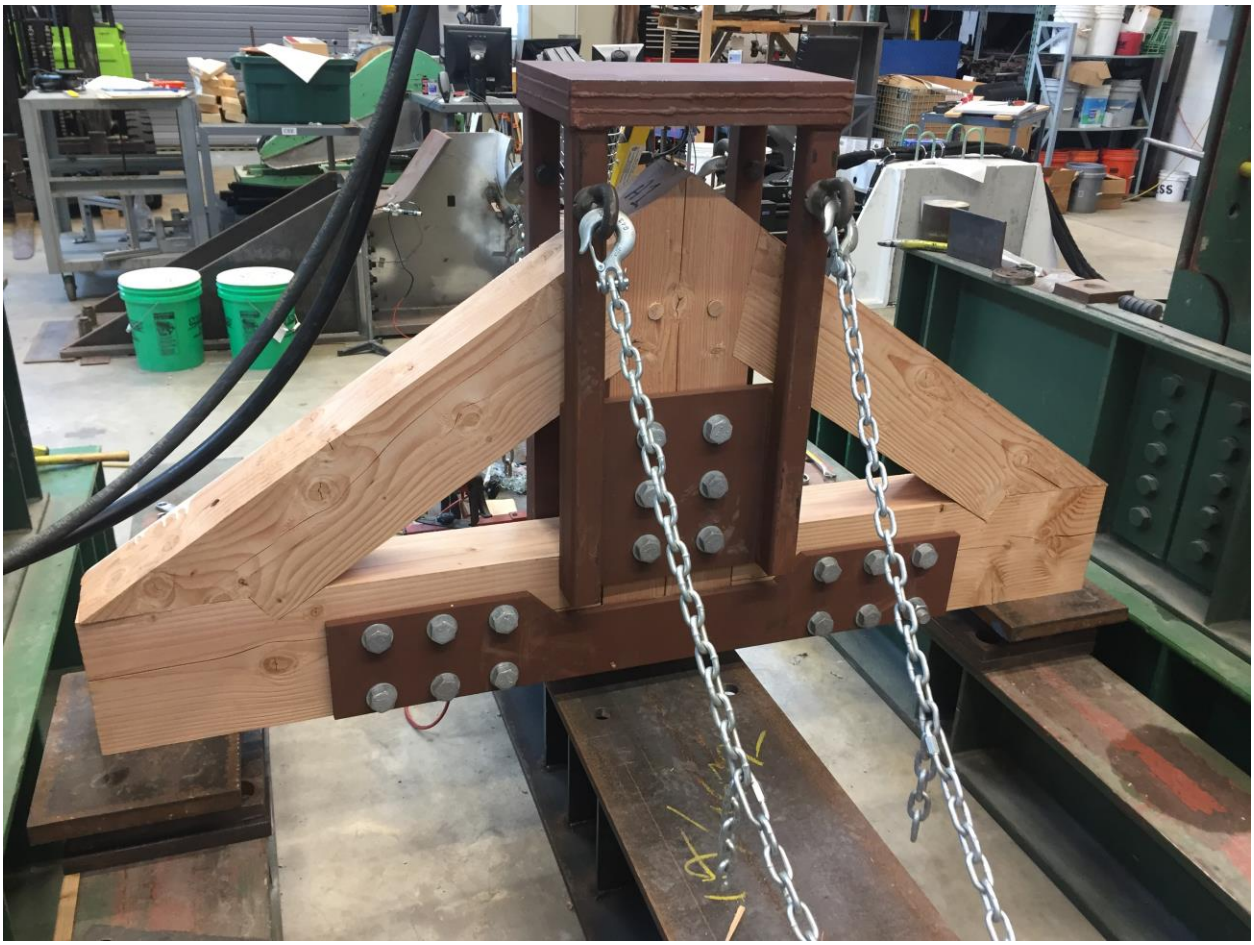

Figure 2-22: Truss in place in the UNH reaction frame (side shown is opposite the DIC painted side).

After the test specimen was placed into position, the various data collection systems were applied to the truss. A Linear Variable Differential Transformer (LVDT) by BDI (model LDC500A, BDI, 740 S Pierce Ave #15, Louisville, CO) was attached to the bottom chord gusset plate using a magnetic base, orientated vertically. A second magnetic base with an aluminum angle was attached to the steel crib on the king post to just engage the LVDT. The magnetic bases were manufactured by Accupro (owned by the Penn Tool Co., 1776 Springfield Ave., Maplewood, NJ) (Figure 2-23).

Figure 2-23: LVDT set up on steel testing frame using magnetic bases.

The load cell was placed in the center of the steel crib directly under the hydraulic ram and attached to the hydraulic ram with the self-aligning spherical seating device. The self-aligning spherical seating device had one end fastened to the hydraulic ram, and one end fastened to the load cell (Section 2.2.3).

Video of the opposite side of each truss, relative to the DIC painted side, was recorded for the duration of the truss test using a standard 1080p webcam and laptop.

2.4.4 Loading Procedure

The trusses were loaded using the hydraulic ram attached to the reaction frame. The ram available did not have sufficient speed control to load the trusses continuously and gradually for the desired 10-minute test duration. The only speed control on the progression of the hydraulic ram (forward or backward) is a manual, rotational ball valve. A preliminary test using 2x4s with

the valve ¼ turn open and a continuous feed showed that the trusses would likely reach their failure limits in 30-60 seconds, which was too rapid to gather sufficient information for each truss test and not a true representation of the desired duration factor for the trusses. To resolve this issue, a sawtooth loading procedure was used to lengthen the trial time to the desired 10-minute timeframe, and the peaks of the stepwise load cell data was correlated with the peaks in the stepwise deflection data for better data analysis and results.

The trusses were loaded in 30 second cycles, with the first two seconds of each cycle engaging the hydraulic ram. Therefore, the loading cycle of the ram was: two seconds forward (down), twenty-eight seconds stationary. The trusses were loaded until there was a distinguishable, ultimate failure, or the deflection limit of ~1 1/2" was reached (i.e., the king post bottomed out on the support beam underneath, or the king post loading frame contacted the gusset plate steel on the bottom chord).

2.4.5 Data Collection

Three forms of data were recorded in addition to a video of the entire test: vertical deflection of the king post relative to the bottom chord, the applied load, and photos for use in the DIC based analysis. The vertical deflection between the king post and bottom chord was recorded using the LVDT. The data was collected with STSLIVE, a Windows® based application by BDI (BDI, 740 S Pierce Ave #15, Louisville, CO). The deflection data was recorded at 1/100 second intervals throughout the length of the test.

The applied load from the hydraulic ram to the truss specimen was recorded using the load cell and a program purposefully written for this project by Noah MacAdam (UNH) in LabVIEW software (National Instruments, 11500 N Mopac Expwy, Austin, TX). The load cell data was recorded in 1/10 second increments throughout the length of the test.

The LVDT data and load cell data were collected independently from each other. To be able to analyze the two data collections together, a MATLAB script was written to:

1. Average the LVDT data every 10 data points to allow for direct comparison to the Loadcell data (i.e., report the LVDT data in 1/10 second intervals).
2. Trim the data series so only the data recorded while the truss was being loaded is analyzed:
    a. The load cell data was truncated for any data points before the load cell registered 200 lbs and for any data points after the load was removed from the truss (i.e., end of test).
    b. The LVDT data was truncated for any data points before the LDVT registered 0.01" and any data points after the load was removed from the truss (i.e., end of test).

The starting values of 200 lbs and 0.01" for the Loadcell and LVDT, respectively, were determined empirically to be the points where both systems began to engage when working with the data following the destructive tests.

The photos for DIC were taken in two separate ways depending on the trial number. For each truss, preliminary photos of each joint under consideration (total three: truss peak, "left" truss heel (heel 1), and "right" truss heel (heel 2)) were taken with an 8"x12" framing square to calibrate the DIC images during analysis. The preliminary trial and Trial #1 used three GOPRO cameras. The cameras were mounted 12" from the face of the timber truss specimens. The cameras took 12 Mega-Pixel (MP) photos, and were set in "linear" photo mode, without fisheye lens modifications. Photos were taken with a GOPRO Smart Remote to take simultaneous photos and to not disturb

the cameras while testing. Two photos were taken in each 30 second loading interval: one at 5 seconds, and another at 25 seconds (i.e., the photos were taken at 10, 20, 10, 20, etc. second intervals). The timing of the photo captures allowed an image to be taken following the loading of each cycle, and another to be taken just before the next loading to determine the movement of the truss joinery between loading cycles.

As discussed previously (Section 2.4.1), the GOPROs were unable to be used for trial 2 through trial 12 due to the aliasing of the DIC data. Therefore, the remainder of the truss trials used three Point Gray Research cameras. The cameras were used with Sigma lenses (SIGMA DG 28-300mm 1:3.5-6.3, SIGMA Corporation of America, 15 Fleetwood Court, Ronkonkoma, NY). F to C adapters (Bower C for Nikon, BowerUSA, 4624 28th St 3rd floor, Long Island City, NY) were required to connect the lenses to the cameras. The cameras were mounted approximately sixteen feet from the truss test setup as Correlated Solutions recommended the longest available focal length be used to reduce noise in the DIC data that can result from out-of-plane motion of the test specimen (Correlated Solutions, n.d.). VIC-SNAP, another Correlated Solutions product, was used to automate the photo collection in 10 second intervals (i.e., three photos were taken in each 30 second loading interval). The loading cycle was started 5 seconds before the DIC photos were taken, so the time stamps for a single load cycle for trials 2 – 12 was:

- 0-2 seconds: Active loading from the hydraulic ram.
- 2-30 seconds: Hydraulic ram stationary.
- 5, 15, 25 seconds: photo taken for DIC data.

3 Results

3.1 Truss Material Measurements

The truss specimens were picked up at Vermont Timber Work's shop on February 24, 2021. They were stored in the humidity and temperature controlled UNH high bay prior to material measurements and physical testing. The storage duration allowed the timbers, fabricated in their green state, to reach typical in-situ states of seasoning for indoor projects (i.e., <19% moisture content). All trusses were weighed, and moisture content (MC) measurements were taken for each member of each truss on May 18th, 2021. The density and specific gravity of each truss was calculated using the measured data, the common truss timber volume of 4.21 cubic feet (Section 2.4.2), and a water density of 62.4 pcf (Table 3-1).

Table 3-1: Material measurements on May 18th, 2021, prior to testing.

Trial Number	Truss Style	Scale Weight (lbs)	Average MC (%)	Density (pcf)	Specific Gravity
0	A1	133.0	10.42	31.6	0.506
1	B3	134.0	14.99	31.8	0.510
2	C3	130.6	13.55	31.0	0.497
3	A1	130.4	11.02	31.0	0.497
4	C3	129.8	15.32	30.8	0.494
5	B2	136.2	14.66	32.4	0.519
6	C1	134.4	13.77	31.9	0.512
7	A1	133.4	13.73	31.7	0.508
8	C2	135.4	14.23	32.2	0.516
9	B1	142.6	16.39	33.9	0.543
10	A3	140.8	16.95	33.5	0.536
11	A2	148.4	18.69	35.3	0.565
12	B2	137.8	16.21	32.7	0.525
Average:		135.9	14.61	14.61	0.518
St. Dev		5.36	2.27	1.27	0.020

Individual weight measurements were rerecorded for each truss on the day each truss was tested. Assuming everything held constant, the only change in weight would be the MC change of the timbers. Therefore, the measured weight was used to calculate the MC, density, and specific

gravity of each specimen on their testing day (Table 3-2 and Table 3-3). The West Coast Lumber Inspection Bureau (WCLIB) and the Western Wood Products Association (WWPA) state an average Specific Gravity of 0.50 for the oven-dried Douglas Fir – Larch species group (NDS, 2018). The measured specific gravity for the Douglas Fir timber material at the time of testing was 0.499 +/- 0.016.

Table 3-2: Material measurements on testing day.

Trial Number	Truss Style	Date Tested (measured)	Lab Temperature (°F)	Lab Relative Humidity (%)	Scale Weight on Day of Test (lbs)	Weight Difference (lbs)*
0	A1	5/11/2021	67.4	32	n/a	-
1	B3	5/28/2021	74.1	22	132.2	1.80
2	C3	6/29/2021	74.3	61	126.8	3.80
3	A1	6/30/2021	71.9	54	128.6	1.80
4	C3	7/2/2021	69.2	64	129	0.80
5	B2	7/2/2021	68.7	64	131.6	4.60
6	C1	7/2/2021	69.8	61	131.8	2.60
7	A1	7/3/2021	66.3	66	129.9	3.50
8	C2	7/7/2021	69.9	59	129.8	5.60
9	B1	7/7/2021	69.8	58	138.2	4.40
10	A3	7/7/2021	73.4	54	133.8	7.00
11	A2	7/8/2021	69.6	55	141.6	6.80
12	B2	7/8/2021	69.2	56	133.2	4.60
Average			70.3	54	132.2	3.64
St. Dev			2.5	12.9	4.2	2.2

*Weight difference is the decrease in measured weight between 5/18/2021 and the testing day.

Table 3-3: Calculated material properties on testing day.

Trial Number	Truss Style	Density Day of Test (pcf)	Specific Gravity Day of Test	Calculated MC on Day of Test (%)
0	A1	n/a	-	n/a
1	B3	31.2	0.499	7.23
2	C3	29.9	0.479	9.12
3	A1	30.3	0.486	10.23
4	C3	30.4	0.487	6.76
5	B2	31.0	0.497	8.56
6	C1	31.1	0.498	8.28
7	A1	30.6	0.491	8.77
8	C2	30.6	0.490	9.50
9	B1	32.6	0.522	7.28
10	A3	31.5	0.505	7.94
11	A2	33.4	0.535	6.77
12	B2	31.4	0.503	7.51
Average		31.2	31.2	8.16
St. Dev		0.992	0.016	1.110

3.2 Numerical Data - Load Cell and LVDT Results

The LVDT and Loadcell data was used to determine five measured and calculated responses to quantify the differences in strength and stiffness between each truss trial. Some responses were derived directly from the data, while others were calculated using the LVDT and Loadcell data in a MATLAB script written for this project by the author. The script produced a scatter plot for each individual truss, with the modified applied load data on the y-axis and the modified vertical deflection data on the x-axis. A trinomial line of best fit (i.e., $ax^3 + bx^2 + cx = y$), forced through the origin, was calculated using MATLAB and included on the Load vs. Deflection plot. Scatter plots containing the Load vs. Deflection data, line of best fit, and line of best fit equations are presented in Section 3.4.

The five responses were (Table 3-4):

1. Maximum load applied to truss (lbs).
2. Maximum vertical deflection between king post and bottom chord (in).

3. Load applied to the truss when the deflection limit was reached (lbs).
    a. The deflection limit used for this experiment is a common roof truss deflection limit for combined dead and live loads. The limit is calculated as the $\frac{span\ length}{180}$. The trusses span 6' (72"), so the deflection limit used was 0.4".
4. The total absorbed energy by each truss (lb*in).
    a. The line of best fit equation was used to find the total absorbed energy by calculating the integral of the fitted equation from the origin (0,0) to the maximum deflection experienced by each truss (i.e., the area under the load vs. deflection curve).
5. The maximum stiffness of each truss (lb/in).
    a. The maximum stiffness was calculated as the maximum slope of the fitted equation using differential calculus.
    b. Each trial experienced the maximum stiffness at a unique location in the fitted equation curve. Most of the trials (9 of 13) experienced maximum stiffness at vertical deflections ranging from 0.245" (Trial 1 Truss B3) to 0.687" (Trial 7 Truss A1). However, for 4 of 13 trials (Trial 0 Truss A1, Trial 6 Truss C1, Trial 9 Truss B1, and Trial 11 Truss A2) the fitted equations were parabolic in shape through the testing window (deflection of 0" – 1.5"), so the maximum stiffness was the slope of the line at the origin (i.e., the initial stiffness of the test).

Table 3-4: Measured and calculated responses for all truss trials.

Test Number	Truss Style	Maximum Load (lbs)	Maximum Deflection (in)	Load on Truss at Deflection Limit (lbs)	Total Absorbed Energy (lb*in)	Maximum Stiffness (lb/in)
0	A1	43,100	1.130	26,300	29,900	70,800
1	B3	23,400	0.616	17,620	7,600	56,500
2	C3	27,200	0.774	15,120	10,220	50,000
3	A1	43,400	1.301	13,200	25,600	42,900
4	C3	29,400	0.826	11,160	10,340	44,500
5	B2	28,100	1.385	10,160	21,100	30,600
6	C1	45,900	1.475	20,800	29,700	71,800
7	A1	48,000	0.921	30,500	28,200	123,500
8	C2	34,400	0.916	16,530	16,380	52,100
9	B1	36,000	1.463	17,270	35,400	51,900
10	A3	36,900	0.941	17,770	19,440	69,100
11	A2	36,200	1.465	15,620	37,800	51,300
12	B2	30,900	1.164	10,690	18,880	35,100
Average		35,600	1.106	17,140	22,300	57,700
Standard Deviation		7,729	0.294	5,950	9,710	23,514

3.3 Joint Failure Mechanisms

3.3.1 Overview

All truss trials were stopped for one of two reasons: either the vertical deflection limit was reached, or an ultimate structural failure occurred. Four out of thirteen trials were ended due to reaching the vertical defection limit of approximately 1 ½", and nine out of thirteen trials ended due to an ultimate structural failure, which was defined as a failure that prevented the truss from carrying additional load. In addition to either the deflection limit or ultimate failure, the thirteen specimens experienced additional failure modes of varying degrees of severity.

Seven failure modes were observed throughout the thirteen trials at the truss peaks and the truss heels: block shear, crack formation, check expansion, shoulder bearing failure (i.e., crushing), mortise and tenon (M&T) bearing failure, peg yielding, and excessive vertical deflection. Most

failures were visually observed in the DIC photos or the DIC software program using the generated strain maps. Failures were also observed with the video recording, while others still were significant enough to be audible and clearly visible to observers during the test. The DIC photos were taken on one side of the truss while the video was taken of the other side. A numerical naming strategy was used for descriptive purposes (Figure 3-1). The numerical naming strategy is consistent for each side, i.e., a failure observed on the DIC side (shown in Figure 3-1) at Heel 1 would be the left heel, whereas a failure observed on the video recording side at Heel 1 would be the right heel.

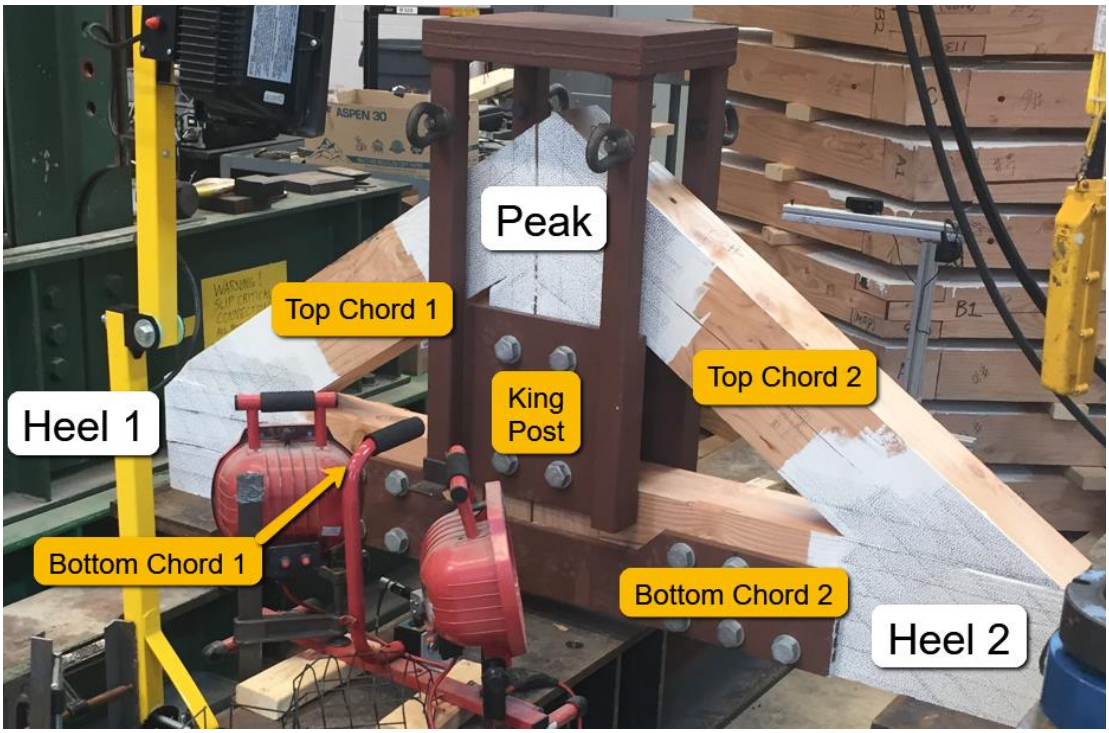

Figure 3-1: Nomenclature of testing set up from DIC side of Truss.

The seven distinct failure modes were not observed for each joint of every truss tested. Some joints were not pushed to failure, as the test was halted due to ultimate failures at different joints, or the deflection limit was met for the trial. Additionally, some of the seven failure modes were specific to certain joint styles (e.g., structural peg yielding for Peak Style B). The observed

failures for each unique joint design were compiled into separate categories to compare the failures between joint types (Table 3-5 and Table 3-6).

Table 3-5: Observed joint failure modes for each Peak joinery style.

Peak connections		
Joinery Style	Possible Failure Method	Failure Label
A	Block Shear Failure	Structural
	Peg Yielding (Relative Deflection ≥ 1/8")	Serviceability
	Tenon Failure (Relative Deflection ≥ 3/16")	Structural
	Crack Formation (Along TC Shoulder)	Serviceability
	Bearing Failure of KP Shoulder	Serviceability
B	Peg Yielding (Relative Deflection ≥ 1/8")	Structural
	Crack Formation (Along TC Shoulder)	Serviceability
	Bearing Failure of KP Shoulder	Structural
C	Block Shear Failure	Structural
	Bearing Failure of KP Shoulder	Structural
	Crack Formation (at reentrant corner of TC)	Serviceability
	Check Expansion	Serviceability

Table 3-6: Observed joint failure modes for each Heel joinery style.

Heel connections		
Joinery Style	Possible Failure Method	Failure Label
1	Block Shear Failure	Structural
	Bearing Failure of BC Shoulder	Structural
	Crack Formation (at reentrant corner of TC)	Serviceability
	Check Expansion	Serviceability
2	Block Shear Failure	Structural
	Peg Yielding (Relative Deflection ≥ 1/8")	Serviceability
	Tenon Failure (Relative Deflection ≥ 3/16")	Structural
	Bearing Failure of BC Shoulder	Serviceability
3	Block Shear Failure	Structural
	Peg Yielding (Relative Deflection ≥ 1/8")	Serviceability
	Tenon Failure (Relative Deflection ≥ 3/16")	Structural
	Bearing Failure of BC Shoulder	Serviceability

The failure modes were labeled as structural failures or serviceability failures, depending on the circumstances of each joinery style. A structural failure is defined as when a critical

component of the joint (i.e., principal load path) fails. The definitions of failures used for this Thesis are discussed in Sections 3.3.2 and 3.3.3. A serviceability failure is defined as when a non-critical component of the joint (i.e., non-principal load path) fails, or the truss exceeds serviceability requirements (i.e., aesthetic concerns, excessive deflection). The truss would still be considered "safe" following the occurrence of a serviceability failure but would be considered "unsafe" following the occurrence of a structural failure in practice. While serviceability failures are important to consider while designing a structure, this thesis will focus on the structural failures experienced by each truss. Both failure types are stated with corresponding concurrent approximate applied loads, and structural failures will be discussed in more detail.

The failure modes are further grouped into sudden failures (i.e., brittle, or semi-brittle failure), or gradual failures (i.e., ductile failures), with corresponding failure mechanism descriptions and accompanying photos from the trials.

3.3.2 Sudden Failures

3.3.2.1 Block Shear

The most common sudden failure observed was block shear. Block shear is a failure mode commonly seen in bolted (fastened) tension connections, where some or all the section of material that is bolted fails as a single piece, or "block." Multiple failure planes occur during a fastened block shear failure: tension rupture along the material plane perpendicular to the direction of load, and shear rupture along the material plane(s) parallel with the direction of load (AISC Manual – 14th ed., 2010).

A different definition is used for this Thesis and for timber compression/bearing joints. Block shear in a traditional timber compression joint refers to one or more shear rupture paths that occur in the tension member at the joint. For example, a birdsmouth shoulder joint (i.e., Heel Style

1, Peak Style C), with the continuous shoulder and no tenon, develops a single shear plane in the tension member (Figure 3-2). The block shear area of this heel connection is the width of the bottom chord (BC - tension member) multiplied by the length of the remaining material of the BC behind the shoulder.

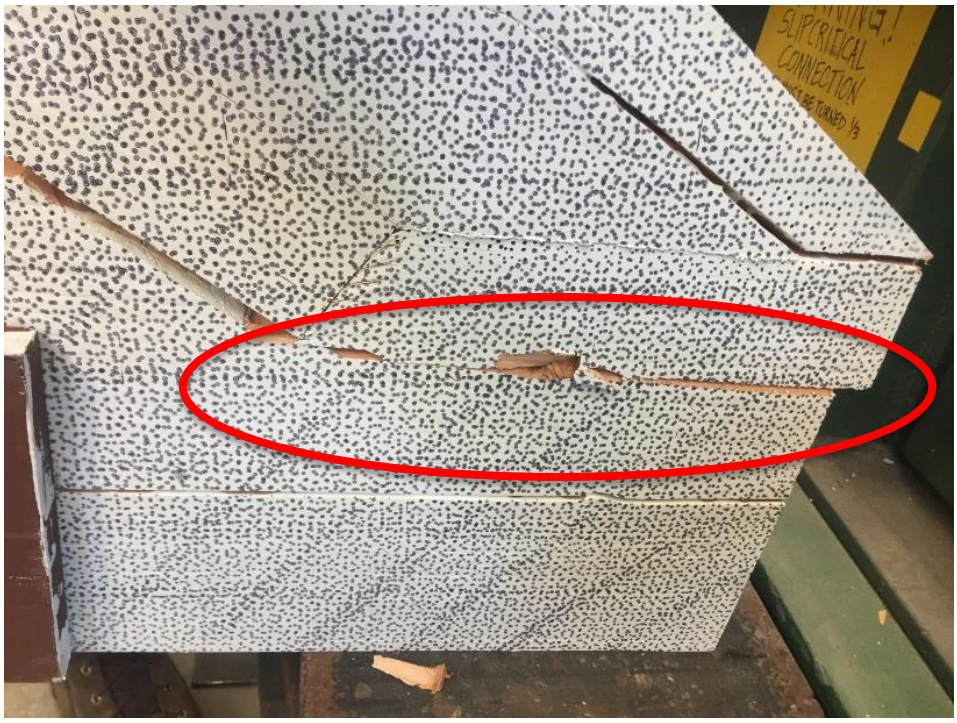

Figure 3-2: Block shear failure along failure plane of Trial 3 Truss A1 Heel 2.

Mortise and tenon (M&T) joinery (i.e., Heel Styles 2 and 3, Peak Styles 1) form two or three polygonal block shear areas (i.e., planes) in the tension members: two shear planes on each side of the tenon and a single shear plane at the bottom of the tenon (Heel Styles only). Block shear in this fashion typically "pushes" a rectangularly shaped section of the tension member out of the end grain in a shape corresponding to the size of the tenon (Figure 3-3).

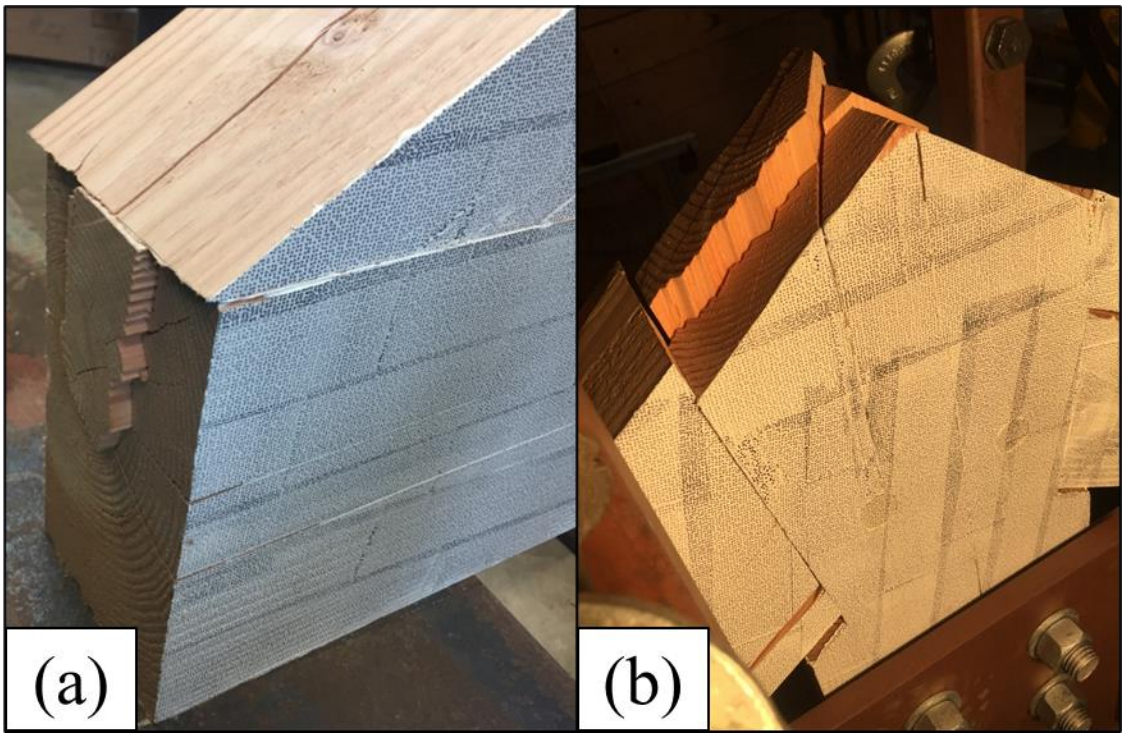

Figure 3-3: (a) Block Shear Failure of Trial 1 Truss B3 Heel 1, (b) Block shear failure of Trial 0 Truss A1 Peak Side 1.

The DIC images and data processing software were able to identify similar failure modes to past research for the birdsmouth shoulder joints, but DIC was unable to identify or predict block shear in the mortise and tenon (M&T) joinery. This is because DIC can only measure surface strain, and the semi-brittle nature of block shear with the M&T joinery prevented the interior failure planes projecting strain to the exterior surfaces prior to the ultimate failure.

Villar-García et al. (2018) identified block shear as a semi-brittle failure mode for the birdsmouth shoulder. Their model predicted a shear stress concentration, confirmed by their physical tests, which began at the bottom of the notch and diminished to zero at the end of the bottom chord. The block shear failure began once this shear stress concentration hit a certain limit and caused an initial crack. Once the initial shear crack was formed in the bottom chord, the remainder of the bottom chord shear plane fails rapidly in a cascading failure. This failure mechanism was observed in this research using the DIC photos. Figure 3-4 shows four photos

spaced 10 seconds apart prior to the block shear failure of Trial 3 Truss A1 Heel 2. The largest shear strain is indicated by red and decreasing strains are indicated by: red, orange, yellow, green, blue, indigo, violet. Figure 3-4a is prior to the initial shear crack. Figure 3-4b shows the formation of the initial shear crack, with the elongation and development of a distinct shear failure plane. Figure 3-4c and Figure 3-4d show the failure plane increasing in length and severity along the bottom chord prior to the cascading block shear failure (Figure 3-2).

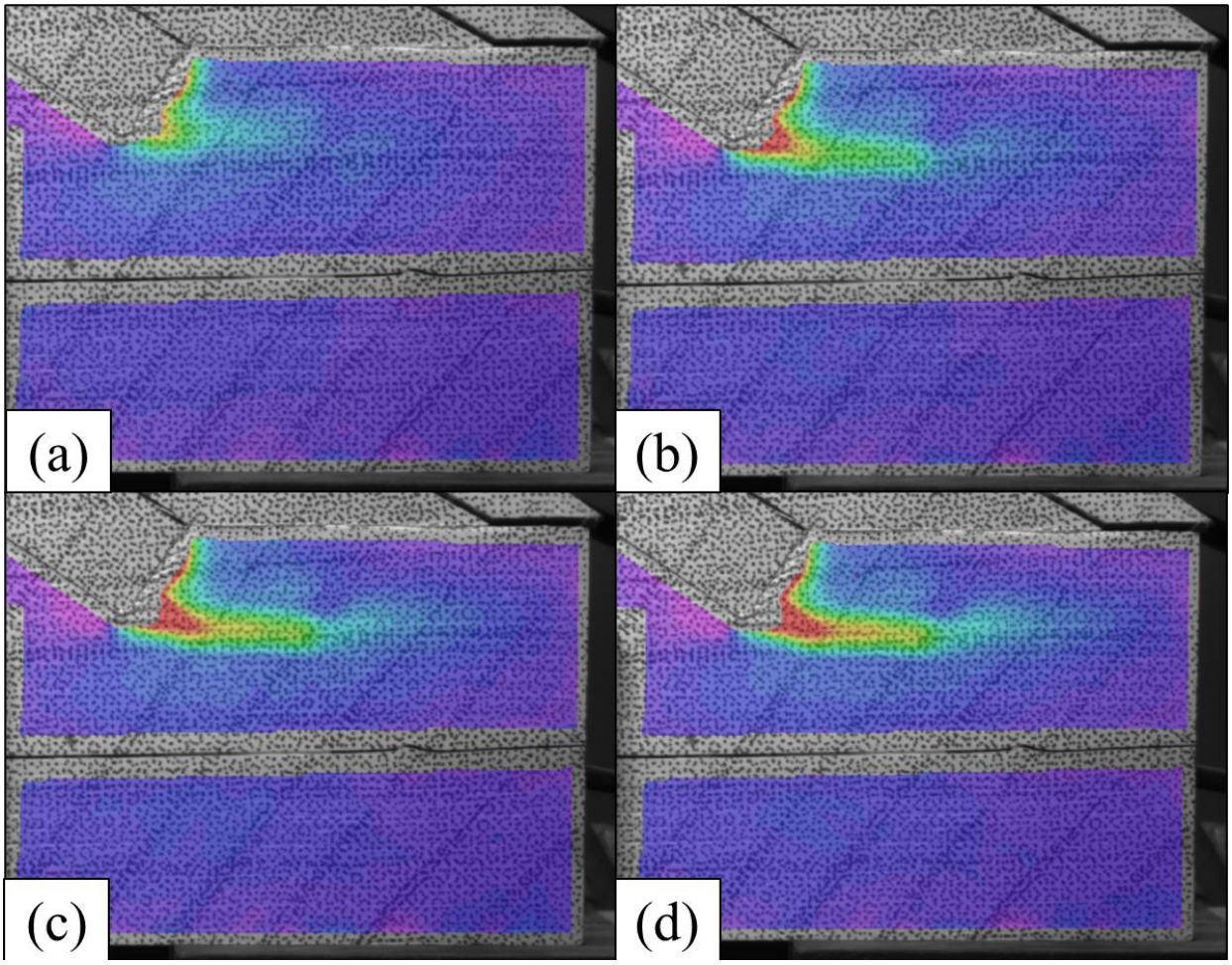

Figure 3-4: (a) Trial 3 Truss A1 Heel 2 shear strain map before initial shear crack, (b) Shear strain map following formation of shear crack, (c) Shear strain map showing shear failure plane elongation, (d) Shear strain map directly prior to block shear failure.

Block shear was the only ultimate structural failure mode observed in this research and was the cause of the nine of thirteen trials to sustain no additional load. For each of the nine trials that had an ultimate failure in block shear, the recorded load of the failure was the maximum recorded load on the truss. Block shear occurred in Heel Styles 1, 2, 3, and Peak Style A.

Conversely, Trial 11 Truss B2 experienced a block shear failure crack (or compression crack) of the king post at the peak on side 1, but the crack did not lead to a full punch-out failure and did not result in the truss being unable to sustain additional load (Figure 3-5). Therefore, the trial was continued until the deflection limit was reached. It is not counted as one of the 9/13 trusses that had an ultimate failure.

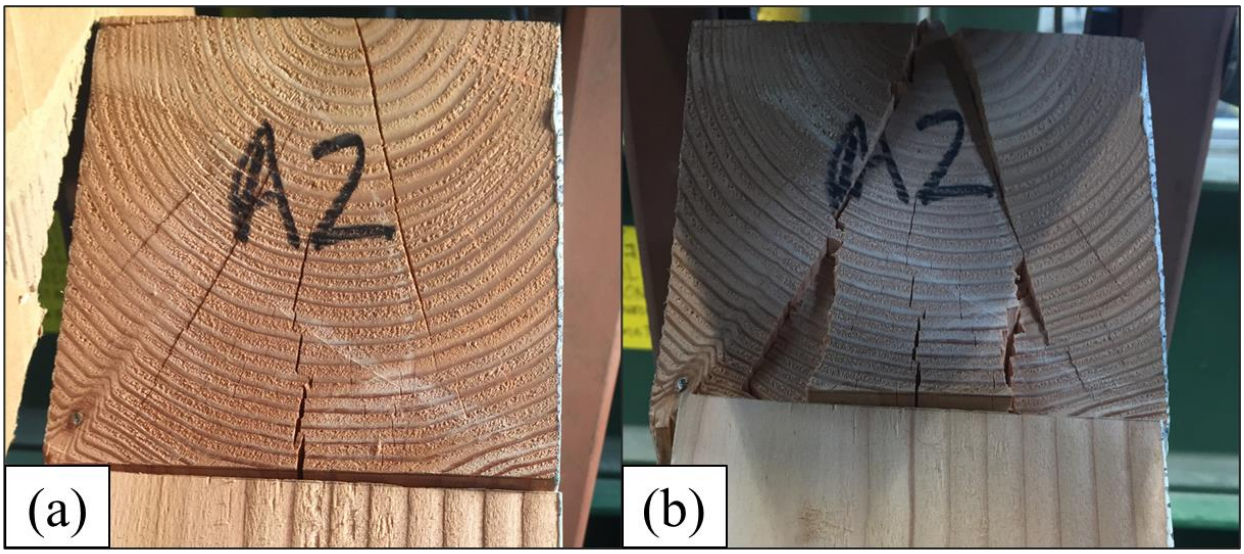

Figure 3-5: (a) King post of Trial 11 Truss B2 Side 1 prior to testing, (b) Block Shear compression crack of King Post at end of test.

3.3.2.2 Crack Formation and Check Expansion

Cracks and checks are defined separately for this thesis. A crack is defined as a split (i.e., separation of wood fibers) in a timber that was formed during the loading process and was not present prior to the truss test. Conversely, checks are defined as existing (prior to the truss test) radial cracks that formed in the timbers. Checks commonly form as timbers age and dry due to the

differential rate of drying shrinkage between radial (along the grain) and tangential (across the grain) dimensions. In general, as timber dries, the perimeter of the timber is drying at a faster rate (i.e., making a smaller circle) than the timber across the grain (i.e., tangential to the grain/perimeter) (TFEC 1-21). This differential rate of shrinkage induces tension perpendicular to grain in the outermost layers of the timber. This tension often exceeds the timber's capacity in perpendicular to grain tension and forms cracks called checks. These checks occur parallel to the grain's long direction, and are generally considered not serious structural defects, as the parallel-to-grain checks do not greatly impact axial compression or tensile capabilities. Checks could be considered serious structural defects in special circumstances if the check goes through the majority of a timber, on both sides of the central pith of the timber, and the checks are near the neutral axis of a bending member. However, the design values in the National Design Specifications (NDS, 2018) already include adjustments for the presence of checks, so typically no further modifications are required (TFEC 1-21).

The crack and check expansions occurred during loading due to induced tension perpendicular to the grain in the timbers. Two common crack locations were observed, as described in the following, and they were best observed with either the DIC photos or the video recording, depending on which side of the timbers the cracks started. The check expansion was difficult to determine an exact moment of failure, but there were auditory sounds on the video that could be used to determine an exact moment. If no auditory sounds were available, then a crack expansion of 1/16" relative to its original width was called a failure, observable only in the DIC photos.

One location of crack formations was at the interior corners of the birdsmouth shoulder joints in the top chords (compression members). This failure was observed in Peak Style A and Heel Style 1 (i.e., birdsmouth shoulder joints) (Figure 3-6). These cracks formed due to induced

perpendicular to grain tension that developed at the interior notch cut in the compression member. The compression of the top chord shoulders onto the tension member shoulders (i.e., king post or bottom chord) caused the tension member shoulder material to plastically deform (i.e., crush). The deformation of the tension member shoulder was in the direction opposite the compressive load and towards the centerline of the tension member (i.e., away from the compressive member centerline). For some of the trials, the plastic deformation was large enough to close the gap between the bearing surface of the two members outside of the designated shoulder location (i.e., the un-notched material). As the load increased further, the bearing shoulder material of the compression member deformed, but the remaining section of the compression member was restrained on the tension member and experienced a reaction against the tension member. This reaction induced perpendicular to grain tension and the resulting crack. This failure can be prevented by providing a back-cut to the compression member material that is not involved in the birdsmouth notch of ~1/8”-1/4” (i.e., the location of note 2 in Figure 3-6). The back-cut allows the material not in the shoulder of the compression member to not contact the tension member when the compression shoulder deforms. This is not a common detail in practice due to aesthetic concerns, so it was not used for this Thesis.

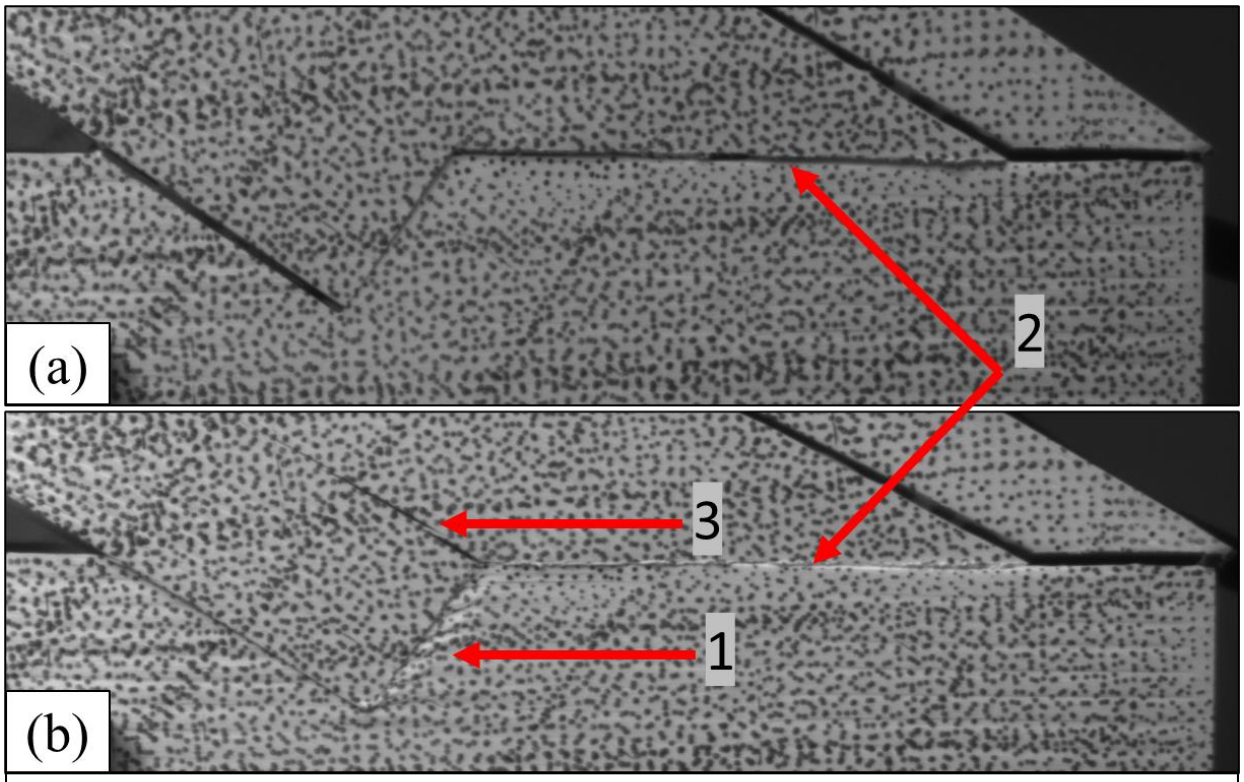

(1) Plastic deformation (i.e., crushing) of tension member shoulder.
(2) Compression member surface not in shoulder begins to bear on tension member material, inducing a positive reaction in the compression member.
(3) Crack formation at interior notch of top chord shoulder due to unintentional perpendicular-to-grain tension induced by reaction onto compression member from tension member material not in the shoulder (2).

Figure 3-6: (a) Trial 3 Truss A1 Heel 2 at start of test, (b) crack formation in top chord and plastic deformation of bottom chord shoulder about 2/3 through test.

The other primary location of crack formation or check expansions occurred along the continuously sloped shoulder design or the no shoulder designs. This failure was observed in Peak Styles A and B and was likely due to the large vertical deflections experienced by the king posts. As the king post was loaded, the top chords resolved the resulting force in compression, either through the bearing on tenons or pegs. However, as the load on the king post increased and the joints began to fail (i.e., bearing failure, peg yielding), the king post deflected vertically down more than the adjacent top chords, as the top chords were still restrained by the tenon or pegs. As

the load increased further, the relative difference in vertical deflection between the top chords above and below the primary load paths (i.e., tenon bearing, peg bearing) increased, causing perpendicular to grain tension in the top chord and the resulting cracks (Figure 3-7 and Figure 3-8). It was observed that the top chord tenons for Peak Style B joints (Trial 1 Truss B3, Trial 5 Truss B2, Trial 9 Truss B1, and Trial 12 Truss B2) met in the middle and began to bear on each other as the trusses were loaded, even with the ~½" included back-cut (Figure 3-9). This observation was only possible for Peak Style B due to the tenons daylighting out of the top of the king post mortise. It is assumed that the bearing of the tenons on one another helped prevent the top chords from deflecting with the king post, which exacerbated the differential deflection and resulting perpendicular-to-grain tension, causing cracks to form. It was unknown if the tenons for Peak Style A met in the middle of the king post, as the load had to be removed from the truss prior to investigating the joints.

Figure 3-7: Cut view of Trial 5 Truss B2 crack formation at lower peg location.

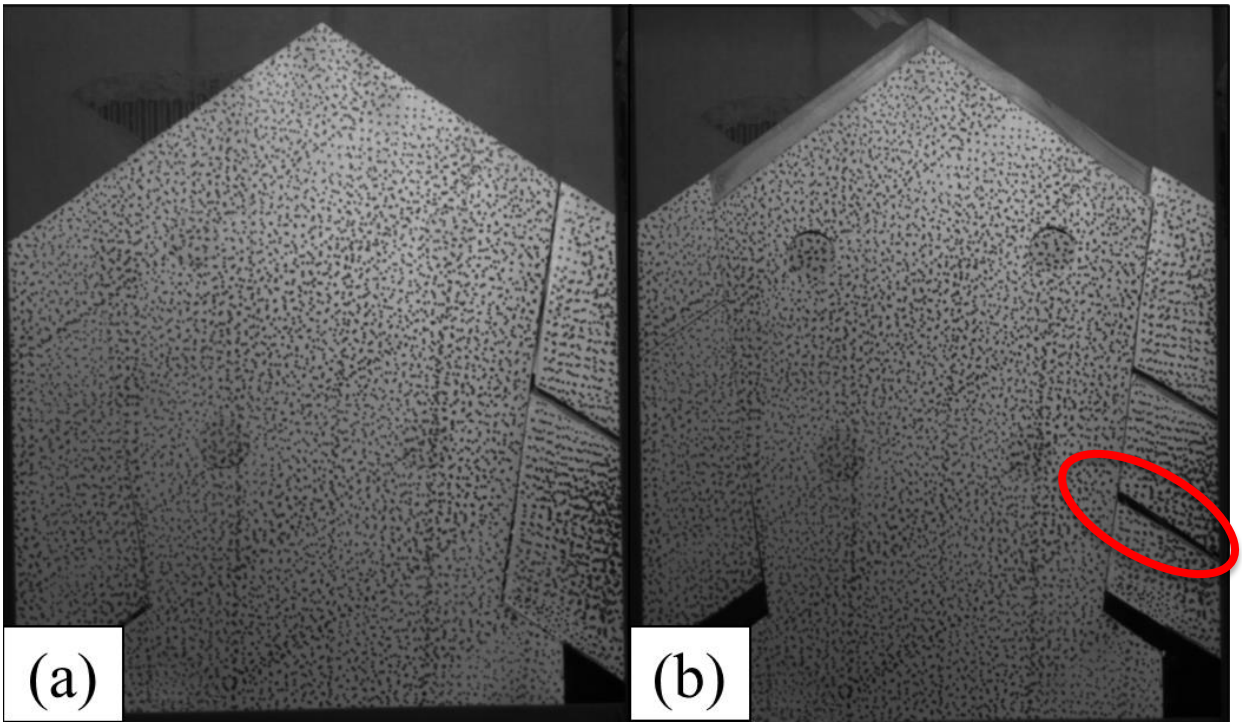

Figure 3-8: (a) Trial 5 Truss B2 at start of test, (b) crack formation of peak side 2 and peg yielding of both sides at end of test.

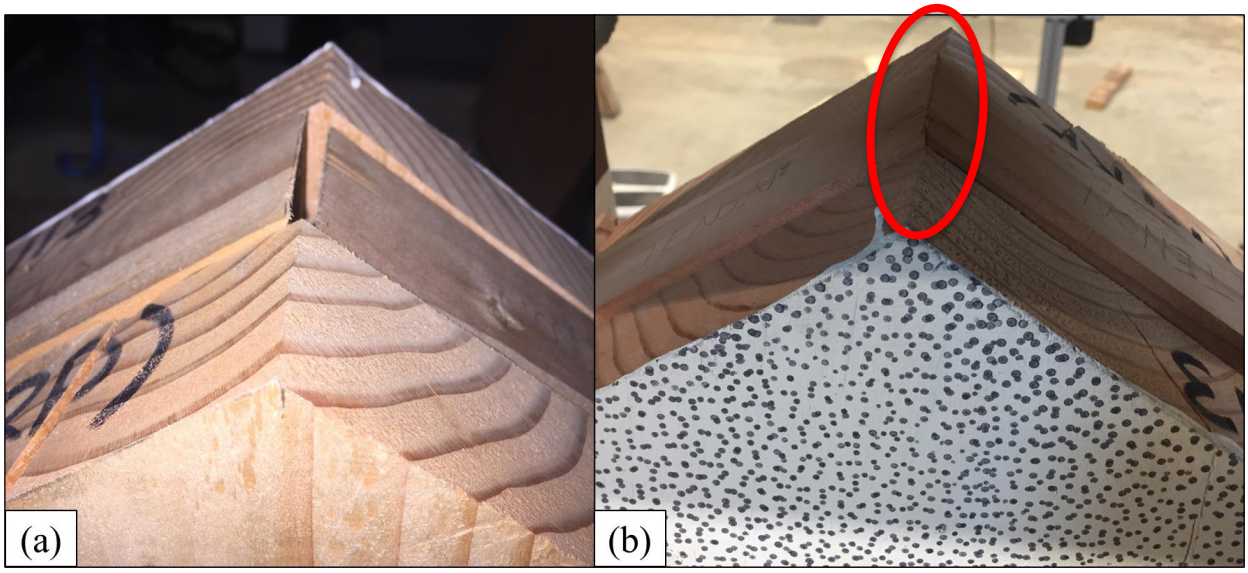

Figure 3-9: (a) Trial 12 Truss B2 top chord tenon separation at peak joint prior to test, (b) Trial 12 Truss B2 top chord tenon bearing and king post vertical deflection following test.

Crack formation and check expansion failures were considered serviceability failures for the purposes of this Thesis for the following reasons:

1. The crack formations and check expansions did not cause any of the truss joints to be unable to sustain additional load.
2. The crack formations at the two birdsmouth joints (Peak Style C and Heel Style 1) could be mitigated by providing a minimum 1/8”-1/4” back-cut on the compression member material that is not in the shoulder joint (see note 2 Figure 3-6). This gap allows for the compression member to bear on the tension member and deform/crush with the tension member without the surfaces outside of the designed shoulder joint meeting, inducing the perpendicular to grain tension that formed the cracks. The gap was not included in this research project because it is not a common detail prevalent in the industry due to aesthetic concerns.
3. The crack formations or check expansions in the M&T joinery were all observed at the truss peak joints under large vertical deflections. These crack formations or check expansions would likely not occur under service loads in trusses designed with a solid bottom chord and diagonal webs, where the vertical deflection of the truss is shared by additional components and not purely sustained by the king post.

3.3.3 Gradual Failures

3.3.3.1 Shoulder Bearing Failure

The West Coast Lumber Inspection Bureau (WCLIB) is one of the two grading agencies that the NDS – 18 recognizes as a grading agency for Douglas Fir-Larch timbers. The other is the Western Wood Product Association. The WCLIB refers to ASTM Standards D2555-17a and D143-21 regarding the empirically measured values of compression perpendicular to grain

(WCLIB Standard #17). The ASTM Standards for small, clear specimens of wood use a 2" x 2" cross section. For perpendicular to grain compression measurements, the test records a load vs. deflection plot up to a limit of 0.04" (ASTM D143-21 and ASTM D2555-17a). Using the 0.04" limit as the limit of linear-elastic material behavior, for a 2"x2" cross section this equivalates to a maximum allowable strain of 0.02. Therefore, for this Thesis, a crushing/bearing failure of the shoulder material is defined when a surface strain of 0.02 is measured using DIC. Feio et al. (2014) also used a 2% strain limit (0.02) to define an ultimate failure for their compression tests of mortise and tenon joints with shoulders.

Shoulder bearing failure was classified as a structural failure for the joints where the shoulder was the primary load path (i.e., birdsmouth shoulder, Peak Style C and Heel Style 1), and as a serviceability failure for the joints where the shoulder was not the primary load path (i.e., M&T joinery: Peak Style A, Heel Style 2, and Heel Style 3, or peg yielding: Peak Style B). The structural failure designation for the birdsmouth shoulder joint is because timber bearing is a required design consideration of the governing timber code (NDS, 2018). However, there is debate in the timber engineering community regarding classifying crushing as a structural failure. Verbist et. al (2016) concluded their paper on compression testing of the single step joint (similar to a birdsmouth joint) with:

> However, the crushing is described as a failure mode in the European Standard whereas it's actually about timber deformation. Must we hence consider the crushing like a failure in the Single Step Joint [birdsmouth shoulder] whereas the shear crack [block shear] will occur as the ultimate failure mode for all the geometrical configurations? This question is fundamental for the timber in general, the Simple Notched Joint but also for the choice of reinforcement technics [techniques] according to the emergence of any failure mode. (p. 20)

This thesis was focused on replicating real-world design methodologies and loading conditions as closely as possible, so bearing strain in excess of 2% in the shoulder area was considered a

structural failure. However, the determination of the failure point using the 0.02 strain limit did not reflect a bearing failure of the entire shoulder. Figure 3-10 shows six images of principal strain maps throughout the test of Trial 3 Truss A1 Heel 2. Principal strain is indicated differently relative to shear strain, mentioned previously (Figure 3-4). For principal strain, the largest strain is indicated with violet, and decreasing strains are indicated by: violet, indigo, blue, green, yellow, orange, red. The truss experienced a principal strain greater than 0.02 between images A and B (approximately 11,600 lbs applied load to king post), but only at the bottom of the bearing shoulder. The top of the bearing shoulder was experiencing strains less than 0.005 when the bearing joint "failed." Therefore, the joint technically failed at the location of maximum strain, but the remaining shoulder material not yet at failure has a lot more capacity in bearing. It was not until image D (approximately 28,450 lbs applied load to king post) when the strain map was consistent along the bottom chord shoulder, but the strains were significantly larger than the failure criteria (approximately 0.10 or greater). Therefore, due to the definition used to define failure for this experiment, most of the approximate loads for structural failures due to shoulder bearing are less than other failures identified in this thesis.

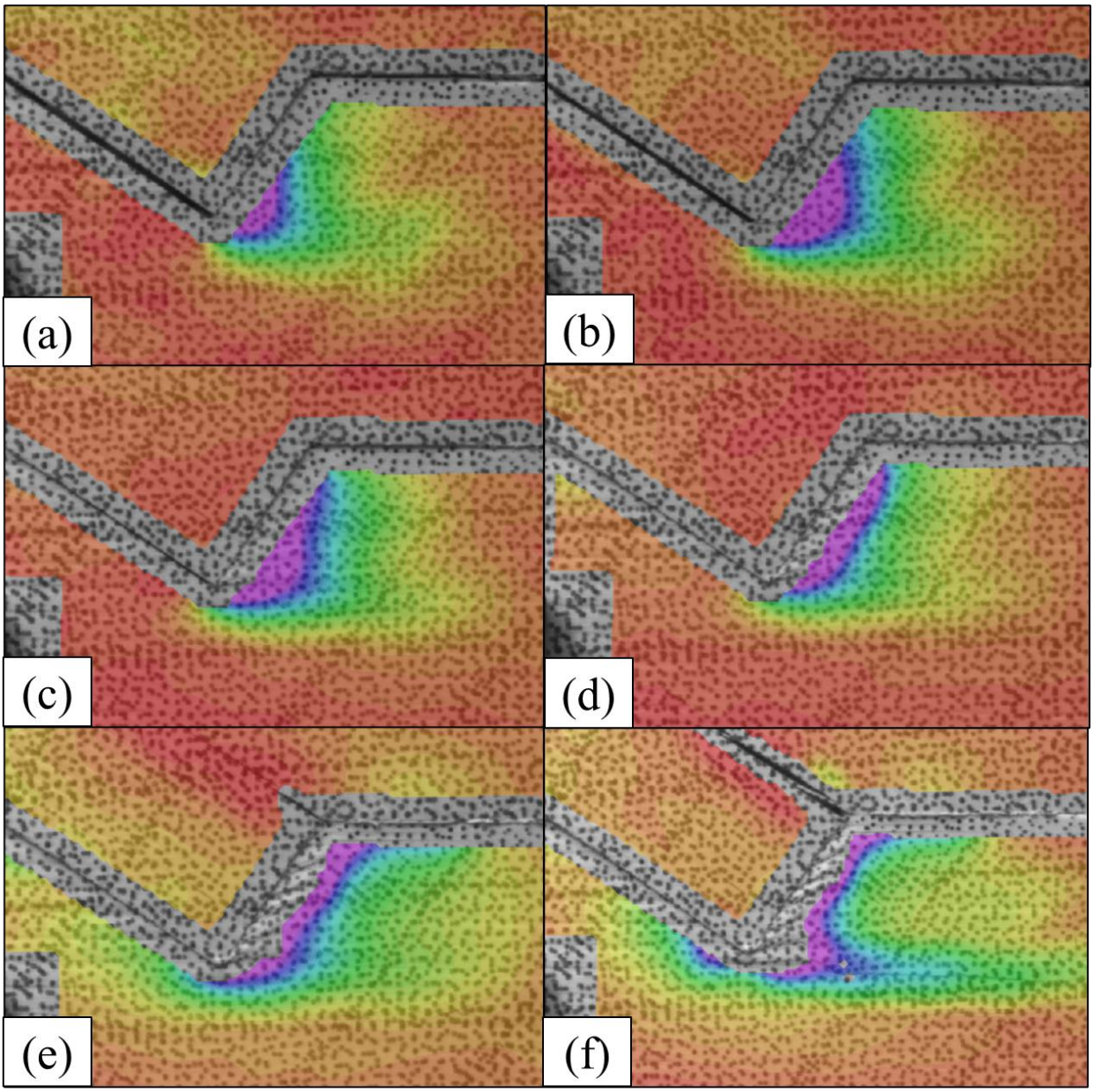

Figure 3-10: Principal strain map of Trial 3 Truss A1 Heel 2 showing strain concentration of the bottom chord shoulder throughout the test. Approximate point loads applied to truss king post: (a) 8160 lbs, (b) 13230 lbs, (c) 22280 lbs, (d) 28450 lbs, (e) 37700 lbs, (f) 43350 lbs (maximum load).

Figure 3-10 also verifies two design methodologies in the NDS – 18:

1. The design process of the bearing stress (Appendix C) shows that the parallel to grain bearing surface of the top chord should have more capacity than the angle-to-grain bearing surface of the bottom chord, and that the bottom chord shoulder surface governs

the capacity of the joint. Throughout the test, the top chord shoulder experiences relatively small strain (deformation), while the bottom chord shoulder experiences relatively large strain (deformation) and reaches the failure limit of 0.02 at a much lower load, thus confirming that the angle-to-grain bottom chord shoulder has less capacity. This is shown in Figure 3-10 by the lack of coloration (i.e., strain) of the top chord shoulder relative to the bottom chord shoulder.

2. Section 3.10.1.3 of the NDS – 18 states that when the actual bearing stress is greater than 75% of the allowable bearing stress ($f_c > 0.75 * F_c'$), a rigid, homogeneous material of sufficient stiffness is required between timber bearing surfaces to evenly distribute the loads through the joint. Figure 3-10 A, B, and C show that there is a distinct stress concentration at a single location that expands to the full section as the load is increased, and the location of maximum stress begins to fail (crush) and spread the load throughout the joint. This may be able to be prevented by using a rigid bearing block between timber surfaces, but this was not used in this experiment to replicate real-world conditions.

3.3.3.2 Peg Yielding

The standard practice for determining peg yielding is based on ASTM D5652-21 and ASTM D5764-97a, which use a 5% fastener diameter offset yield method (ASTM D5652-21 and ASTM D5764-97a). This method uses the load-displacement curve for a single fastener connection in double shear loaded uniaxially (i.e., single direction). Due to the nature of the truss tests conducted for this thesis, where multiple fasteners may be loaded in two dimensions simultaneously, the yield limit for a single fastener (i.e., peg) cannot be accurately determined using this method.

As part of their Thesis, Miller et. Al (2004) conducted tests using the ASTM D5652-21 and ASTM D5764-97a protocols for varying peg species with a 1” diameter in Yellow Poplar mortise and tenon connections. Their findings state the mean yield deflection for the peg tests occurred at deflection of 0.138 inches, and a mean yield load of 5,549 lbs (Miller et. al., 2004). This thesis used the failure deflection obtained by Miller et. al (2004) to define the failure of a peg empirically. Therefore, a peg was considered “failed” if the difference of deflection between members, either vertical (truss peak) or horizontal (truss heel), met or exceeded a limit of 1/8” (0.125”). The relative deflection was measured using the DIC data.

Peg yielding was considered a structural failure for Peak Style B, as peg yielding was the primary load path to resist the vertical vector of the top chord compression. Peg yielding was considered a serviceability failure for every other joint, as the primary loads paths were either M&T bearing and block shear, and the pegs were considered yielded if those failures occurred (Figure 3-11).

Figure 3-11: Yielded peg failure concurrent with block shear of the BC at Trial 4 Truss C3 Heel 2.

3.3.3.3 Mortise and Tenon Bearing Failure

Mortise and Tenon (M&T) bearing failure was observed with the DIC results in 4 of 13 truss trials. This failure occurs when the block shear capacity of the tension member (i.e., bottom chord, king post) exceeds the capacity of the M&T to resist bearing force. From engineering mechanics, timber material properties, and associated calculations (Appendix C), it is assumed that pegs yielded prior to M&T faces failing in bearing. It was impossible to determine the true yield point of the bearing M&T connection due to the lack of visibility, so an indirect relationship with relative displacement was used to define failure of the M&T connection. Using the DIC data for each of the applicable connections, a M&T was considered "failed" if the difference in deflection between members, either vertical (truss peak) or horizontal (truss heel), met or exceeded

a limit of 3/16” (0.1875”). This limit is 1/16” larger than the peg failure limit, and if reached it is assumed that the peg has yielded, and that the M&T material has failed in a bearing failure.

Two of the four M&T failures were tenon specific failures, observed both with the DIC results and visual observations of the tenons post-test (Figure 3-12). For these two failures, the large compressive force and vertical deflection experienced by the trusses caused localized bearing failure and tear-out of the tenon fibers against the mortise. The tenon material appeared to experience buckling of the wood fibers, which cascaded throughout the tenon and resulted in large horizontal deflection of the top chord, large vertical deflection of the king post, and the truss being unable to sustain additional load. Both truss trials which experienced tenon specific failure were stopped due to excessive vertical deflection.

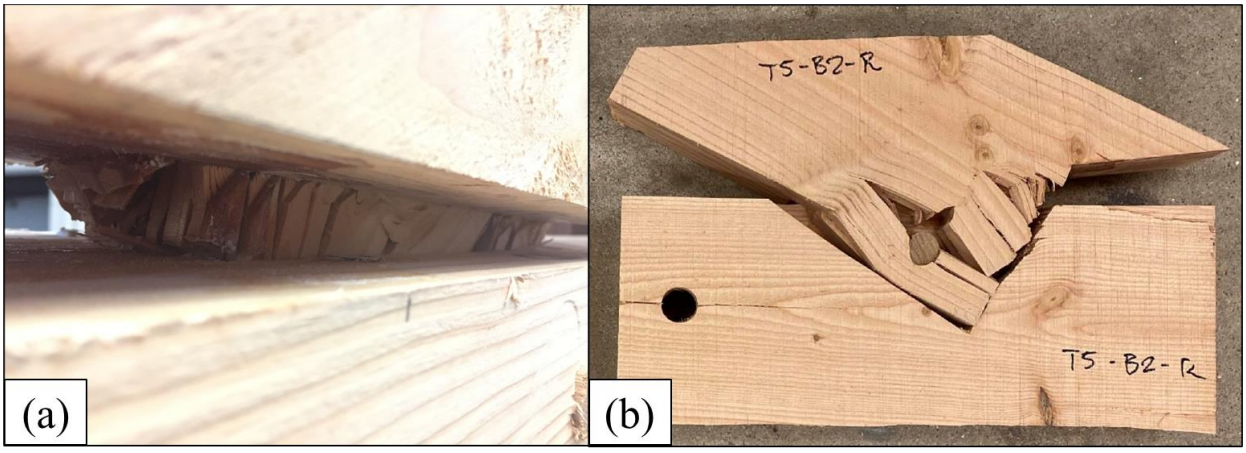

Figure 3-12: Trial 5 Truss B2 Heel 2 localized tenon failure and tenon tear-out (a) view from exterior of joint, (b) interior view when cut in half vertically.

3.3.3.4 Excessive Vertical Deflection

Excessive deflection is a serviceability-only concern that is considered in the design phase of each structural engineering project. For this thesis, each truss greatly surpassed the least strict deflection limit of L/180 at loads above the allowable design loads. This is partly due to the geometry of the testing rig and truss, where the king post was able to slip past the bottom chord,

partly due to the excessive live load applied to the trusses, and partly due to the short span of the trusses. The maximum vertical deflection was recorded, but otherwise no additional metrics or calculations were used regarding the excessive vertical deflection.

3.4 Individual Trial Results

The following sections will provide the results for the individual truss trials: Load vs. Deflection plot, numerical data table, and joint failure table. The joint failure table will state individual joint failures with concurrent approximate applied loads experienced by each truss. If the truss experienced an ***ultimate failure***, it is identified with ***bold and italicized text.*** Block shear was the only failure mode that caused the nine of thirteen trials to experience an ultimate failure, where the truss was unable to carry additional load. **Structural failures** are indicated with **bold text.** All trials experienced some structural failures, most of which were not ultimate failures, meaning that a structural part of the joint (i.e., primary load path) failed, but the truss was still able to carry additional load (e.g., peg yielding, shoulder bearing, mortise and tenon bearing). Serviceability failures do not have bold or italicized text. The loads provided for comparison (approximate failure load, allowable load) are all point loads applied to the truss king post. The provided allowable point loads are based upon the governing failure mechanism for each joint type (Appendix C).

For trial 0 and trial 1, the DIC strain data was not able to be used due to issues with processing the images in the software (Section 2.4.1). Therefore, the failure modes determined by using the DIC strain data were not able to be determined. However, the relative deflections were able to be determined, as the relative deflections were measured using specific areas of the DIC dot pattern not impacted by the aliasing of the overall data.

3.4.1 Preliminary Trial (0) Truss A1

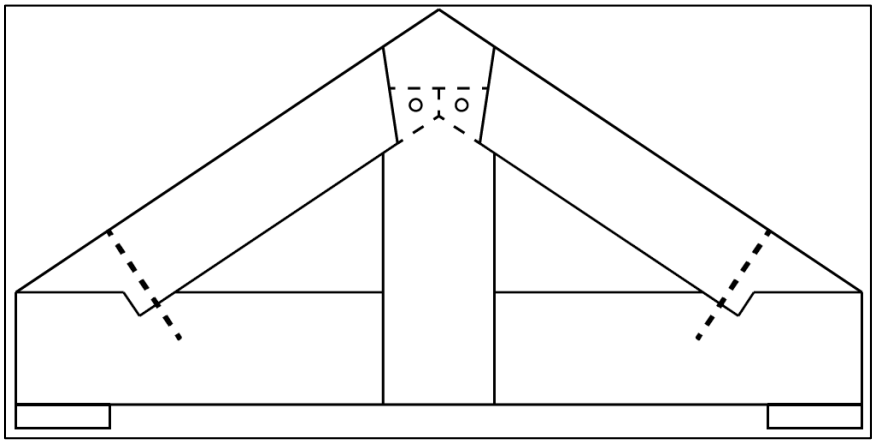

Figure 3-13: Truss A1 elevation view.

The LVDT data for Trial 0 did not record adequately, so the deflection data was entered manually from a graphical readout of the LVDT data in 12 second increments. Therefore, the deflection data for Trial 0 is 120 times less precise compared to the other truss trials, but a Load vs. Deflection plot was still able to be created (Figure 3-14).

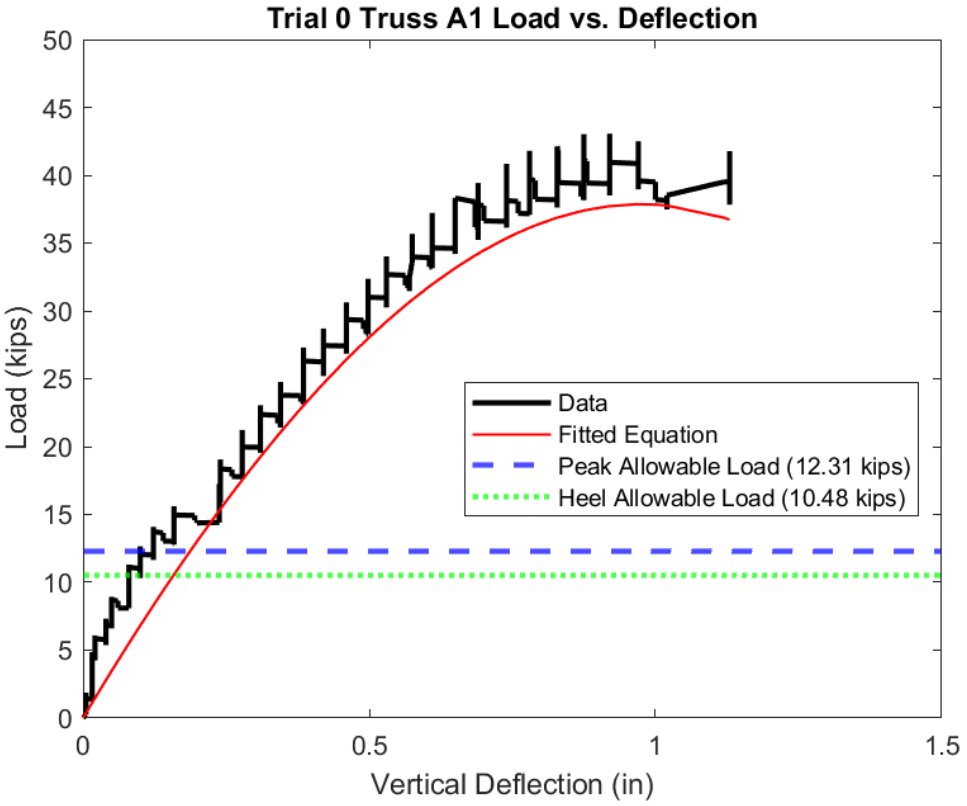

Figure 3-14: Load vs. Deflection plot for Trial 0 Truss A1.

Table 3-7: Responses from numerical data and measurements for Trial 0 Truss A1.

Trial 0 Truss Style A1 - Tested 05/11/21		
Response	Value	Units
Test Day Moisture Content	10.0	%
Test Day Specific Gravity	0.506	-
Maximum Load	43,100	lb
Maximum Deflection	1.130	in
Load on Truss at Deflection Limit	26,300	lb
Total Absorbed Energy	29,900	lb*in
Maximum Stiffness	70,800	lb/in
Best Fit Equation: $f(x) = -7173 * x^3 - 25799 * x^2 + 70803 * x$		

Trial 0 was stopped due to an ultimate failure of block shear at the Truss Peak on Side 1. It was the only truss to have an ultimate structural failure at the truss peak, and the block shear of the king post was the only structural failure experienced by the truss. The remaining failures were all serviceability failures (Table 3-8).

Table 3-8: Trial 0 Truss A1 failures.

Joint Type	Failure mode*	Sustained Load at Failure (lbs)	Allowable load by code calculations (lbs)	Factor of Safety
Heel Style 1, Side 1	Crack Formation (at reentrant corner of TC)	32,400	10,480	3.09
Heel Style 1, Side 2	Crack Formation (at reentrant corner of TC)	30,900	10,480	2.95
Peak Style A, Side 1	***Block Shear Failure***	***43,100***	***12,310***	***3.50***
	Peg Yielding (Relative Deflection ≥ 1/8")	21,900	12,310	1.78
	Crack Formation (Along TC Shoulder)	38,600	12,310	3.14
Peak Style A, Side 2	Peg Yielding (Relative Deflection ≥ 1/8")	21,900	12,310	1.78

*Note: Bold and italicized text indicates ultimate failure. Bold text indicates structural failure. Plain text indicates serviceability failure.

3.4.2 Trial 1 Truss B3

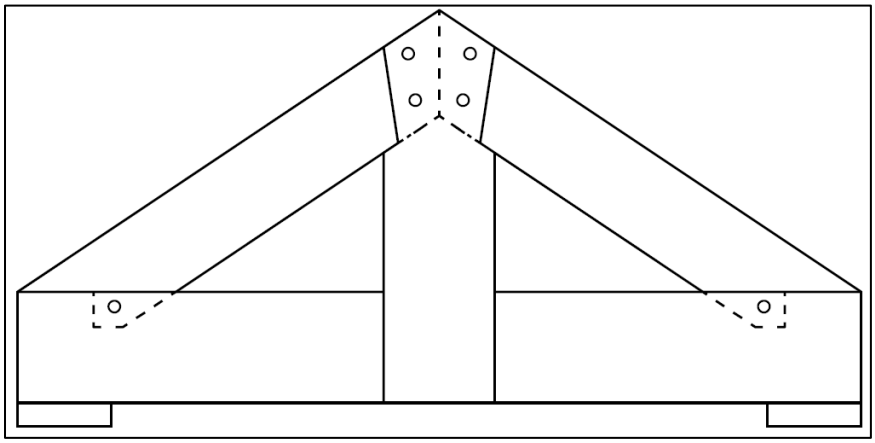

Figure 3-15: Truss B3 elevation view.

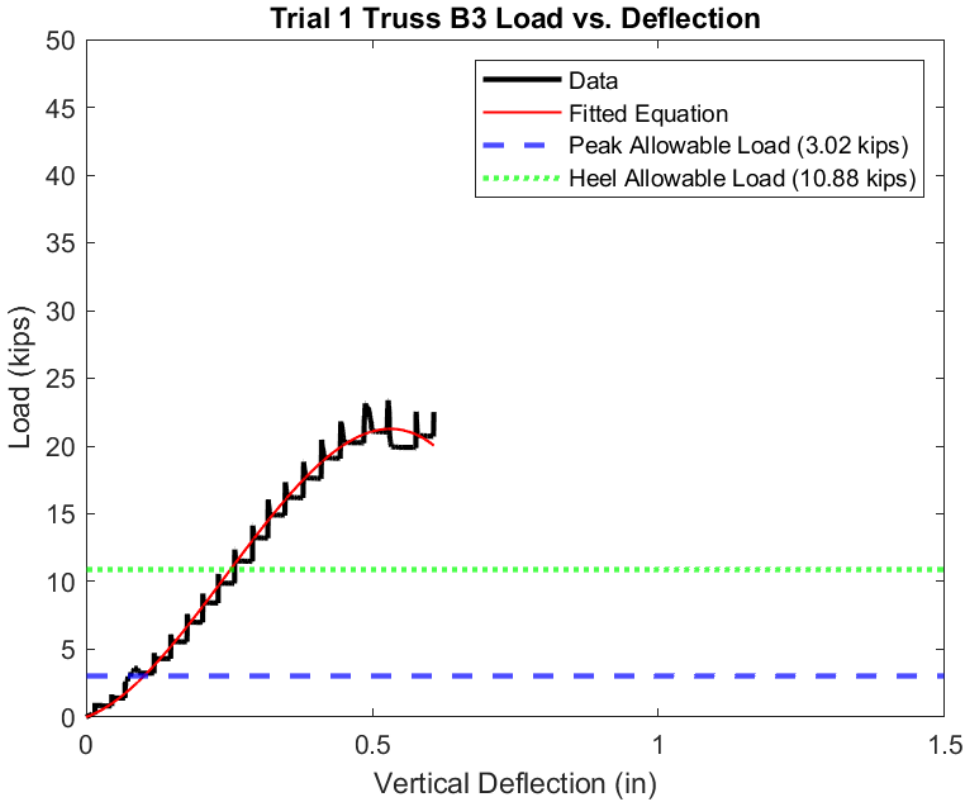

Figure 3-16: Load vs. Deflection plot for Trial 1 Truss B3.

Table 3-9: Responses from numerical data and measurements for Trial 1 Truss B3

Trial 1 Truss Style B3 - Tested 05/28/21		
Response	Value	Units
Test Day Moisture Content	7.23	%
Test Day Specific Gravity	0.499	-
Maximum Load	23,400	lb
Maximum Deflection	0.616	in
Load on Truss at Deflection Limit	17,600	lb
Total Absorbed Energy	7,600	lb*in
Maximum Stiffness	56,500	lb/in
Best Fit Equation: $f(x) = -228771 * x^3 + 168059 * x^2 + 15316 * x$		

Trial 1 was stopped due to an ultimate failure of Block Shear at Heel 1, but experienced structural failures of peg yielding at both sides of the peak joint prior to the ultimate failure. The peg yielding failures were well above the allowable loads at the peak for Peak Style B. The ultimate failure of block shear at Heel 1 was the lowest recorded ultimate failure of the 9/13 trusses that experienced an ultimate failure (Table 3-10).

Table 3-10: Trial 1 Truss B3 failures.

Joint Type	Failure mode*	Sustained Load at Failure (lbs)	Allowable load by code calculations (lbs)	Factor of Safety
Heel Style 3, Side 1	***Block Shear Failure***	***23,400***	***10,880***	***2.15***
Heel Style 3, Side 2	No notable failures		10,880	-
Peak Style B, Side 1	**Peg Yielding (Relative Deflection ≥ 1/8")**	**14,670**	**3,020**	**4.85**
Peak Style B, Side 2	**Peg Yielding (Relative Deflection ≥ 1/8")**	**21,900**	**3,020**	**7.24**

*Note: Bold and italicized text indicates ultimate failure. Bold text indicates structural failure. Plain text indicates serviceability failure.

3.4.3 Trial 2 Truss C3

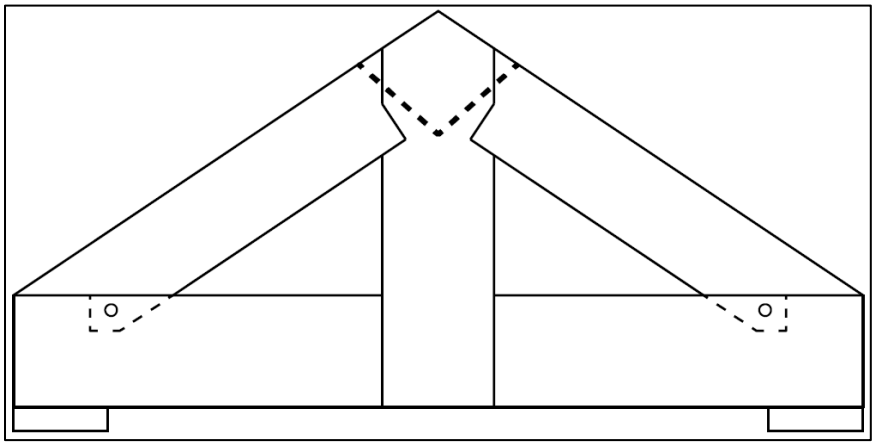

Figure 3-17: Truss C3 elevation view.

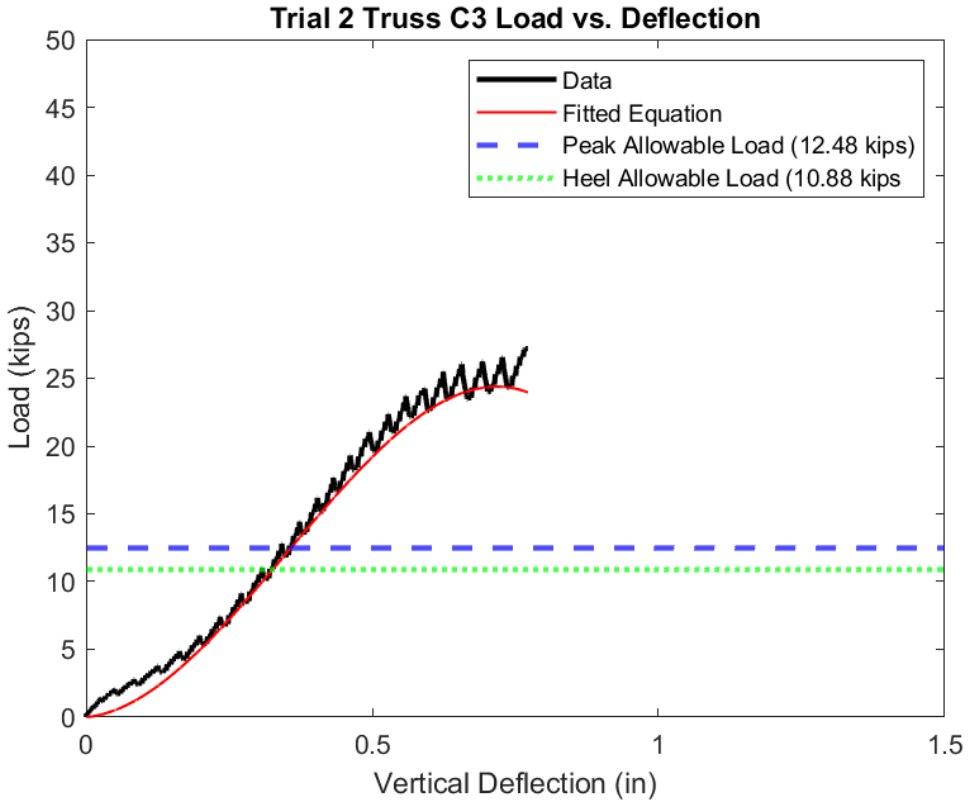

Figure 3-18: Load vs. Deflection plot for Trial 2 Truss C3.

Table 3-11: Responses from numerical data and measurements for Trial 2 Truss C3

Trial 2 Truss Style C3 - Tested 06/29/21		
Response	Value	Units
Test Day Moisture Content	9.12	%
Test Day Specific Gravity	0.479	-
Maximum Load	27,200	lb
Maximum Deflection	0.774	in
Load on Truss at Deflection Limit	15,120	lb
Total Absorbed Energy	10,200	lb*in
Maximum Stiffness	50,000	lb/in
Best Fit Equation: $f(x) = -124578 * x^3 + 131429 * x^2 + 3816 * x$		

Trial 2 was stopped due to an ultimate failure of Block Shear at Heel 1 but experienced a structural bearing failure of the king post shoulder (side 1) prior to the ultimate failure. The peak joints and heel joints were all analyzed separately, but it was observed that the structural bearing failure of the king post shoulder (side 1), and the two serviceability failures of bearing of the bottom chord shoulder (Heel 1) and check expansion at the truss peak (side 2) all occurred simultaneously (Table 3-12).

Table 3-12: Trial 2 Truss C3 failures.

Joint Type	Failure mode*	Sustained Load at Failure (lbs)	Allowable load by code calculations (lbs)	Factor of Safety
Heel Style 3, Side 1	***Block Shear Failure***	***27,200***	***10,880***	***2.50***
	Peg Yielding (Relative Deflection ≥ 1/8")	24,600	10,880	2.26
	Bearing Failure of BC Shoulder	22,800	10,880	2.10
Heel Style 3, Side 2	Bearing Failure of BC Shoulder	10,400	10,880	0.96
Peak Style C, Side 1	**Bearing Failure of KP Shoulder**	**22,800**	**12,470**	**1.83**
Peak Style C, Side 2	Check Expansion	22,800	12,470	1.83

*Note: Bold and italicized text indicates ultimate failure. Bold text indicates structural failure. Plain text indicates serviceability failure.

3.4.4 Trial 3 Truss A1

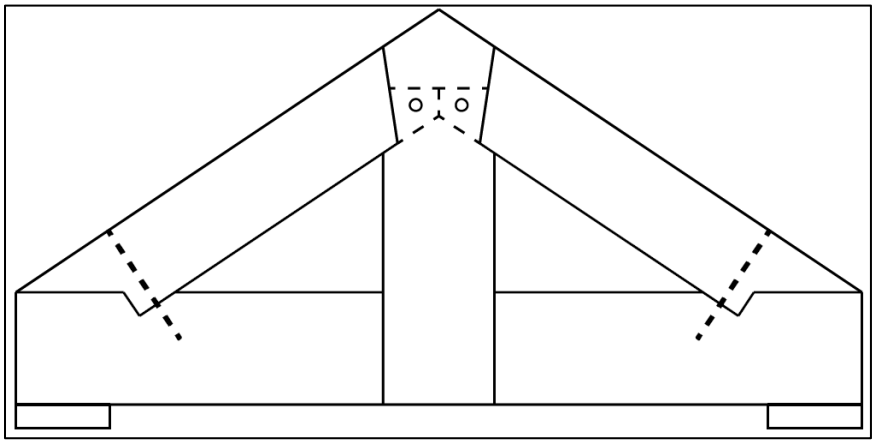

Figure 3-19: Truss A1 elevation view.

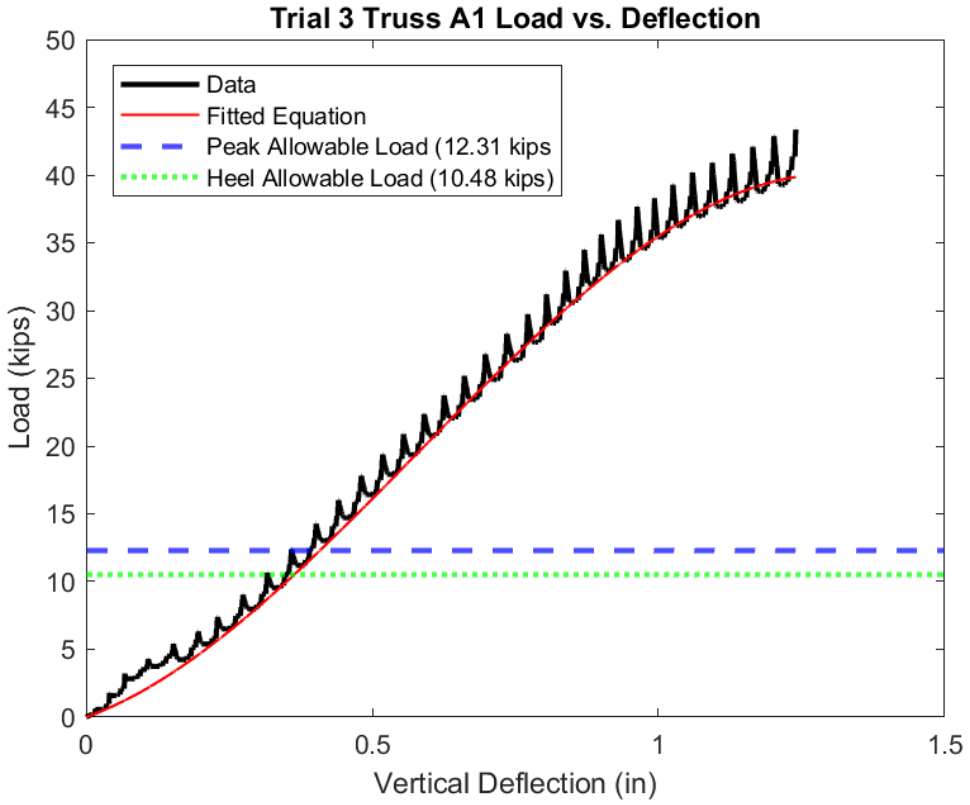

Figure 3-20: Load vs. Deflection plot for Trial 3 Truss A1.

Table 3-13: Responses from numerical data and measurements for Trial 3 Truss A1

Trial 3 Truss Style A1 - Tested 06/30/21		
Response	Value	Units
Test Day Moisture Content	10.23	%
Test Day Specific Gravity	0.486	-
Maximum Load	43,400	lb
Maximum Deflection	1.301	in
Load on Truss at Deflection Limit	13,200	lb
Total Absorbed Energy	25,600	lb*in
Maximum Stiffness	42,900	lb/in
Best Fit Equation: $f(x) = -27710 * x^3 + 48124 * x^2 + 15073 * x$		

Trial 3 was stopped due to an ultimate failure of Block Shear at Heel 2 but experienced structural bearing failures of both bottom chord shoulders (sides 1 and 2) prior to the ultimate failure. The first structural bearing failure occurred just over the allowable load limit (Table 3-14).

Table 3-14: Trial 3 Truss A1 failures.

Joint Type	Failure mode*	Sustained Load at Failure (lbs)	Allowable point load by code calculations (lbs)	Factor of Safety
Heel Style 1, Side 1	**Bearing Failure of BC Shoulder**	**17,900**	**10,480**	**1.71**
Heel Style 1, Side 2	***Block Shear Failure***	***43,400***	***10,480***	***4.14***
	Bearing Failure of BC Shoulder	**11,600**	**10,480**	**1.10**
	Crack Formation (at reentrant corner of TC)	34,200	10,480	3.26
Peak Style A, Side 1	Crack Formation (Along TC Shoulder)	35,500	12,310	2.88
Peak Style A, Side 2	Peg Yielding (Relative Deflection ≥ 1/8")	34,100	12,310	2.77

*Note: Bold and italicized text indicates ultimate failure. Bold text indicates structural failure. Plain text indicates serviceability failure.

3.4.5 Trial 4 Truss C3

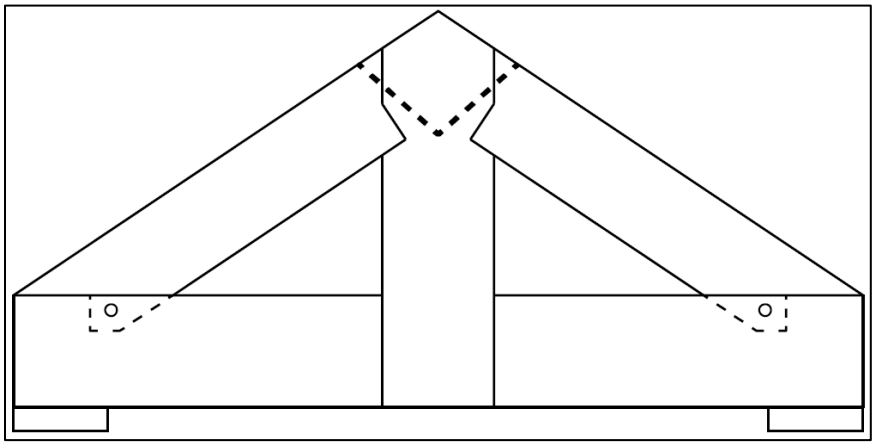

Figure 3-21: Truss C3 elevation view.

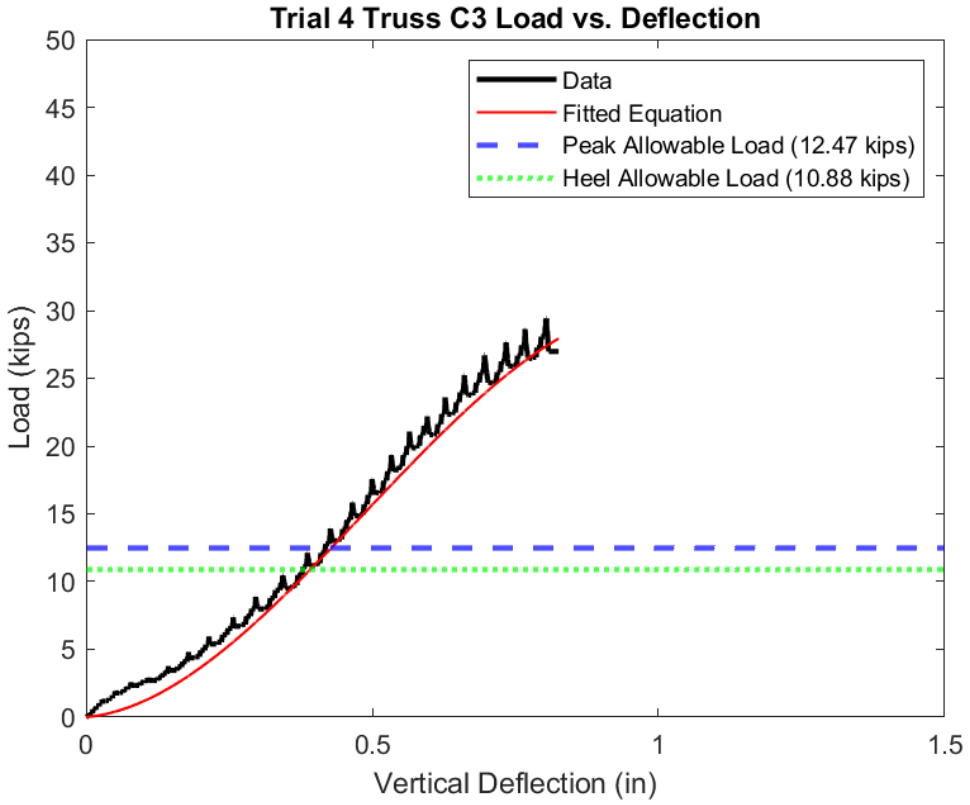

Figure 3-22: Load vs. Deflection plot for Trial 4 Truss C3.

Table 3-15: Responses from numerical data and measurements for Trial 4 Truss C3

Trial 4 Truss Style C3 - Tested 07/02/21		
Response	Value	Units
Test Day Moisture Content	6.76	%
Test Day Specific Gravity	0.487	-
Maximum Load	29,400	lb
Maximum Deflection	0.826	in
Load on Truss at Deflection Limit	11,160	lb
Total Absorbed Energy	10,300	lb*in
Maximum Stiffness	44,500	lb/in
Best Fit Equation: $f(x) = -57177 * x^3 + 83508 * x^2 + 3868 * x$		

Trial 4 was stopped due to an ultimate failure of Block Shear at Heel 2 but experienced structural bearing failures of both sides of the king post shoulder joints prior to the ultimate failure. The loading was balanced at the truss peak, with both bearing shoulder failures occurring simultaneously (Table 3-16).

Table 3-16: Trial 4 Truss C3 failures.

Joint Type	Failure mode*	Sustained Load at Failure (lbs)	Allowable point load by code calculations (lbs)	Factor of Safety
Heel Style 3, Side 1	Bearing Failure of BC Shoulder	22,900	10,880	2.10
Heel Style 3, Side 2	***Block Shear Failure***	***29,400***	***10,880***	***2.70***
	Bearing Failure of BC Shoulder	18,500	10,880	1.70
Peak Style C, Side 1	**Bearing Failure of KP Shoulder**	**24,600**	**12,470**	**1.97**
Peak Style C, Side 2	**Bearing Failure of KP Shoulder**	**24,600**	**12,470**	**1.97**
	Crack Formation (at reentrant corner of TC)	20,200	12,470	1.62

*Note: Bold and italicized text indicates ultimate failure. Bold text indicates structural failure. Plain text indicates serviceability failure.

3.4.6 Trial 5 Truss B2

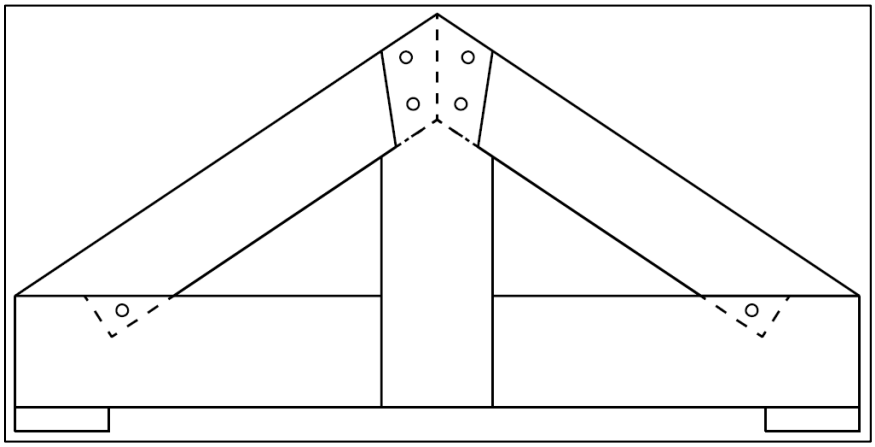

Figure 3-23: Truss B2 elevation view.

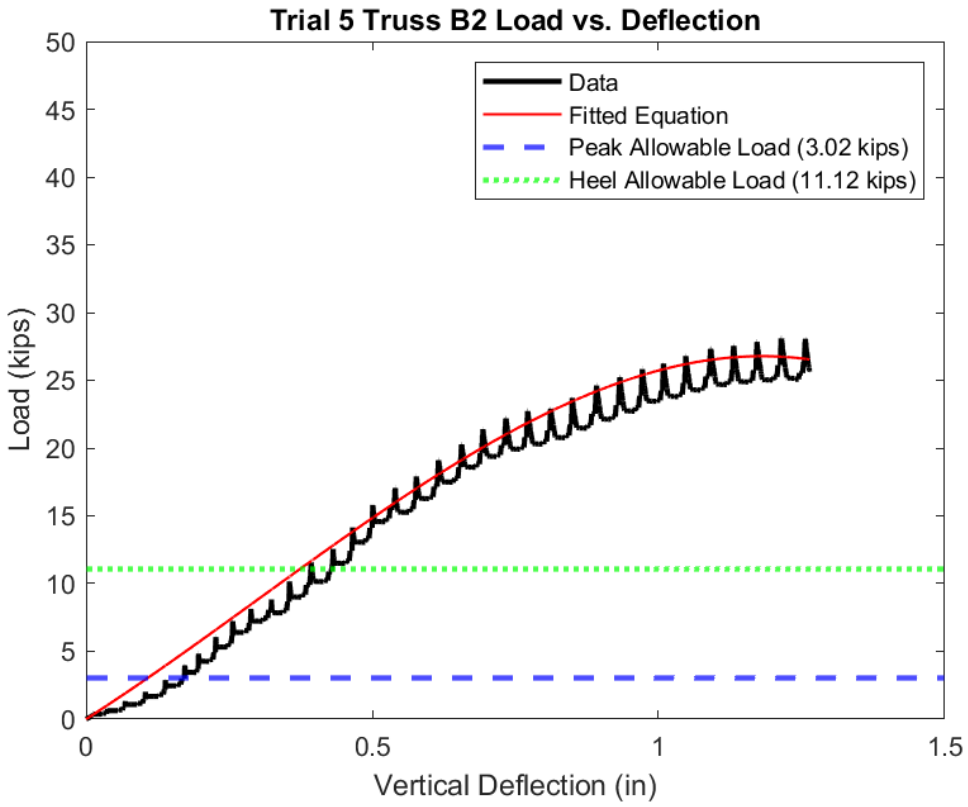

Figure 3-24: Load vs. Deflection plot for Trial 5 Truss B2.

Table 3-17: Responses from numerical data and measurements for Trial 5 Truss B2

Trial 5 Truss Style B2 - Tested 07/02/21		
Response	Value	Units
Test Day Moisture Content	8.56	%
Test Day Specific Gravity	0.497	-
Maximum Load	28,100	lb
Maximum Deflection	1.385	in
Load on Truss at Deflection Limit	10,160	lb
Total Absorbed Energy	21,100	lb*in
Maximum Stiffness	30,600	lb/in
Best Fit Equation: $f(x) = -13103 * x^3 + 11753 * x^2 + 27071 * x$		

Trial 5 was stopped due to the truss reaching the deflection limit of the testing rig; 1 ½". Prior to reaching the deflection limit, the truss experienced numerous structural and serviceability failures. Each structural failure occurred at a load above the allowable loads, whereas the serviceability failures for the heels occurred below the allowable loads (Table 3-18). The tenon failure experienced at heel side 2 was one of the two tenon-specific "buckling" failures (Trial 11 was the other).

Table 3-18: Trial 5 Truss B2 failures.

Joint Type	Failure mode*	Sustained Load at Failure (lbs)	Allowable Point Load (lbs)	Factor of Safety
Heel Style 2, Side 1	Peg Yielding (Relative Deflection ≥ 1/8")	7,960	11,120	0.72
	Tenon Failure (Relative Deflection ≥ 3/16")	**23,700**	**11,120**	**2.13**
	Bearing Failure of BC Shoulder	6,500	11,120	0.58
Heel Style 2, Side 2	Peg Yielding (Relative Deflection ≥ 1/8")	11,000	11,120	0.99
	Tenon Failure (Relative Deflection ≥ 3/16")	**20,000**	**11,120**	**1.80**
	Bearing Failure of BC Shoulder	8,100	11,120	0.73
Peak Style B, Side 1	**Peg Yielding (Relative Deflection ≥ 1/8")**	**11,800**	**3,020**	**3.91**
	Crack Formation (Along TC Shoulder)	23,600	3,020	7.79
	Bearing Failure of KP Shoulder	6,500	3,020	2.15
Peak Style B, Side 2	**Peg Yielding (Relative Deflection ≥ 1/8")**	**11,800**	**3,020**	**3.91**
	Crack Formation (Along TC Shoulder)	19,700	3,020	6.51

*Note: Bold and italicized text indicates ultimate failure. Bold text indicates structural failure. Plain text indicates serviceability failure.

3.4.7 Trial 6 Truss C1

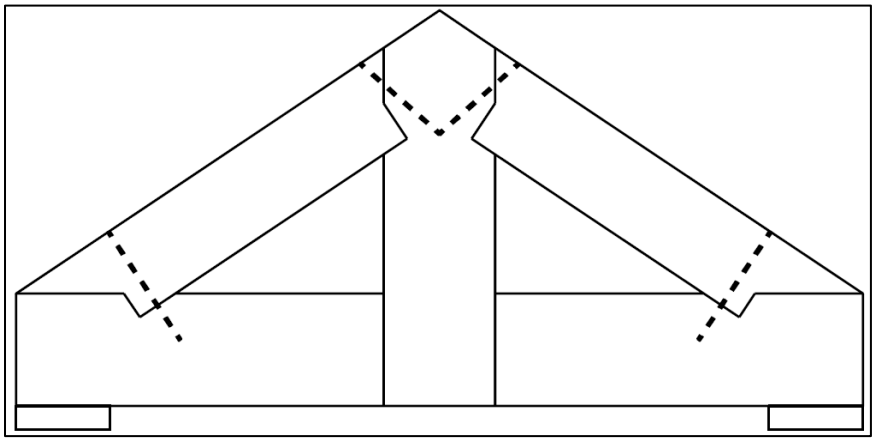

Figure 3-25: Truss C1 elevation view.

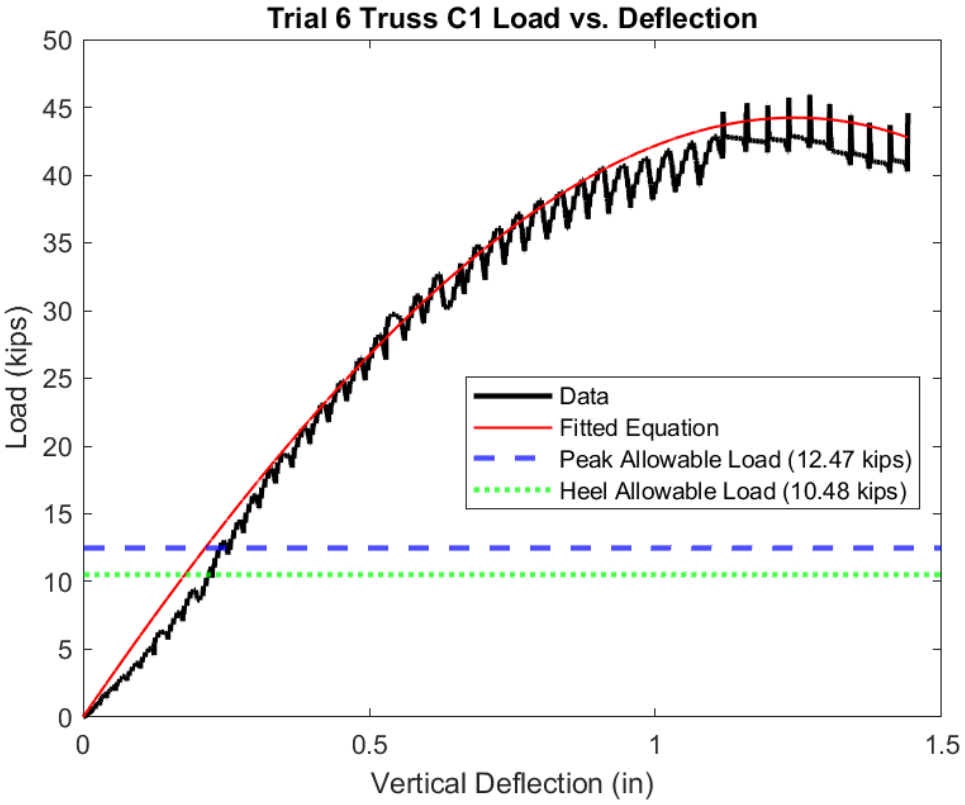

Figure 3-26: Load vs. Deflection plot for Trial 6 Truss C1.

Table 3-19: Responses from numerical data and measurements for Trial 6 Truss C1.

Trial 6 Truss Style C1 - Tested 07/02/21		
Response	Value	Units
Test Day Moisture Content	8.28	%
Test Day Specific Gravity	0.498	-
Maximum Load	42,800	lb
Maximum Deflection	1.475	in
Load on Truss at Deflection Limit	20,800	lb
Total Absorbed Energy	29,000	lb*in
Maximum Stiffness	71,800	lb/in
Best Fit Equation: $f(x) = -6042 * x^3 - 13497 * x^2 + 61710 * x$		

Trial 6 was stopped due to the truss reaching the deflection limit of the testing rig; 1 ½". Prior to reaching the deflection limit, the truss experienced structural bearing failures at both Heel 1 (bottom chord shoulder) and Peak side 2 (king post shoulder). The bearing failure of peak side 2 occurred at a load below the allowable load, which was only one of two structural failures recorded that occurred below the allowable load (Table 3-20).

There was a unique situation regarding crack formation and check expansion failure for Trial 6 Truss C1. Crack formation and check expansion were considered serviceability failures for this thesis, as their presence were not at primary load paths, they were often minor, and they did not affect the truss' ability to sustain additional load (Section Crack Formation and Check Expansion). However, for Trial 6, the crack formation at the truss peak (side 1) and check expansion at the truss peak (side 2) cascaded throughout the top chords, resulting in splits greater than ½" across by the end of the test. These failures did not impact the truss' ability to sustain additional load, but in this instance the serviceability failures of crack formation and check expansion were much greater than the other trusses (Figure 3-27).

Table 3-20: Trial 6 Truss C1 failures.

Joint Type	Failure mode*	Sustained Load at Failure (lbs)	Allowable point load by code calculations (lbs)	Factor of Safety
Heel Style 1, Side 1	**Bearing Failure of BC Shoulder**	**12,400**	**10480**	**1.18**
	Crack Formation (at reentrant corner of TC)	2,000	10480	0.19
Heel Style 1, Side 2	Crack Formation (at reentrant corner of TC)	43,500	10480	4.15
	Check Expansion	38,900	10480	3.71
Peak Style C, Side 1	**Bearing Failure of KP Shoulder**	**2,200**	**12470**	**0.18**
	Crack Formation (at reentrant corner of TC)	21,900	12470	1.75
Peak Style C, Side 2	**Bearing Failure of KP Shoulder**	**8,700**	**12470**	**0.70**
	Check Expansion	26,600	12470	2.14

*Note: Bold and italicized text indicates ultimate failure. Bold text indicates structural failure. Plain text indicates serviceability failure.

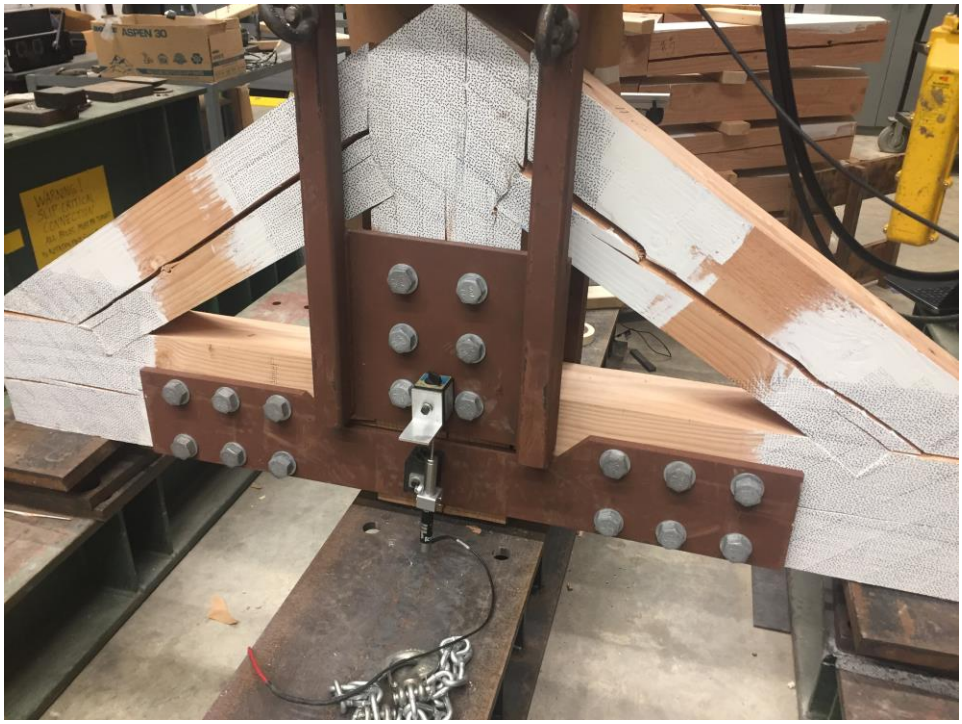

Figure 3-27: Full-length splits of both top chords of Trial 6 Truss C1.

3.4.8 Trial 7 Truss A1

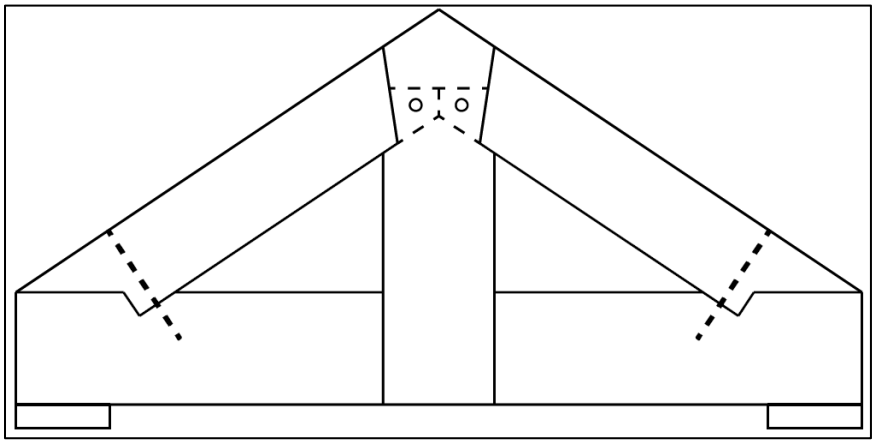

Figure 3-28: Truss A1 elevation view.

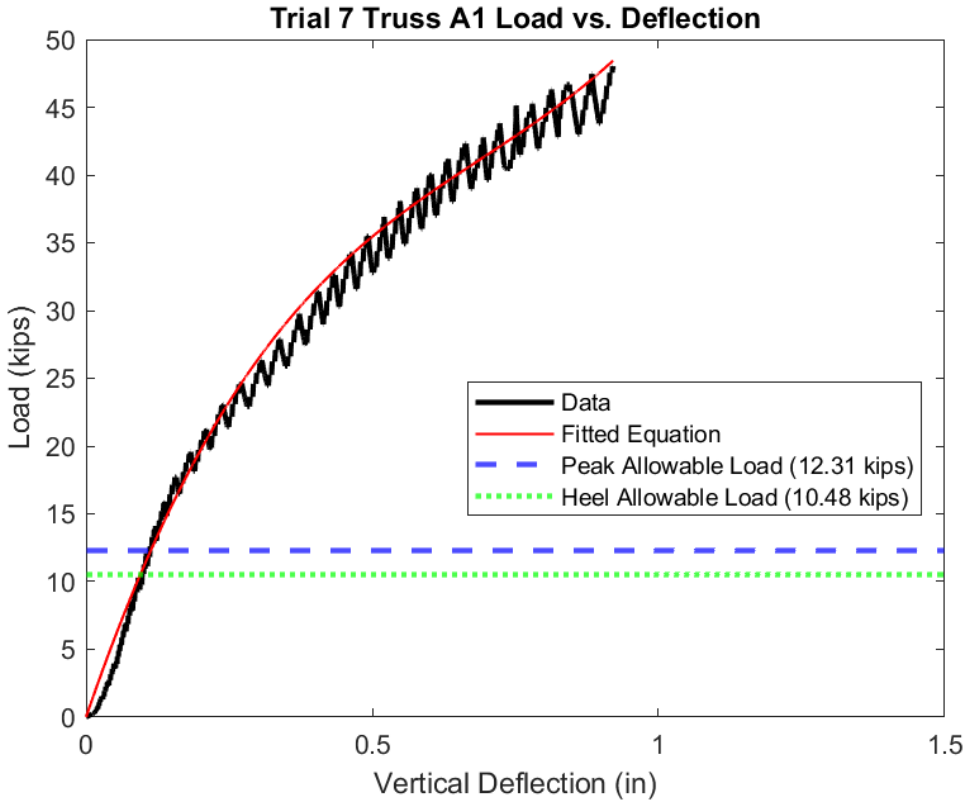

Figure 3-29: Load vs. Deflection plot for Trial 7 Truss A1.

Table 3-21: Responses from numerical data and measurements for Trial 7 Truss A1.

Trial 7 Truss Style A1 - Tested 07/03/21		
Response	Value	Units
Test Day Moisture Content	8.77	%
Test Day Specific Gravity	0.491	-
Maximum Load	48,000	lb
Maximum Deflection	0.921	in
Load on Truss at Deflection Limit	30,500	lb
Total Absorbed Energy	28,200	lb*in
Maximum Stiffness	123,500	lb/in
Best Fit Equation: $f(x) = 67156 * x^3 - 138870 * x^2 + 123544 * x$		

Trial 7 was stopped due to an ultimate failure of Block Shear at Heel 2 but experienced structural bearing failures of the bottom chord at Heel 1 and Heel 2, and a structural tenon failure at the truss peak at side 2 (Table 3-22).

Table 3-22: Trial 7 Truss A1 failures.

Joint Type	Failure mode*	Sustained Load at Failure (lbs)	Allowable point load by code calculations (lbs)	Factor of Safety
Heel Style 1, Side 1	**Bearing Failure of BC Shoulder**	**27,900**	**10,480**	**2.66**
	Crack Formation (at reentrant corner of TC)	41,400	10,480	3.95
Heel Style 1, Side 2	***Block Shear Failure***	***48,000***	***10,480***	***4.58***
	Bearing Failure of BC Shoulder	**20,300**	**10,480**	**1.93**
	Crack Formation (at reentrant corner of TC)	34,100	10,480	3.25
Peak Style A, Side 1	Peg Yielding (Relative Deflection ≥ 1/8")	41,200	12,310	3.35
Peak Style A, Side 2	Peg Yielding (Relative Deflection ≥ 1/8")	24,200	12,310	1.97
	Tenon Failure (Relative Deflection ≥ 3/16")	**38,800**	**12,310**	**3.15**
	Bearing Failure of KP Shoulder	27,900	12,310	0.79

*Note: Bold and italicized text indicates ultimate failure. Bold text indicates structural failure. Plain text indicates serviceability failure.

3.4.9 Trial 8 Truss C2

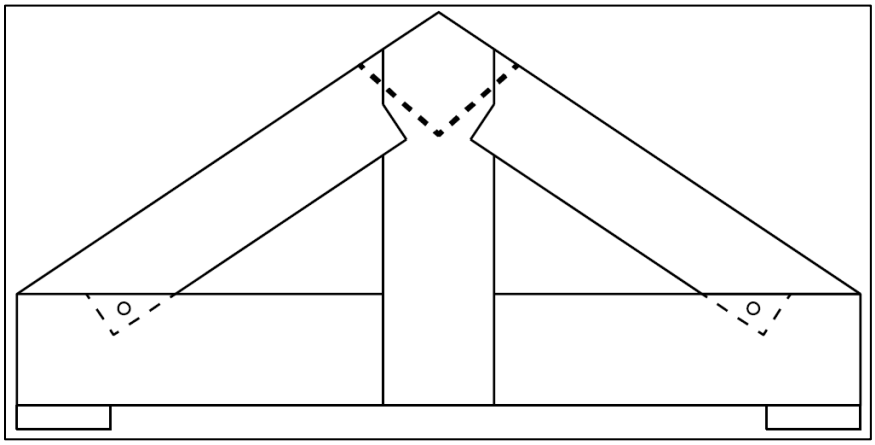

Figure 3-30: Truss C2 elevation view.

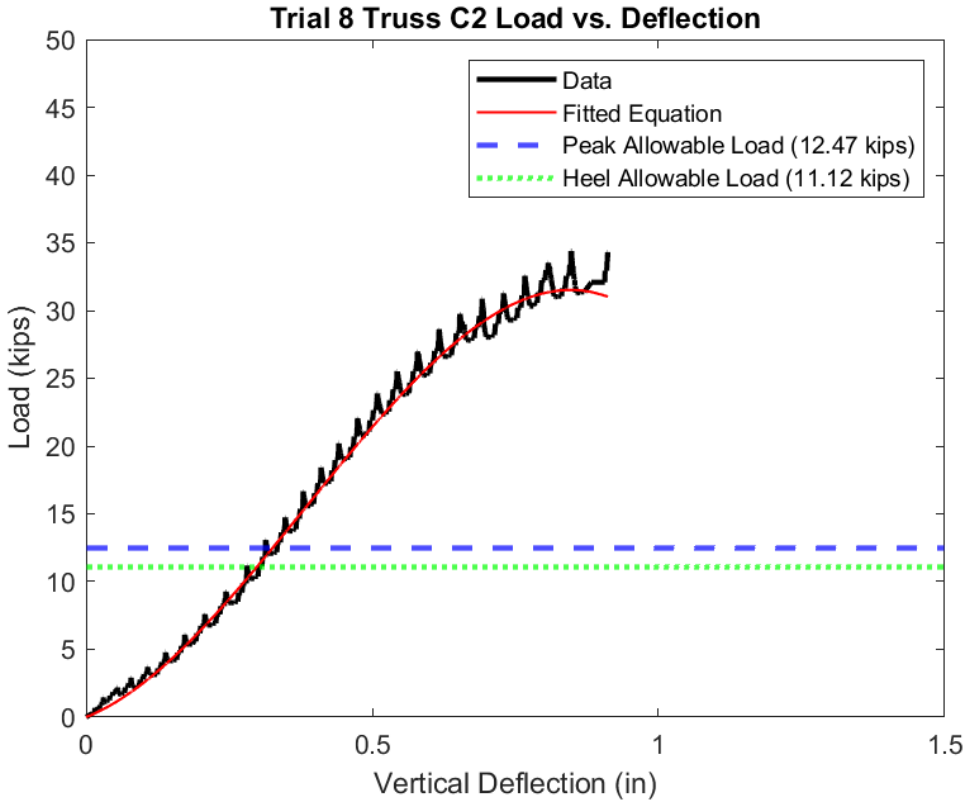

Figure 3-31: Load vs. Deflection plot for Trial 8 truss C2.

Table 3-23: Responses from numerical data and measurements for Trial 8 Truss C2

Trial 8 Truss Style C2 - Tested 07/07/21		
Response	**Value**	**Units**
Test Day Moisture Content	9.50	%
Test Day Specific Gravity	0.490	-
Maximum Load	34,400	lb
Maximum Deflection	0.916	in
Load on Truss at Deflection Limit	16,530	lb
Total Absorbed Energy	16,380	lb*in
Maximum Stiffness	52,100	lb/in
Best Fit Equation: $f(x) = -80500 * x^3 + 92324 * x^2 + 16764 * x$		

Trial 8 was stopped due to an ultimate failure of Block Shear at Heel 2 but experienced numerous serviceability failures and structural bearing failures at every joint: Heel 1, Heel 2, Peak Side 1, and Peak Side 2 (Table 3-24).

Table 3-24: Trial 8 Truss C2 failures.

Joint Type	Failure mode*	Sustained Load at Failure (lbs)	Allowable point load by code calculations (lbs)	Factor of Safety
Heel Style 2, Side 1	**Bearing Failure of BC Shoulder**	**12,200**	**11,120**	**1.10**
Heel Style 2, Side 2	***Block Shear Failure***	***34,400***	***11,120***	***3.09***
	Peg Yielding (Relative Deflection ≥ 1/8")	32,200	11,120	2.90
	Bearing Failure of BC Shoulder	**29,500**	**11,120**	**2.65**
Peak Style C, Side 1	**Bearing Failure of KP Shoulder**	**14,200**	**12,470**	**1.14**
	Check Expansion	28,500	12,470	2.28
Peak Style C, Side 2	**Bearing Failure of KP Shoulder**	**4,220**	**12,470**	**0.34**
	Check Expansion	22,700	12,470	1.82

*Note: Bold and italicized text indicates ultimate failure. Bold text indicates structural failure. Plain text indicates serviceability failure.

3.4.10 Trial 9 Truss B1

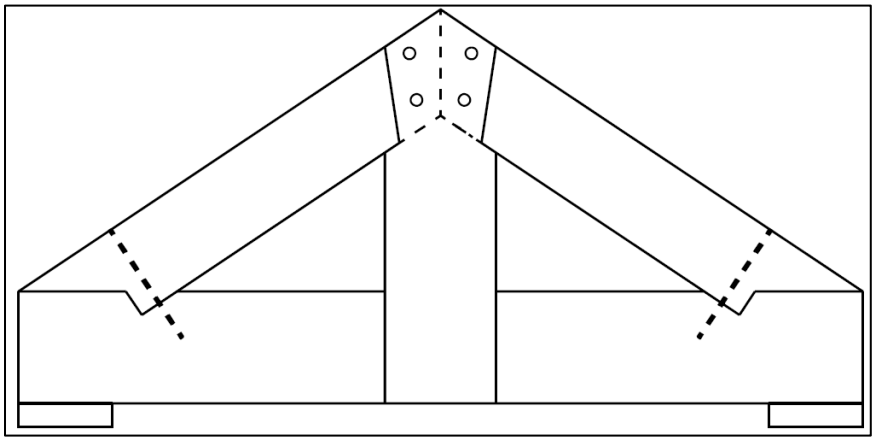

Figure 3-32: Truss B1 elevation view.

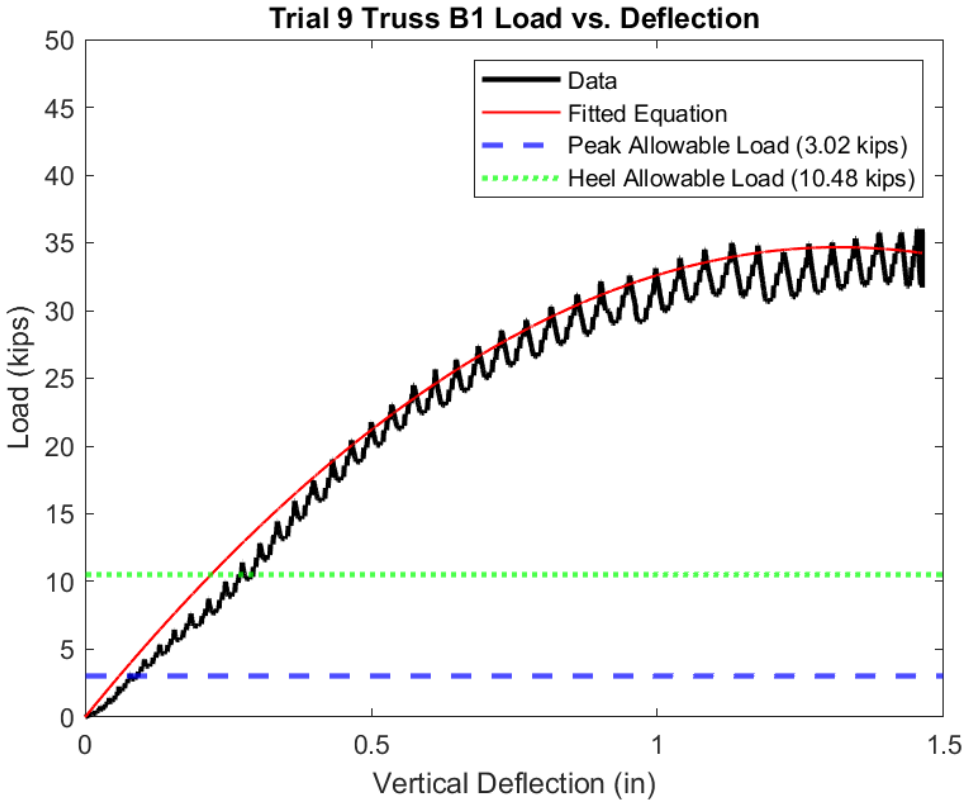

Figure 3-33: Load vs. Deflection plot for Trial 9 Truss B1.

Table 3-25: Responses from numerical data and measurements for Trial 9 Truss B1.

Trial 9 Truss Style B1 - Tested 07/07/21		
Response	Value	Units
Test Day Moisture Content	7.28	%
Test Day Specific Gravity	0.522	-
Maximum Load	36,000	lb
Maximum Deflection	1.463	in
Load on Truss at Deflection Limit	17,270	lb
Total Absorbed Energy	35,400	lb*in
Maximum Stiffness	51,900	lb/in
Best Fit Equation: $f(x) = -397 * x^3 - 18920 * x^2 + 51933 * x$		

Trial 9 was stopped due to the truss reaching the deflection limit of the testing rig; 1 ½". Prior to reaching the deflection limit, the truss experienced structural failures at every joint; bearing failures at both heel joints, and structural peg yielding failures at both sides of the peak joint (Table 3-26).

Table 3-26: Trial 9 Truss B1 failures.

Joint Type	Failure mode*	Sustained Load at Failure (lbs)	Allowable Point Load (lbs)	Factor of Safety
Heel Style 1, Side 1	**Bearing Failure of BC Shoulder**	**15,340**	**10,480**	**1.46**
Heel Style 1, Side 2	**Bearing Failure of BC Shoulder**	**11,750**	**10,480**	**1.12**
Peak Style B, Side 1	**Peg Yielding (Relative Deflection ≥ 1/8")**	**16,466**	**3,020**	**5.45**
Peak Style B, Side 2	**Peg Yielding (Relative Deflection ≥ 1/8")**	**11,750**	**3,020**	**3.89**
	Crack Formation (Along TC Shoulder)	28,200	3,020	9.34

*Note: Bold and italicized text indicates ultimate failure. Bold text indicates structural failure. Plain text indicates serviceability failure.

3.4.11 Trial 10 Truss A3

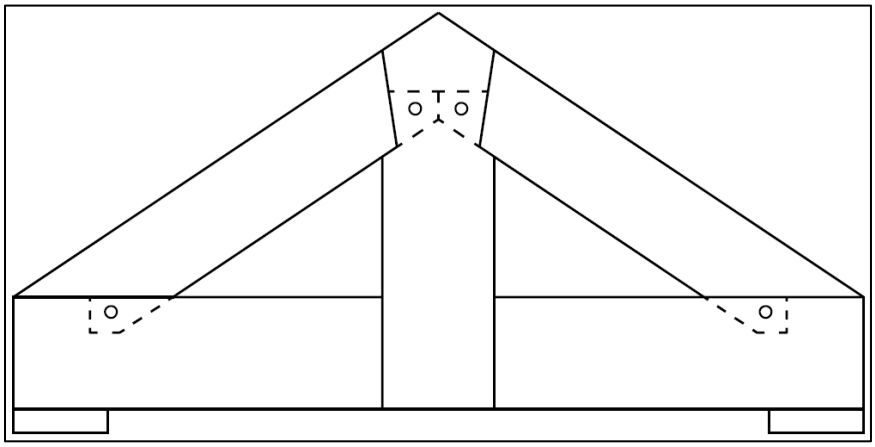

Figure 3-34: Truss A3 elevation view.

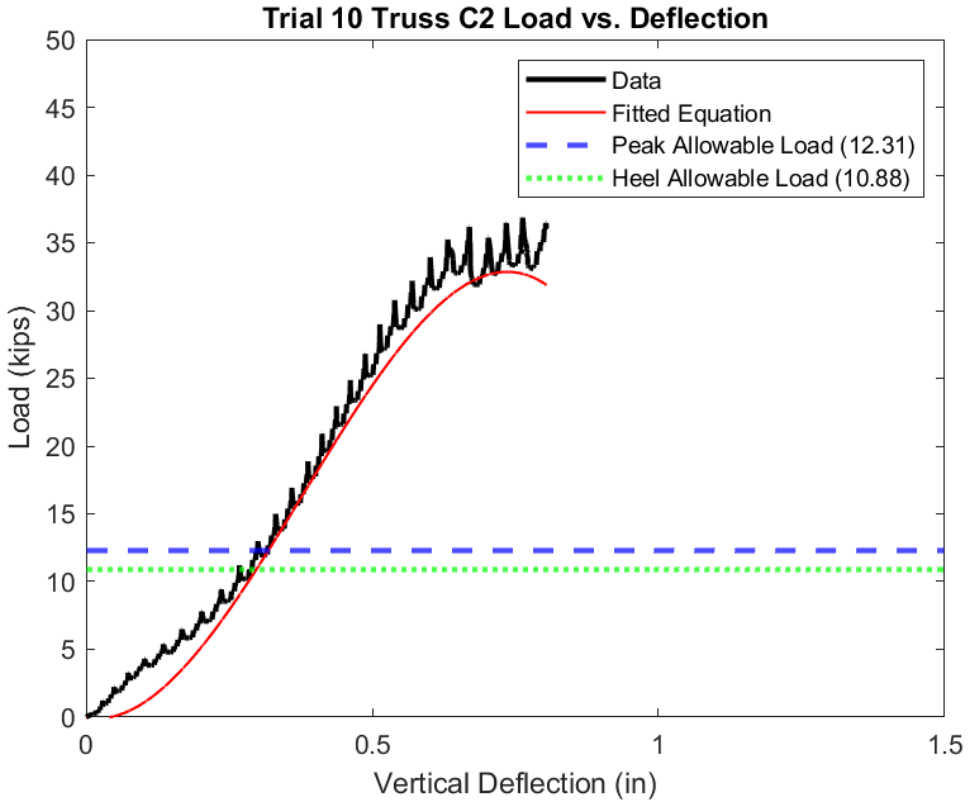

Figure 3-35: Load vs. Deflection plot for Trial 10 Truss C2.

Table 3-27: Responses from numerical data and measurements for Trial 10 Truss A3.

Trial 10 Truss Style A3 - Tested 07/07/21		
Response	Value	Units
Test Day Moisture Content	7.94	%
Test Day Specific Gravity	0.505	-
Maximum Load	36,900	lb
Maximum Deflection	0.941	in
Load on Truss at Deflection Limit	17,770	lb
Total Absorbed Energy	19,440	lb*in
Maximum Stiffness	69,100	lb/in
Best Fit Equation: $f(x) = -180003 * x^3 + 204282 * x^2 - 8212 * x$		

Trial 10 was stopped due to an ultimate failure of Block Shear at Heel 1 but experienced numerous serviceability failures and a structural tenon/mortise failure at the same location prior to the ultimate failure (Table 3-28).

Table 3-28: Trial 10 Truss A3 failures.

Joint Type	Failure mode*	Sustained Load at Failure (lbs)	Allowable point load by code calculations (lbs)	Factor of Safety
Heel Style 3, Side 1	***Block Shear Failure***	***36,900***	***10,880***	***3.39***
	Peg Yielding (Relative Deflection ≥ 1/8")	30,300	10,880	2.78
	Tenon Failure (Relative Deflection ≥ 3/16")	**33,400**	**10,880**	**3.07**
	Bearing Failure of BC Shoulder	16,380	10,880	1.51
Heel Style 3, Side 2	Bearing Failure of BC Shoulder	26,100	10,880	2.40
Peak Style A, Side 1	Peg Yielding (Relative Deflection ≥ 1/8")	25,600	12,310	2.08
	Bearing Failure of KP Shoulder	10,700	12,310	0.87
Peak Style A, Side 2	Peg Yielding (Relative Deflection ≥ 1/8")	35,600	12,310	2.89
	Crack Formation (Along TC Shoulder)	32,900	12,310	2.68
	Bearing Failure of KP Shoulder	25,600	12,310	2.08

*Note: Bold and italicized text indicates ultimate failure. Bold text indicates structural failure. Plain text indicates serviceability failure.

3.4.12 Trial 11 Truss A2

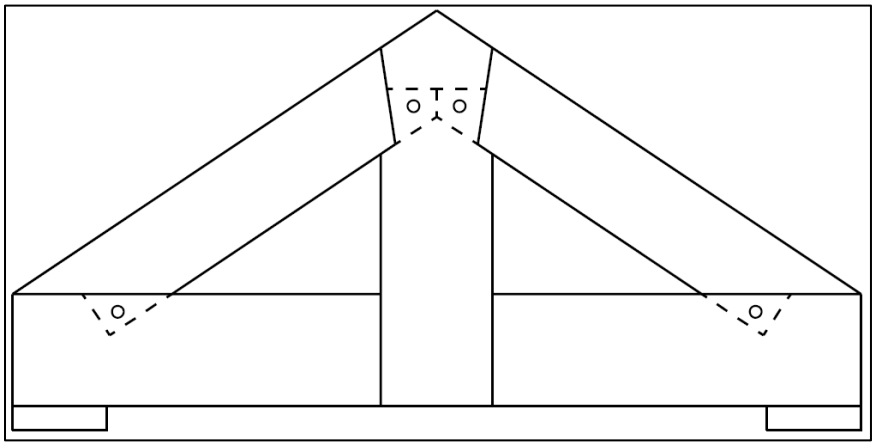

Figure 3-36: Truss A2 elevation view.

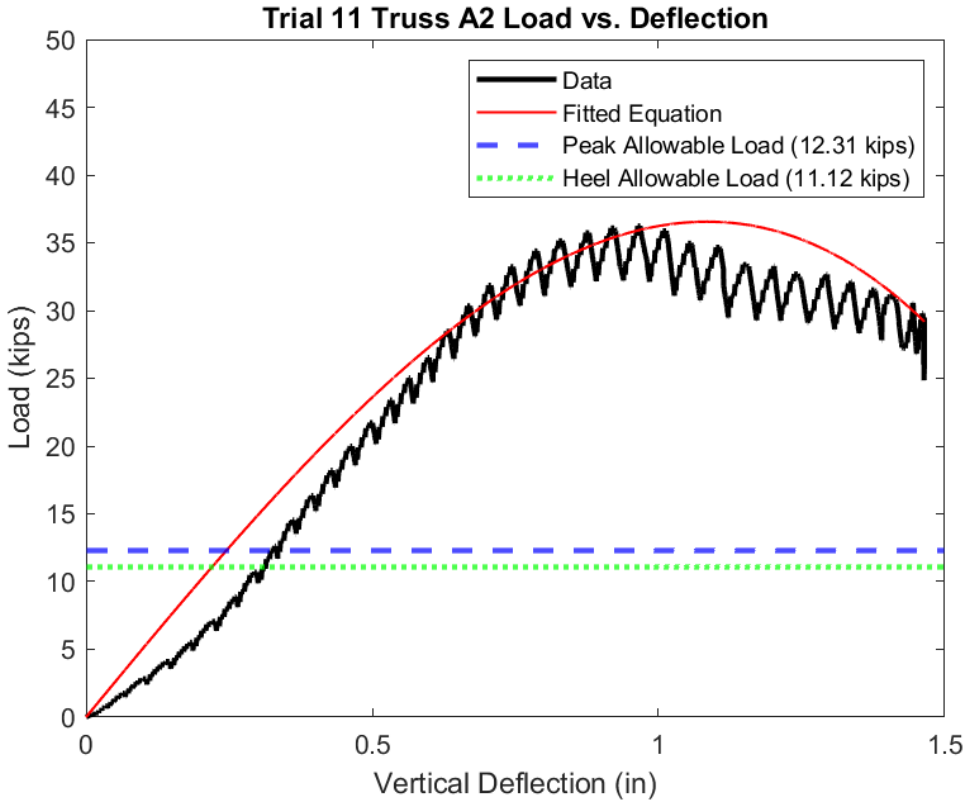

Figure 3-37: Load vs. Deflection plot for Trial 11 Truss A2.

Table 3-29: Responses from numerical data and measurements for Trial 11 Truss A2.

Trial 11 Truss Style A2 - Tested 07/08/21		
Response	Value	Units
Test Day Moisture Content	6.77	%
Test Day Specific Gravity	0.535	-
Maximum Load	36,200	lb
Maximum Deflection	1.465	in
Load on Truss at Deflection Limit	15,620	lb
Total Absorbed Energy	37,800	lb*in
Maximum Stiffness	51,300	lb/in
Best Fit Equation: $f(x) = -13680 * x^3 - 1388 * x^2 + 51300 * x$		

Trial 11 was stopped due to the truss reaching the deflection limit of the testing rig; 1 ½". Prior to reaching the deflection limit, the truss experienced numerous serviceability failures and structural tenon failures at every joint (Table 3-30). The tenon failure experienced by Trial 11 heel side 1 was one of two tenon-specific failures (Trial 5 was the other).

Table 3-30: Trial 11 Truss A2 failures.

Joint Type	Failure mode*	Sustained Load at Failure (lbs)	Allowable point load by code calculations (lbs)	Factor of Safety
Heel Style 2, Side 1	Peg Yielding (Relative Deflection ≥ 1/8")	33,200	11,120	2.98
	Tenon Failure (Relative Deflection ≥ 3/16")	**33,800**	**11,120**	**3.04**
Heel Style 2, Side 2	Peg Yielding (Relative Deflection ≥ 1/8")	34,500	11,120	**3.10**
	Tenon Failure (Relative Deflection ≥ 3/16")	**31,300**	**11,120**	**2.82**
	Bearing Failure of BC Shoulder	22,400	11,120	2.01
Peak Style A, Side 1	Peg Yielding (Relative Deflection ≥ 1/8")	32,300	12,310	2.62
	Tenon Failure (Relative Deflection ≥ 3/16")	**32,500**	**12,310**	**2.64**
	Bearing Failure of KP Shoulder	6,540	12,310	0.53
Peak Style A, Side 2	Peg Yielding (Relative Deflection ≥ 1/8")	32,300	12,310	2.62
	Tenon Failure (Relative Deflection ≥ 3/16")	**31,500**	**12,310**	**2.56**
	Bearing Failure of KP Shoulder	10,060	12,310	0.82

*Note: Bold and italicized text indicates ultimate failure. Bold text indicates structural failure. Plain text indicates serviceability failure.

3.4.13 Trial 12 Truss B2

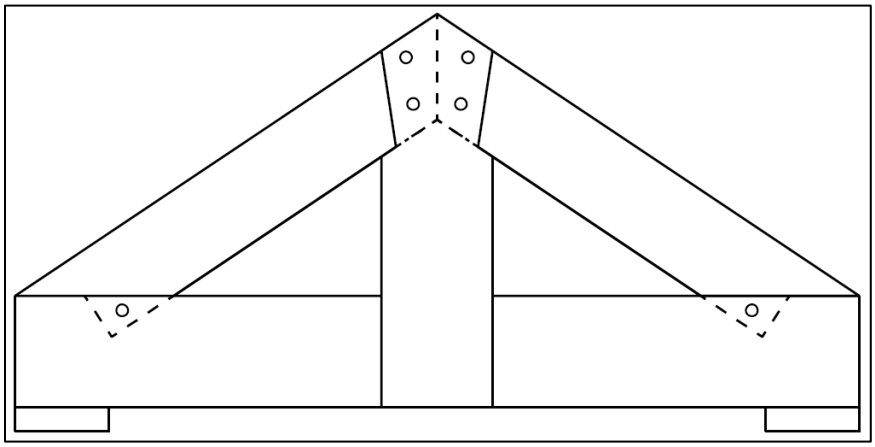

Figure 3-38: Truss B2 elevation view.

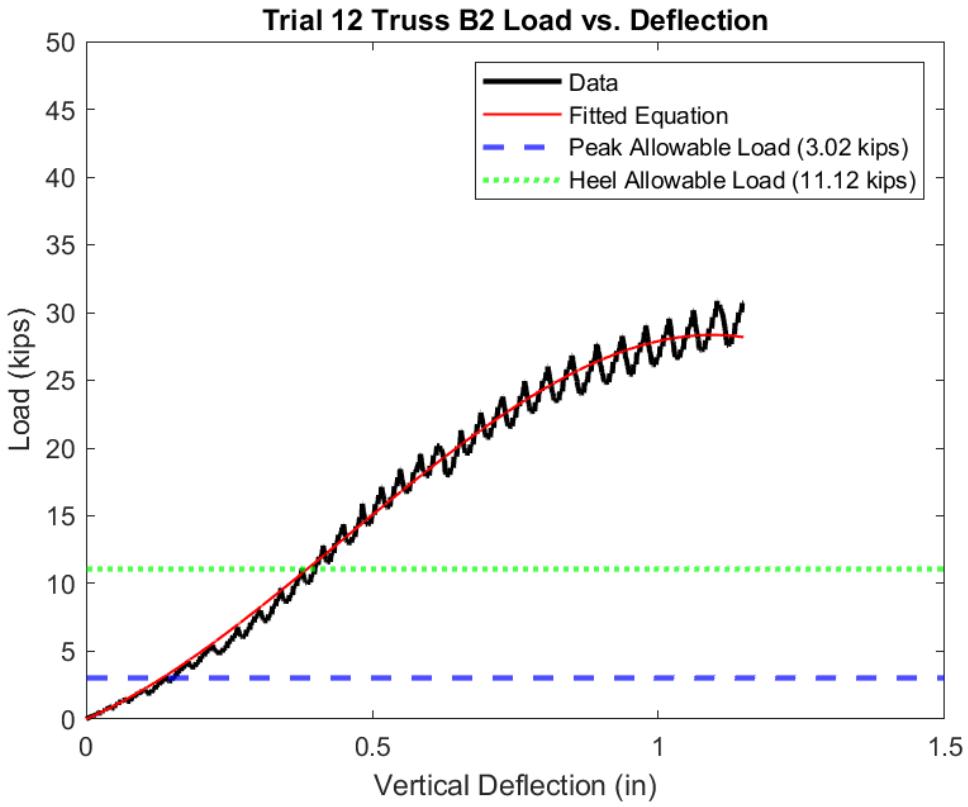

Figure 3-39: Load vs. Deflection plot for Trial 12 Truss B2.

Table 3-31: Responses from numerical data and measurements for Trial 12 truss B2.

Trial 12 Truss Style B2 - Tested 07/08/21		
Response	Value	Units
Test Day Moisture Content	7.51	%
Test Day Specific Gravity	0.503	-
Maximum Load	30,900	lb
Maximum Deflection	1.164	in
Load on Truss at Deflection Limit	10,690	lb
Total Absorbed Energy	18,880	lb*in
Maximum Stiffness	35,100	lb/in
Best Fit Equation: $f(x) = -28000 * x^3 + 37563 * x^2 + 18329 * x$		

Trial 12 was stopped due to an ultimate failure of Block Shear at Heel 2 but experienced numerous serviceability failures and structural peg yielding failures at both sides of the truss peak prior to the ultimate failure (Table 3-32).

Table 3-32: Trial 12 Truss B2 failures.

Joint Type	Failure mode*	Sustained Load at Failure (lbs)	Allowable Point Loads	Factor of Safety
Heel Style 2, Side 1	Bearing Failure of BC Shoulder	15,980	11,120	1.44
Heel Style 2, Side 2	***Block Shear Failure***	***30,900***	***11,120***	***2.78***
	Bearing Failure of BC Shoulder	25,000	11,120	2.25
Peak Style B, Side 1	**Peg Yielding (Relative Deflection ≥ 1/8")**	**19,060**	**3,020**	**6.30**
	Bearing Failure of KP Shoulder	10,190	3,020	3.37
Peak Style B, Side 2	**Peg Yielding (Relative Deflection ≥ 1/8")**	**23,900**	**3,020**	**7.90**
	Crack Formation (Along TC Shoulder)	23,300	3,020	7.70
	Bearing Failure of KP Shoulder	13,240	3,020	4.38

*Note: Bold and italicized text indicates ultimate failure. Bold text indicates structural failure. Plain text indicates serviceability failure.

4 Discussion

4.1 Trial Specimen Performance Comparisons

The thirteen truss trials all had maximum imposed loads in excess of their calculated design loads, with every trial exceeding their calculated design loads by at least a factor of 2.0. Every truss trial also had imposed loads in excess of their calculated design loads when the trusses reached the deflection limit (0.4”), but the margin between the allowable loads and measured loads were much smaller (e.g., Trial 4 Truss C3 had an allowable load of 10,883 lbs and had an imposed load at the deflection limit of 11,161 lbs, or a factor of safety of 1.03). This was an expected result, as the truss set up was designed to focus on loading the truss joints in compression only, which used a configuration that enabled the king post to slide past the bottom chord (Section 2.2.3). This truss design led to a less stiff truss than if the bottom chord could carry some of the vertical load at the king post in bending. Additionally, settling deflection is also a natural occurrence in all timber structures, as the traditional bearing joints cannot be cut perfectly and therefore have some displacement that must occur prior to the joints fully engaging. This initial deflection is generally impossible to calculate, as it is dependent on many parameters (e.g., slop in joints, number of joints, size of joints, size of structure). For this thesis, the trusses were fabricated with shortened member lengths to fit the trusses in the available testing apparatus at UNH (Section 2.2.3). Therefore, the initial deflection due to the timber joints was magnified relative to the span of the trusses, as it could be expected trusses with the same joint types and member sizes, but longer lengths could span 20 - 40 feet in practice and would therefore occur similar initial deflection, which would not figure so prominently in the overall truss performance with a larger span.

The maximum loads imposed on each trial are presented in Table 4-1, and are arranged from best performance to worst performance. It was observed that Peak Style A and Heel Style 1 were the best performing Peak and Heel Styles, respectively, with every truss type containing one or both of those styles resolving more than the average load, and the three A1 style trusses were within the top four performers. There were only two trials containing Peak Style B or C that performed above average, and both trusses contained Heel Style 1.

Table 4-1: Maximum load applied to trusses arranged from best to worst performance.

Test Number	Truss Style	Maximum Load (lbs)
7	A1	48,000
6	C1	45,900
3	A1	43,400
0	A1	43,100
10	A3	36,900
11	A2	36,200
9	B1	36,000
8	C2	34,400
12	B2	30,900
4	C3	29,400
5	B2	28,100
2	C3	27,200
1	B3	23,400
Average		35,600
St. Dev.		7,700

The maximum vertical deflection experienced by each truss was determined in one of two ways: either the truss experienced an ultimate failure (i.e., block shear) where it was unable to sustain additional load, in which case the maximum deflection experienced by the truss was the vertical deflection at the time of failure; or the truss reached the vertical deflection limit of the testing set up of approximately 1 ½" (Section 2.4.4). The maximum vertical deflections are presented in Table 4-2, and are arranged from best performance to worst performance. It was observed that the results for maximum deflection were approximately inverse to the maximum

load results. The two which had the smallest maximum load (Trial 1 and Trial 2) had the smallest maximum vertical deflection, and most trials containing Peak Style A and Heel Style 1 joinery methods had maximum vertical deflections that were larger than the average of all the trials (5 of 7).

Table 4-2: Maximum deflection results arranged from best to worst performance.

Test Number	Truss Style	Maximum Deflection (in)
1	B3	0.615
2	C3	0.773
4	C3	0.825
8	C2	0.916
7	A1	0.921
10	A3	0.940
0	A1	1.129
12	B2	1.163
3	A1	1.301
5	B2	1.384
9	B1	1.462
11	A2	1.464
6	C1	1.475
Average		1.106
Standard Deviation		0.294

This inverse relationship between the maximum load results and the maximum deflection results could be explained by either:

- The weaker trusses (i.e., Trial 1 (B3), Trial 2 (C3), Trial 4 (C3)) failed at a lower maximum load, which prevented the truss from experiencing a larger vertical deflection.
- The trusses that could support a higher maximum load (i.e., joinery styles A, C, 1) contained joinery styles that were able to distribute the loads through their joints (i.e., away from principal failure planes), which resulted in the higher maximum loads and higher vertical deflections.

Therefore, less emphasis was placed upon the maximum deflection as a measured response to compare the capacities of different trusses and joint types compared to the other four responses (maximum load applied, load applied to truss at deflection limit, total absorbed energy, and maximum stiffness).

The loads applied to each truss at the deflection limit are presented in Table 4-3, and are arranged from best performance to worst performance. All trusses sustained loads at the deflection limit above the truss allowable loads, but the lower values were just over the limit. The results were less conclusive relative to the maximum applied load, but most trusses containing joint styles 1 and A (heel and peak, respectively) performed at or near the top, and both B2 trusses performed the worst (Table 4-3).

Table 4-3: Loads on Truss at deflection limit.

Test Number	Truss Style	Load on Truss at Deflection limit (0.4") (lbs)
7	A1	30,500
0	A1	26,300
6	C1	20,800
10	A3	17,770
1	B3	17,620
9	B1	17,270
8	C2	16,530
11	A2	15,620
2	C3	15,120
3	A1	13,200
4	C3	11,160
12	B2	10,690
5	B2	10,160
Averages		17,140
St. Dev.		5,960

The performance of each trial regarding maximum stiffness of each truss very similar to the load on truss at the deflection limit results (Table 4-4), with the only changes being some of the trials changing places, with a maximum movement of one spot. It was observed that, like the

load on truss at the deflection limit, Truss Style A1 was the best performer and Truss Style B2 was the worst performer, and trusses in the top three positions contained Heel Style 1.

Table 4-4: Maximum stiffness arranged from best to worst performance.

Test Number	Truss Style	Maximum Stiffness (lb/in)
7	A1	123,500
0	A1	70,800
10	A3	69,100
1	B3	56,500
6	C1	55,000
8	C2	52,100
9	B1	51,900
11	A2	51,300
2	C3	50,000
4	C3	44,500
3	A1	42,900
12	B2	35,100
5	B2	30,600
Averages		56,400
St. Dev.		23,100

The total absorbed energy of each truss (the area under the load vs. deflection curve) had similar results to the maximum load applied to each truss but with less conclusive results (Table 4-5). The principal observations were that the trials that absorbed the most energy contained mostly Peak Style A (top 4/6) and Heel Style 1 (top 5/6), and the trials that absorbed the least energy contained mostly Heel Style 3 (bottom 3/3).

Table 4-5: The total absorbed energy arranged from best to worst performance.

Test Number	Truss Style	Total Absorbed Energy (lb*in)
11	A2	37,800
9	B1	35,400
0	A1	29,900
6	C1	29,700
7	A1	28,200
3	A1	25,600
5	B2	21,100
10	A3	19,440
12	B2	18,880
8	C2	16,380
4	C3	10,340
2	C3	10,220
1	B3	7,600
Averages		22,300
St. Dev.		9,700

4.1.1 Truss Style A1

Three truss style A1s were tested throughout the experiment to show the variability of timber as a natural material and traditional fabrication techniques. The three truss performances were all above average regarding maximum load, but only Trial 0 and Trial 7 were above average for load applied at deflection limit, total absorbed energy, and maximum stiffness, whereas Trial 3 was below average. These differences in performance are shown on the combined Load vs. Deflection plot (Figure 4-1). The Truss Style A1 load vs. deflection curves show similar maximum loads and maximum deflections but exemplify the differences of variability in timber as a natural material.

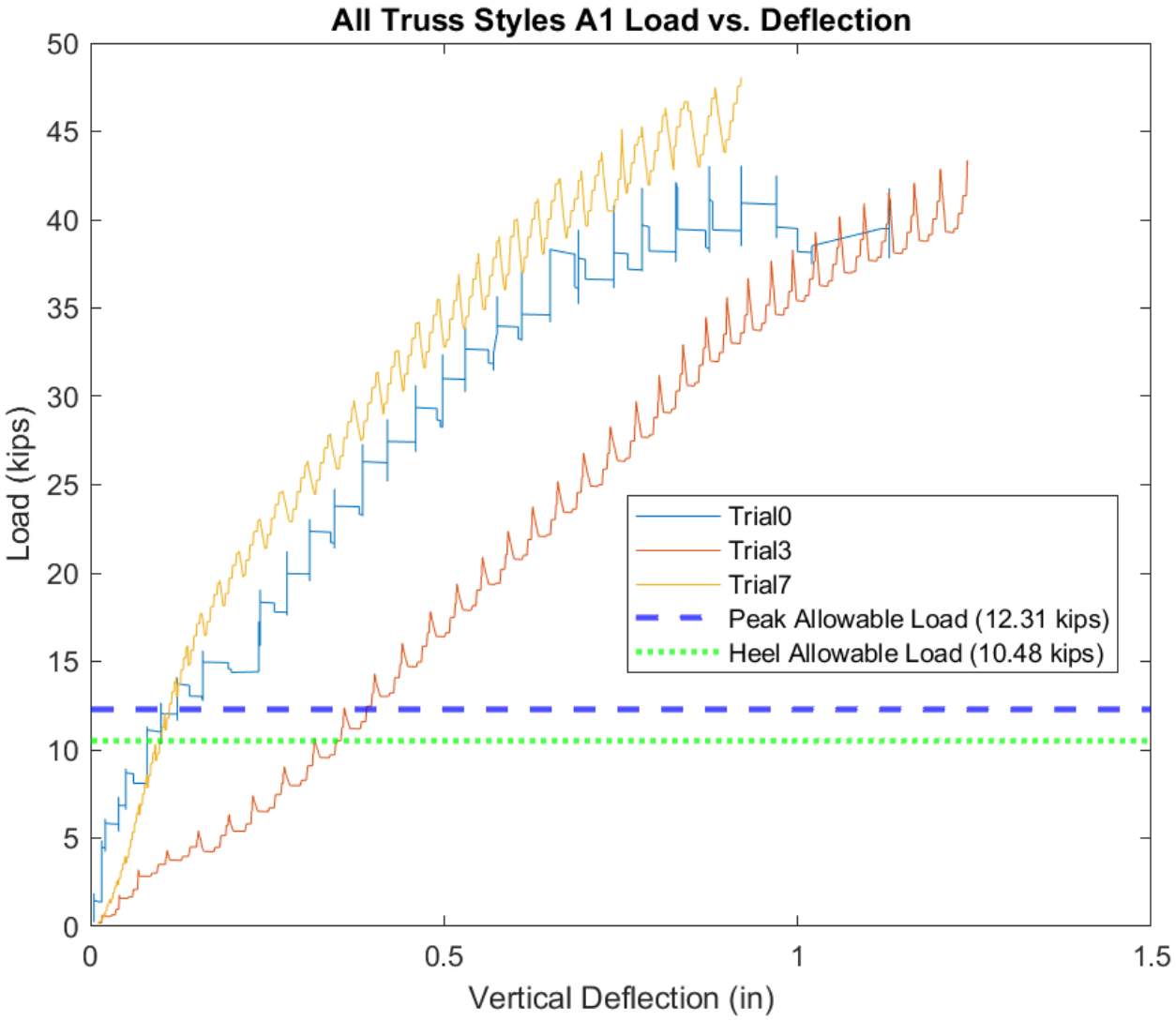

Figure 4-1: Truss style A1 combined Load vs. Deflection plot.

4.1.2 Truss Style B2

Two truss style B2s were tested throughout the experiment. Their performances were below average for every measured and calculated response. The B2 load vs. deflection curves were similar through the Heel and Peak allowable loads, and both failed around similar loads and deflections (Figure 4-2).

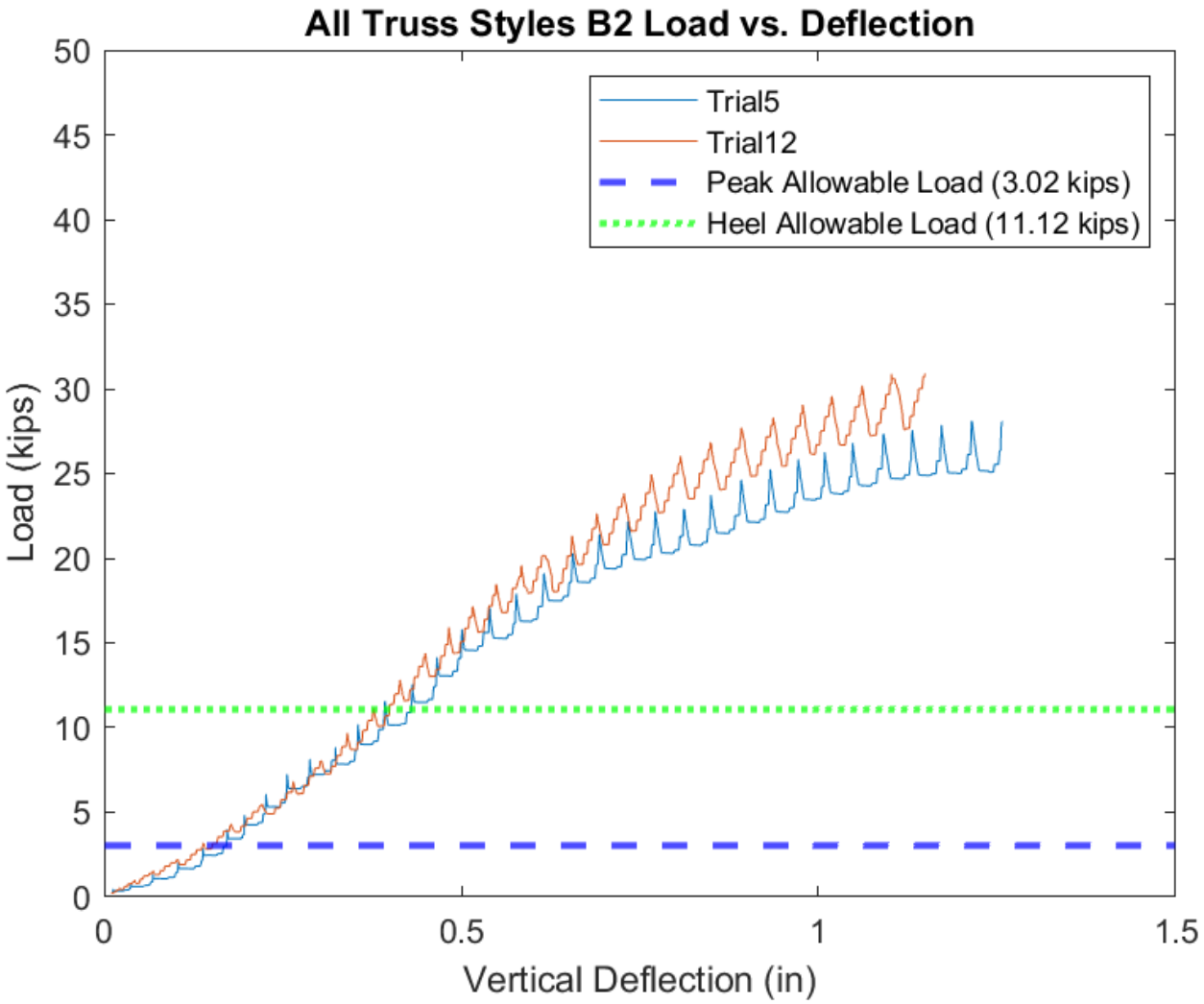

Figure 4-2: Truss style C3 combined Load vs. Deflection plot.

4.1.3 Truss Style C3

Two truss style C3s were tested throughout the experiment (Figure 4-3). Their performances were below average for every measured and calculated response. The C3 load vs. deflection curves were similar throughout the test, and both failed around similar loads and deflections.

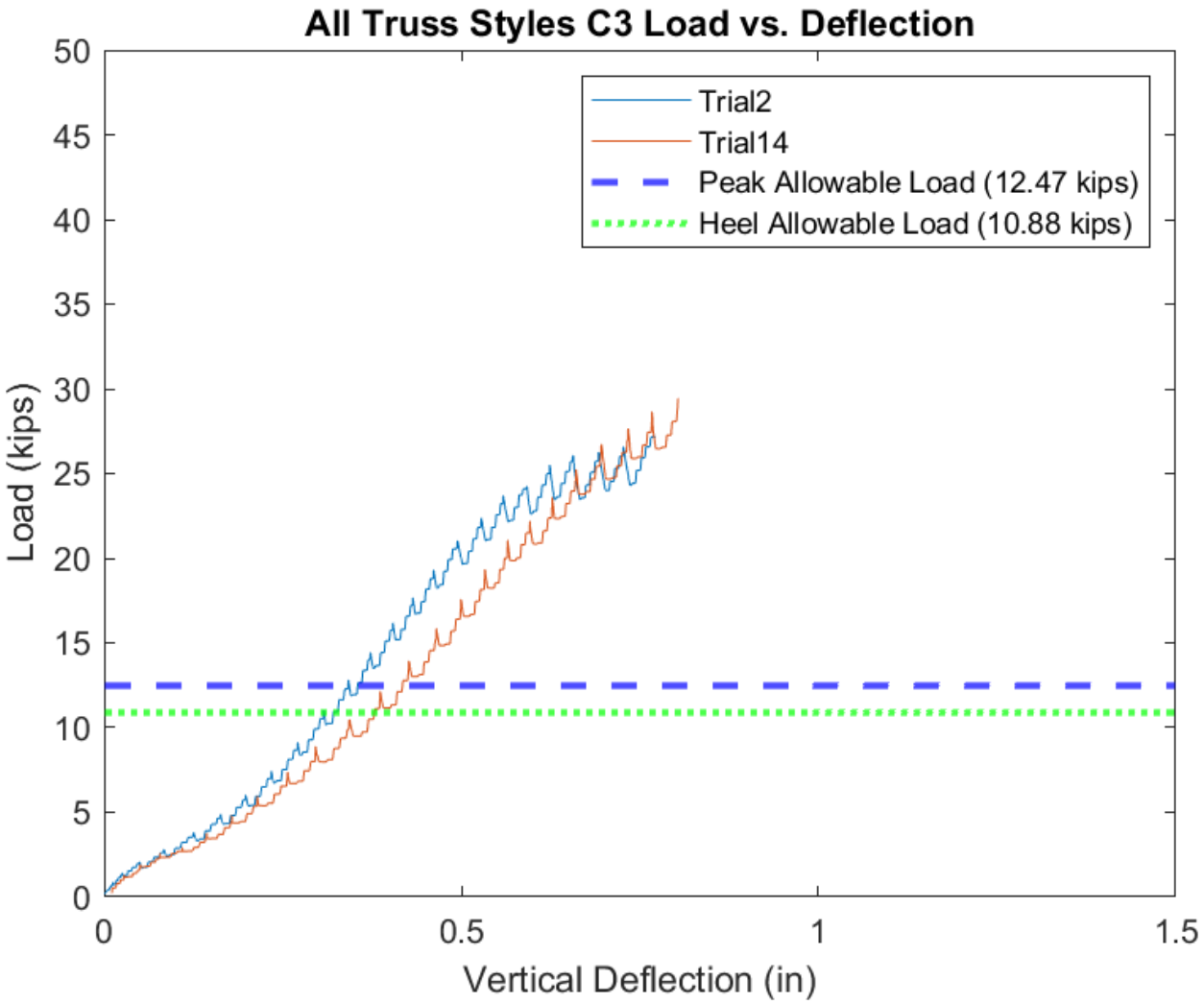

Figure 4-3: Truss style C3 combined Load vs. Deflection plot.

4.2 Joint Failures

The following sections discuss the joint failures, concurrent approximate loads, and corresponding factors of safety for each structural failure experienced by the specimens and the similarities and differences between the joint styles.

4.2.1 Joint Failure Observations

Structural joints are designed in practice with a minimum factor of safety of 1.0, meaning that all components of the joint are designed to resist the maximum anticipated structural loads (e.g., a combination of dead and snow loads). However, it is common to have factors of safety of 2.0 and greater, due to the uncertainty of the materials, the structure, and the actual loads experienced by the structure. It is additionally preferred, from an engineering standpoint, to have gradual failures occur prior to sudden failures if a joint is overloaded. The longer duration between initial signs of failure for gradual failures (e.g., for this Thesis: relative deflection of joints to observe peg yielding or mortise and tenon bearing failure and bearing strain observations using DIC) allow for time to vacate the structure and address the loading issues or failing joints. Conversely, a sudden, ultimate failure (e.g., for this Thesis: block shear) could cause a structural collapse or numerous other issues without adequate warning. To design this in practice, structural engineers can incorporate a larger factor of safety for sudden failures (e.g., block shear) relative to the factor of safety for gradual failures (e.g., peg yielding, bearing).

The results of this Thesis show that all structural failure modes (excluding shoulder bearing failure for Peak Style C and Heel Style 1) sustained loads at failure greater than the designed allowable load, which correlated to a factor of safety greater than 1.0. It was also observed for all joint types (excluding Heel Style 3) that gradual, ductile failures (e.g., shoulder bearing, peg yielding, mortise and tenon bearing) occurred, on average, at lower loads relative to ultimate, sudden failures (e.g., for this Thesis: block shear).

The equation for block shear was the only equation for calculating the design allowable loads that contained a direct factor of safety incorporated in the equation of 2.0 (Appendix C). The other three failure modes (peg yielding, shoulder bearing, mortise and tenon bearing) have inherent

factors of safety incorporated into their equations based off previous research and ASTM Standards (Schmidt and MacKay (1997); Schmidt and Daniels (1999); Miller and Schmidt (2004); Miller (2009); ASTM D143-21; ASTM D2555-17a), but no direct factor of safety is incorporated in the equations. It is the opinion of the author, based off the experimental specimens and observed failures by the observational methods stated in this Thesis, that the factors of safety used in practice are adequate for the four observed structural failure modes. The ultimate failure of block shear had factors of safety ranging from 2.15 (Heel Style 3) to 4.14 (Heel Style 1), which met the criteria of at least a factor of safety of 2.0 per the design equation and provided some additional safety factor for certain joint types. Peg yielding had an average factor of safety of 5.43 for Peak Style B, but due to the empirical definition used to define failure for this Thesis (Section 3.3.3.2), a definitive recommendation to increase or decrease the design capacity of a single peg cannot be determined. Mortise and tenon bearing failure had factors of safety ranging from 2.32 (Heel Style 2) to 2.90 (Heel Style 3), all of which were above 2.0 but only by 16% to 45%. Shoulder bearing was the only structural failure that experienced failures below the design allowable load (both Peak Style C and Heel Style 1), correlating to a factor of safety less than 1.0, but that is partially due to the definition of failure used for this Thesis (Section 3.3.3.1). However, the average factor of safety for both trials that experienced shoulder bearing was above 1.0.

4.2.2 Peak Style A

The allowable load calculations for Peak Style A resulted in predicted failure modes of top chord (TC) tenon bearing and block shear of the king post (KP). The allowable loads for both failures were similar in magnitude, but it was predicted that the TC tenon would fail in bearing prior to the KP block shear failure. Both failure loads were observed in the physical tests (Table 4-6).

Peak Style A joints were the most tested peak style joints but experienced the least number of structural failures and had the highest average sustained load at failure. Trial 0 experienced the only ultimate structural failure (block shear) out of the three Peak Styles. Two of five trials experienced no structural failures, which was only observed for the two Peak Style A joints and one Heel Style 1 joint. The data shows that it could be expected that the tenon bearing surface would fail prior to the joint failing in block shear.

Table 4-6: Compiled structural failures for Peak Style A joints.

Trial #	Peak Style A	Failure Method	Sustained Load at Failure (lbs)	Allowable Point Load (lbs)	Factor of Safety
Trial 0	Side 1	Block Shear Failure	43,000	12,620	3.41
Trial 3	No Structural Failures				
Trial 7	Side 2	Tenon Failure (Relative Deflection ≥ 3/16")	38,800	12,310	3.15
Trial 10	No Structural Failures				
Trial 11	Side 1	Tenon Failure (Relative Deflection ≥ 3/16")	32,500	12,310	2.64
Trial 11	Side 2	Tenon Failure (Relative Deflection ≥ 3/16")	31,500	12,310	2.56
Average ± Standard Deviation Sustained Load at Failure (Excluding Block Shear)			34,300 ± 3,930	12,310	2.78 ± 0.41
Minimum Block Shear Failure Load			43,000	12,620	3.41

4.2.3 Peak Style B

The allowable load calculations for Peak Style B resulted in predicted failure of peg yielding. The calculated allowable load for peg yielding was much less than other predicted failures for Peak Style B (e.g., block shear of pegs), so peg yielding was the only expected failure mode (Table 4-7).

Peak Style B joints did not experience an ultimate failure, but both sides of every joint experienced structural failure of peg yielding. The structural failures had the second lowest average

sustained load at failure out of any joint (second to Peak Style C), but the highest average factor of safety due to the relatively low allowable point load of the joint. Peak Style B was one of two joinery styles to have a 100% structural failure rate (Heel Style 3 was the other).

Table 4-7: Compiled structural failures for Peak Style B joints.

Trial #	Peak Style B	Failure Method	Sustained Load at Failure (lbs)	Allowable Point Load (lbs)	Factor of Safety
Trial 1	Side 1	Peg Yielding (Relative Deflection ≥ 1/8")	14,670	3,020	4.85
Trial 1	Side 2	Peg Yielding (Relative Deflection ≥ 1/8")	21,900	3,020	7.24
Trial 5	Side 1	Peg Yielding (Relative Deflection ≥ 1/8")	11,810	3,020	3.91
Trial 5	Side 2	Peg Yielding (Relative Deflection ≥ 1/8")	11,810	3,020	3.91
Trial 9	Side 1	Peg Yielding (Relative Deflection ≥ 1/8")	16,470	3,020	5.45
Trial 9	Side 2	Peg Yielding (Relative Deflection ≥ 1/8")	11,750	3,020	3.89
Trial 12	Side 1	Peg Yielding (Relative Deflection ≥ 1/8")	19,060	3,020	6.30
Trial 12	Side 2	Peg Yielding (Relative Deflection ≥ 1/8")	23,900	3,020	7.90
Average ± Standard Deviation Sustained Load at Failure (Excluding Block Shear)			16,400 ± 4,786	3,020	5.43 ± 1.58

4.2.4 Peak Style C

The allowable load calculations for Peak Style C resulted in predicted failure modes of king post (KP) shoulder bearing and block shear of the KP. Both failure loads were similar, but it was predicted that the KP shoulder would fail in bearing prior to the KP block shear failure. Only bearing failure of the KP shoulder was observed in the physical tests (Table 4-8).

Peak Style C joints experienced structural failures of KP shoulder bearing at all but one of the joint sides (Trial 2 Side 2 was the exception). Peak Style C had the lowest average sustained

load at failure and the second lowest factor of safety for structural failures (Heel Style 1 had the lowest). This is partly due to the definition of failure used (Section 3.3.2.1), where the joints partially failed at lower loads than expected.

Table 4-8: Compiled structural failures for Peak Style C joints.

Trial #	Peak Style C	Failure Method	Sustained Load at Failure (lbs)	Allowable Point Load (lbs)	Factor of Safety
Trial 2	Side 1	Bearing Failure of KP Shoulder	22,800	12,470	1.83
Trial 4	Side 1	Bearing Failure of KP Shoulder	24,600	12,470	1.97
Trial 4	Side 2	Bearing Failure of KP Shoulder	24,600	12,470	1.97
Trial 6	Side 1	Bearing Failure of KP Shoulder	2,210	12,470	0.18
Trial 6	Side 2	Bearing Failure of KP Shoulder	8,700	12,470	0.70
Trial 8	Side 1	Bearing Failure of KP Shoulder	14,170	12,470	1.14
Trial 8	Side 2	Bearing Failure of KP Shoulder	4,220	12,470	0.34
Average ± Standard Deviation Sustained Load at Failure Excluding Block Shear			14,460 ± 9,682	12,470	1.16 ± 0.78

4.2.5 Heel Style 1

The allowable load calculations for Heel Style 1 resulted in predicted failure modes of bottom chord (BC) shoulder bearing and block shear of the BC. The BC shoulder bearing failure mode was calculated to have approximately 45% more capacity compared to BC block shear failure mode. Both failure loads were observed in the physical tests (Table 4-9).

Heel Style 1 joints experienced two ultimate failures of block shear and structural failures of BC shoulder bearing at most of the joints. The average sustained load at failure of Heel Style 1 was the lowest experienced by the Heel Styles which resulted in the lowest factor of safety of any

joint style. This result was partly due to the definition of failure used (Section 3.3.2.1), where the joints partially failed in bearing at much lower loads than expected. The two ultimate block shear failures of Heel Style 1 were the only ultimate failures observed for either of the two birdsmouth shoulder joints (Peak Style C and Heel Style 1). Heel Style 1 had the highest minimum block shear failure load out of any of the joint styles. The data shows that it could be expected that the BC would fail in bearing failure of the shoulder prior to block shear, which is opposite of the expected result from the allowable load calculations but preferred from a structural engineering standpoint. Trial 0 did not experience any structural failures, but that is likely due to DIC being unable to be used for this trial, so bearing failures could not be observed using the strain data.

Table 4-9: Compiled structural failures for Heel Style 1 joints.

Trial #	Heel Style 1	Failure Method	Sustained Load at Failure (lbs)	Allowable Point Load (lbs)	Factor of Safety
Trial 0	No Structural Failures				
Trial 3	Side 1	Bearing Failure of BC Shoulder	17,890	15,090	1.19
Trial 3	Side 2	Block Shear Failure	43,400	10,483	4.14
Trial 3	Side 2	Bearing Failure of BC Shoulder	11,560	15,090	0.77
Trial 6	Side 1	Bearing Failure of BC Shoulder	12,350	15,090	0.82
Trial 7	Side 1	Bearing Failure of BC Shoulder	27,900	15,090	1.85
Trial 7	Side 2	Block Shear Failure	48,000	10,483	4.58
Trial 7	Side 2	Bearing Failure of BC Shoulder	20,300	15,090	1.34
Trial 9	Side 1	Bearing Failure of BC Shoulder	15,340	15,090	1.02
Trial 9	Side 2	Bearing Failure of BC Shoulder	11,750	15,090	0.78
Average ± Standard Deviation Sustained Load at Failure Excluding Block Shear			16,720 ± 5,928	15,090	1.108 ± 0.393
Minimum Block Shear Failure Load			43,400	10,483	4.14

4.2.6 Heel Style 2

The allowable load calculations for Heel Style 2 resulted in predicted failure modes of bottom chord (BC) mortise pocket bearing and block shear of the BC. Both allowable failure loads were similar, but it was predicted that the BC mortise would fail in bearing prior to the BC block shear failure. Both failure loads were observed in the physical tests (Table 4-10).

Heel Style 2 experienced two ultimate failures of block shear in the BC and multiple mortise and tenon bearing failures. The average sustained load at failure of Heel Style 2 is similar to Heel Style 3 and greater than Heel Style 1, but the minimum block shear load was much less than Heel Style 1. The data shows that it could be expected that the mortise and tenon would fail in bearing prior to the joint failing in block shear.

Table 4-10: Compiled structural failures for Heel Style 2 joints.

Trial #	Heel Style 2	Failure Method	Sustained Load at Failure (lbs)	Allowable Point Load (lbs)	Factor of Safety
Trial 5	Side 1	Tenon Failure (Relative Deflection ≥ 3/16")	23,700	11,700	2.02
Trial 5	Side 2	Tenon Failure (Relative Deflection ≥ 3/16")	20,000	11,700	1.71
Trial 8	Side 2	Block Shear Failure	34,400	12,030	2.86
Trial 11	Side 1	Tenon Failure (Relative Deflection ≥ 3/16")	33,800	11,700	2.89
Trial 11	Side 2	Tenon Failure (Relative Deflection ≥ 3/16")	31,300	11,700	2.68
Trial 12	Side 2	Block Shear Failure	30,900	12,030	2.57
Average ± Standard Deviation Sustained Load at Failure Excluding Block Shear			27,200 ± 6,430	11,700	2.32 ± 0.55
Minimum Block Shear Failure Load			30,900	12,026	2.57

4.2.7 Heel Style 3

The allowable load calculations for Heel Style 3 resulted in predicted failure modes of Top chord (TC) tenon bearing and block shear of the bottom chord (BC). Both failure loads were similar, but it was predicted that the BC would fail in block shear prior to the TC tenon bearing failure. Both failure loads were observed in the physical tests (Table 4-11).

Heel Style 3 experienced the highest percentage of ultimate failure of block shear out of any joint style, with 100% of the trusses containing Heel Style 3 failing in an ultimate block shear failure at the truss heel. An average sustained load at failure could not be determined for Heel Style 3, as there was only one observed structural failure that was not block shear. Heel Style 3 had the lowest minimum block shear failure load out of all trials that experienced block shear.

Table 4-11: Compiled structural failures for Heel Style 3 joints.

Trial #	Heel Style 3	Failure Method	Sustained Load at Failure (lbs)	Allowable Point Load (lbs)	Factor of Safety
Trial 1	Side 1	Block Shear Failure	23,400	10,880	2.15
Trial 2	Side 1	Block Shear Failure	27,200	10,880	2.50
Trial 4	Side 2	Block Shear Failure	29,400	10,880	2.70
Trial 10	Side 1	Block Shear Failure	36,900	10,880	3.39
Trial 10	Side 1	Tenon Failure (Relative Deflection ≥ 3/16")	33,400	11,530	2.90
Average ± Standard Deviation Sustained Load at Failure Excluding Block Shear			n/a	n/a	n/a
Minimum Block Shear Failure Load			23,400	10,880	2.15

4.3 Truss Joint Recommendations

4.3.1 Decision Matrix for Optimum Joint Performance

The truss joints were analyzed and compared between similar joint geometry (i.e., truss peak joints and truss heel joints were compared separately). The analysis was based upon multiple factors observed in this Thesis: ease of fabrication (determined from the survey), measured and

calculated responses (determined from the vertical load and the vertical deflection data), average sustained load at failure, and minimum block shear failure load. A decision matrix was created to compare the joint styles (Table 4-12 and Table 4-13). The truss peak options and truss heel options were ranked one to three for each factor, with one being the best performance and three being the worst performance. A "T" in the table indicates two joint styles "tied," i.e., had the same performance for a given factor.

Table 4-12: Decision Matrix (1/2)

Joint Style		Ease of fabrication (from survey)	Maximum load	Load on Truss at deflection limit	Total Absorbed energy
Peak Style Comparison	A	3	1	1	1
	B	T-1	3	3	2
	C	T-1	2	2	3
Heel Style Comparison	1	1	1	1	1
	2	3	2	3	2
	3	2	3	2	3

Table 4-13: Decision Matrix (2/2)

Joint Style		Maximum stiffness	Average Sustained Load at Failure	Minimum Block Shear Failure Load	Total Value
Peak Style Comparison	A	T-1	1	-	8
	B	3	2	-	14
	C	T-1	3	-	12
Heel Style Comparison	1	1	-	1	6
	2	3	-	2	15
	3	2	-	3	15

The comparisons of the ease of fabrication factors were determined from the survey results (Appendix A). Due to the design of the survey, direct comparisons between shoulder-only joints and mortise and tenon joints was not possible. However, the joint styles were still able to be ordered by combining the two result sections.

The comparisons of the measured and calculated responses were determined from the tables that arranged the different responses from best performance to worst performance (Table

4-1, Table 4-3, Table 4-4, and Table 4-5). The order was determined numerically, where the best performing truss received a score of 1, and the worst performing truss received a score of 13. The total value of each joint performance was used to determine the order. Four of the five responses were used due to the inverse relationship between the maximum vertical load and maximum vertical deflection results. Therefore, only the maximum vertical load, load on truss at deflection limit, maximum stiffness, and total absorbed energy responses were used to compare the trusses.

The average sustained load at failure was used to compare the truss peak joints only, due to Heel Style 3 not having sufficient data to formulate an average sustained load at failure. Conversely, the minimum block shear load was used to compare the truss heel joints only, as Peak Style B and Peak Style C did not experience block shear failures, resulting in insufficient data to compare with Peak Style A.

The total value in Table 4-13 indicates the performance of the joints relative to the joints of the same configuration, where the lower the score indicates the better the joint style performed. For this Thesis, Peak Style A and Heel Style 1 were the optimum joints (i.e., best score) with all factors in Table 4-12 and Table 4-13 having the same weight. In the author's opinion, with a structural engineering background, the structural capacity factors are more important factors to consider than ease of fabrication (Section 4.2). With this consideration, the relative performance of Peak Style A and Heel Style 1 would be magnified, as they both performed the best in the two categories. However, other engineers and designers could have different opinions, and weigh the factors differently based on their individual judgement.

4.3.2 Optimum Truss Peak

Based on the results of this research project, the optimum joinery style of the truss peak (three-member configuration) is Peak Style A. This is a great result for the industry, as Peak Style A was the most popular joinery style from the survey results (Section 2.1.3 and Appendix A).

Trusses containing Peak Style A all performed above average regarding the maximum applied load, with the five trusses containing Peak Style A performing in the top six, regardless of Heel Styles. Only 2 of 8 trusses containing either Peak Style B or Peak Style C performed above average regarding maximum applied load, but those two trials were also in the bottom three of the maximum deflection results. Additionally, trusses containing Peak Style A were the best performers in maximum stiffness (top 3 of 4), total absorbed energy (top 4 of 6), and load absorbed to deflection limit (top 3 of 4), and trusses containing either Peak Style B or Peak Style C were the worst performers for every metric.

There was only one occurrence of an ultimate failure of block shear at the truss peak throughout the thirteen trials (Trial 0 Truss A1), which had a factor of safety (FS) of 3.41. This was not a surprising result, as the Peak Styles (excluding Peak Style B) had higher allowable loads relative to the Heel Styles, which predicted failures at the truss heels prior to the truss peaks. Therefore, the differences between the truss peaks due to ultimate failure of block shear is unclear, so the average sustained load at failure for structural failures will be used to compare peak styles.

Peak Style A was the most tested Peak Style but experienced the least number of structural failures and had the highest structural average sustained load at failure for of any joint type. Additionally, Peak Style A had the second highest factor of safety (FS) for structural failures excluding block shear (2.78), second to Peak Style B. However, the FS for Peak Style B structural failure due to peg yielding was abnormally high due to the relatively low allowable load, which

inflated the FS relative to the rest of the joint styles. All but one side of one truss peak containing styles B or C experienced a structural failure, and the two Peak Styles had the two lowest average sustained loads at failure of all six joinery options. Only two trusses experienced no structural failures at the peak, and they both contained Peak Style A (Trial 3 Truss A1 and Trial 10 Truss A3).

Peak Style A is the most labor-intensive option for the truss peak, but it is the opinion of the author that the extra time and expense in the design and labor of this style is recommended due to the improvement in load carrying capacity, higher factors of safety, and overall joint performance.

4.3.3 Optimum Truss Heel

Based on the results of this research project, the optimum joinery style of the truss heel (two-member configuration) is Heel Style 1. This also is a great result for the industry, as Heel Style 1 was the most popular joinery style from the survey results (Section 2.1.4 and Appendix C).

Trusses containing Heel Style 1 all performed above average regarding the maximum applied load, with the top four performers all containing Heel Style 1, regardless of Peak Style. Only one truss trial containing Heel Style 2 (Trial 11 Truss A2) and containing Heel Style 3 (Trial 10 Truss A3) were above average for maximum load, all other truss trials containing Heel Style 2 or 3 performed below average. Additionally, trusses containing Heel Style 1 were the top 3 of 3 for load applied to truss at deflection limit and maximum stiffness, and trusses containing Heel Style 1 were in the top 5 of 6 for total absorbed energy.

The failure occurrences and corresponding loads were not as clear regarding the heel joints relative to the peak joints. Heel Style 1 and Heel Style 2 both had two ultimate failures of block shear, while Heel Style 3 had four ultimate failures of block shear (i.e., 100% ultimate failure rate).

Heel Style 1 had the lowest structural sustained load at failure out of the heel joints, and Heel Style 3 had the highest. However, the lower structural failure load average for Heel Style 1 was partly due to the definition of failure used for this Thesis, (localized crushing of the shoulders - Section 3.3.2.2), and Heel Style 1 had the highest minimum block shear failure load of any joint type, with the corresponding larger factor of safety.

Heel Style 1 was determined to be the optimum joinery style because it was voted the easiest to fabricate in the survey (Section 2.1.4), the performance of Heel Style 1 was the best for every measured and calculated response, and Heel Style 1 had the highest minimum block shear factor of safety (4.14).

5 Conclusions

5.1 Project Summary

This research project was designed to fill a research gap regarding traditional timber framing joinery for bearing connections at an angle. Angled bearing connections are prevalent in the timber framing industry, as they are used in truss joinery and lateral resistance joinery (i.e., braces) to resolve compression. However, there is limited research regarding how traditional bearing joints act under loading, how they fail, and what their true load capacities are.

The primary objective of this Thesis was to determine the optimum style for the truss heel connection (i.e., single compression member) and truss peak connection (i.e., two compression members) (Figure 1-1) using the survey responses, measured and calculated responses, and observed joint failure modes with concurrent loads. The secondary objective was to identify and categorize the observed failure modes and concurrent loads to determine factors of safety relative to the allowable loads of the joints calculated with modern codes.

A survey was written and distributed through the Timber Frame Engineering Council (TFEC) to determine the industry's preferred materials and methods for fabricating timber frame joinery, and the preferred joinery styles for both the truss heel and truss peak connections. The three most popular joinery styles were selected for each joint configuration based on the survey results (Peak Styles A, B, C; Heel Styles 1, 2, 3) (Section 2.1.5). The joinery styles were used to design nine unique specimens (i.e., truss configurations), and four replicates were added to compare the results of the specimens with the same configurations. All parameters other than joinery style (e.g., wood species and grade, member sizes, shape, geometry, loading procedures) were kept consistent to limit variability.

The thirteen specimens were tested using The University of New Hampshire's reaction frame. The reaction frame loaded the simply supported trusses from above with a hydraulic

actuator. A steel frame allowed the actuator to load the king post of the truss below the truss peak, developing axial loads in the truss members. The specimens were loaded continuously, in a stepwise manner, until the specimen experienced a failure where the specimen was unable to sustain additional load (9 of 13 trials), or the vertical deflection limit of the testing aparatus was reached (4 of 13 trials). The ultimate failure method, where the 9 of 13 trials were stopped due to a failure where the specimen was unable to sustain additional load, was block shear for every instance. All thirteen specimens experienced additional structural and servicibility failures that did not prevent the specimen from sustaining additiona load.

The vertical load data and vertical deflection data from each trial was evaluated and compared. Each truss was able to sustain vertical loads with at least a factor of safety of 2.0 relative to their calculated allowable loads. The strongest truss carried approximately five times the calculated allowable load. The vertical deflection of each trial at the allowable load was just above the vertical deflection limit of L/180. Each truss greatly surpased the deflection limit at loads above the calculated allowable loads. Peak Style A and Heel Style 1, most used according to the survey, were observed to be at or near the top for every response other than maximum vertical deflection.

The individual joints for each specimen were evaluated using the observed joint failures and their corresponding loads. Seven unique failure mechanisms were identified, with each joint style experiencing a combination of the seven depending on the design. The results confirmed the measured and calculated responses that Peak Style A and Heel Style 1 provided the best performance: Heel Style 1 had the highest factor of safety regarding ultimate failure of block shear. Peak Style A experienced the highest average sustained load at failure for all trials and experienced the least amount of structural failures for any of the six joint options. It was therefore decided that Peak Style A and Heel Style 1 were the optimum joint styles for each configuration (Figure 5-1).

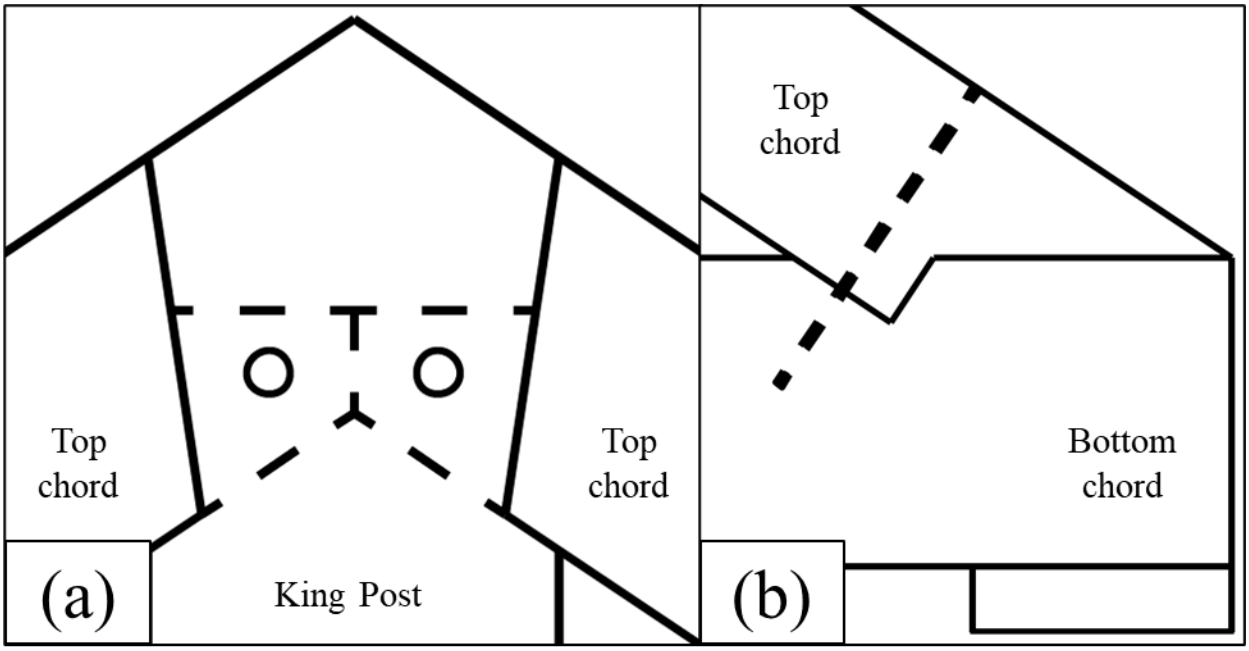

Figure 5-1: (a) Optimum peak joint: Peak Style A, (b) Optimum peak joint: Heel Style 1.

5.2 Principal Conclusions

- The timber framing community has numerous opinions regarding how the truss peak connection and the truss heel connection should be designed. The most popular design choice (birdsmouth shoulder at truss heel) received 70% of the votes, with the other design options only receiving ~30% or less.
- The optimum joinery style for the truss peak was determined to be Peak Style A. Though it is the most labor-intensive option cited by survey respondents, the extra labor was considered less of a concern than the superior strength and stiffness capacity of the joint. Peak Style A also experienced the least number of structural failures, had the highest average sustained load at failure, and the corresponding highest factor of safety for structural failures.

- The optimum joinery style for the truss heel was determined to be Heel Style 1. Trusses containing Heel Style 1 generally outperformed trusses containing Heel Styles 2 and 3. Heel Style 1 was found to have the highest ultimate failure (block shear) load average and corresponding factor of safety. Heel Style 1 was also cited by survey respondents as the easiest to fabricate.
- Each truss was able to carry at least twice the allowable calculated design load, demonstrating a factor of safety greater than 2.0.
- Each truss was able to meet the deflection criteria of L/180 (0.4") for the allowable load.
- The capacities and stiffness of the different joint styles varied: the maximum force applied to the trusses varied from 23,390 lbs to 48,023 lbs, and the maximum vertical deflection of the trusses varied from 0.616 in to 1.475 in.
- The assumed failure modes for the allowable load calculations (a combination of mortise and tenon bearing failure, shoulder bearing failure, block shear, and peg yielding) were all observed.
- Block shear was the only failure mechanism where the truss was unable to sustain additional load once the failure occurred. Mortise and tenon bearing failure, shoulder bearing failure, and peg yielding all were ductile enough to allow the truss to carry increasing loads, though a decrease in truss stiffness became apparent following these failure mechanisms.
- For all trusses (except Heel Style 3) where block shear was a possible failure mode, gradual bearing failures (either shoulder or mortise and tenon) typically occurred at lower loads compared to sudden failures of block shear.

- All structural failure modes, excluding shoulder bearing for Peak Style C and Heel Style 1, had average factors of safety greater than 2.0 for all joint types.
- Three unanticipated failure mechanisms were observed (a combination of crack formation, check expansion, and excessive vertical deflection), but all three were considered serviceability failures, as their occurrence did not prevent the truss from carrying additional load and they occurred outside of the principal load path(s) (i.e., not along block shear planes or at shoulder bearing locations).
- Digital Image Correlation (DIC) proved to be a useful tool for data collection regarding relative displacements between members and surface strains of the timbers. It is important that the placement and resolution of the camera equipment and dot pattern size are appropriate for the analysis software used.

5.3 Project Limitations and Future Work

Findings from this research are specific to the materials, loading procedure, and geometric properties stated in this research project. Each design parameter, excluding the joinery styles, was kept constant across the trials to better compare the differences between each joinery method. Additional experimentation using other wood species, varying angles of compression members, longer span trusses, and different loading durations are recommended to verify the results under different conditions.

Different timber species have unique properties that could alter their failure paths and limits. Two of the most important material properties for determining design characteristics in timber are the modulus of elasticity (E) and specific gravity (G), which vary widely across popular timber framing species (Table 5-1) (NDS, 2018). It was concluded that Peak Style A and Heel

Style 1 were the optimum configurations for Douglas Fir-Larch timbers using the given variables for this Thesis, but different joint configurations could prove superior for different species.

Table 5-1: Material properties for various timber species.

	Modulus of Elasticity (E - psi)	Specific Gravity (G)
Douglas Fir-Larch	1,600,000	0.50
Eastern White Pine	1,100,000	0.36
Hem-Fir	1,200,000	0.41
White Oak	1,000,000	0.73

Various angles of the compression member should also be investigated. The angle changes the vector forces, which alter the allowable load calculations and expected failure paths accordingly. It would be beneficial to know if the experimental failure modes and loads similarly alter under angle changes. This project used a roof pitch of 8/12, but roof pitches of 4/12 to 12/12 are common in the timber framing industry, and the author has worked on projects with roof pitches ranging from 2/12 up to 18/12.

The trusses used for this Thesis have full-size joinery at the truss peak and truss heels but shortened member lengths to fit into the available testing apparatus. The vertical deflections of the king post and top chords at the truss peak develop larger rotational angles at the truss heels compared to the same vertical deflection for a larger span truss. It could be expected that trusses with the same joint types and member sizes could span 20 - 40 feet in practice, which would develop less rotation at the truss heels compared to the six-foot span trusses used for this Thesis. Longer span trusses should be tested to determine if the longer span trusses develop similar failure modes and loads experienced by the short-span trusses.

Changes to the load duration and loading mechanism should also be investigated. Timber as a material is unique in that most strength capacities change under different loading durations. The design load duration for this project was approximately 10 minutes and required a stepwise

loading procedure due to the limitations of the loading mechanism. The load duration could be lengthened to replicate real-world conditions of roof live loads (seven days) and snow loads (two months) to determine if the joints behave in a similar way to the short duration loads used herein. Various loading methods could also be investigated: monotonic compression to failure (i.e., no stepwise loading) and cyclic loading of the joints at design service loads.

Based on the laboratory research outcomes from this thesis, it is recommended that a finite element analysis (FEA) model be created and developed for the joinery designs used in this Thesis and calibrated using the data collected. Previous studies have incorporated FEA models to model the behavior of traditional timber framing joints under compression loads in addition to laboratory testing (Villar et al., 2007; Villar-García et al., 2018; Verbist et al., 2017), but these studies were limited to shoulder-only joints (i.e., birdsmouth shoulder, single step joint). Modeling of mortise and tenon joints should be investigated to allow for analysis of different design parameters (e.g., roof pitch, timber species, loading duration). Additional physical tests may need to be conducted to verify model after development.

References

2018 National Design Specification. (2018). American Wood Council.

AISC. (2011). *Steel Construction Manual* (14th ed.). American Institute of Steel Construction.

ASTM D143 − 21: Standard Test Methods for Small Clear Specimens of Timber. (2021). ASTM International.

ASTM D2555 − 17a: Standard Practice for Establishing Clear Wood Strength Values. (2017). ASTM International.

ASTM D5652 − 21: Standard Test Methods for Single-Bolt Connections in Wood and Wood-Based Products. (n.d.). ASTM International.

ASTM D5764 − 97a: Standard Test Method for Evaluating Dowel-Bearing Strength of Wood and Wood-Based Products. (n.d.). ASTM International.

Benson, T., & Gruber, J. (1995). *Building the Timber Frame House* (First Fireside Edition). Simon and Schuster.

Bramwell, M. (1976). *The International book of wood*. Simon and Schuster.

Branco, J. M., Verbist, M., & Descamps, T. (2018). Design of three Step Joint typologies: Review of European standardized approaches. *Engineering Structures, 174*, 573–585. https://doi.org/10.1016/j.engstruct.2018.06.073

Branco, J., Piazza, M., Cruz, P., & Varum, H. (2006). *Modelling of timber joints in traditional structures*. 15.

Brungraber, R. L. (1985). *Traditional Timber Joinery: A Modern Analysis*. Stanford University.

Correlated Solutions. (n.d.). *VIC-2D-V6 Testing Guide*. Correlated Solutions. Retrieved July 30, 2021, from http://www.correlatedsolutions.com/supportcontent/Vic-2D-v6-Testing-Guide.pdf

Feio, A. O., Lourenço, P., B., & Machado, J. S. (2014). Testing and modeling of a traditional

timber mortise and tenon joint. *Materials and Structures*, *47*, 213–225.

Foliente, G. (2000). History of Timber Construction. In S. Kelley, J. Loferski, A. Salenikovich, & E. Stern (Eds.), *Wood Structures: A Global Forum on the Treatment, Conservation, and Repair of Cultural Heritage* (pp. 3-3–20). ASTM International. https://doi.org/10.1520/STP13370S

Jacoby, Henry S. (1913). *Structural Details or Elements of Design in Timber Framing* (First Edition). John Wiley & Sons.

Lewandoski, Jan, Levin, Ed, & Sobon, Jack. (2004). Historic American Roof Trusses: III. Kingpost Trusses. *Journal of the Timber Framers Guild*, *No. 72*, 16–24.

Li, H., Dai, Y., Qiu, H., & He, X. (2022). Application of Multi-Camera Digital Image Correlation in the Stability Study of the Long Timber Column with the Circular Cross-Section under Axial Compression. *BioResources*, *17*(1), 1717–1728.

Li, X., Zhao, J., Ma, G., & Huang, S. (2015). Experimental Study on the Traditional Timber Mortise-Tenon Joints. *Advances in Structural Engineering*, *18*(12), 2089–2102. https://doi.org/10.1260/1369-4332.18.12.2089

McCormick, N., & Lord, J. (2010). Digital Image Correlation. *Materials Today*, *13*(12), 52–54. https://doi.org/10.1016/S1369-7021(10)70235-2

Miller, J. F. (2009). *Capacity of Pegged Connections*. Timber Frame Engineering Council.

Miller, J. F., & Schmidt, R. J. (2004). *CAPACITY OF PEGGED MORTISE AND TENON JOINERY*. University of Wyoming.

Nehil, T., & Schmidt, D. (2021). *TFEC DG 1—Design Guide for Timber Trusses*. Timber Frame Engineering Council.

Schmidt, R. J., & Daniels, C., E. (1999). *Design Considerations for Mortise and Tenon*

Connections. University of Wyoming.

Schmidt, R. J., & MacKay, R. B. (1997). *TIMBER FRAME TENSION JOINERY*. University of Wyoming.

Standard no. 17: Grading Rules for West Coast Lumber. (n.d.). West Coast Lumber Inspection Bureau.

TFEC. (2019). *Standard for Design of Timber Frame Structures and Commentary (TFEC 1-2019).* (p. 51) [Standard]. Timber Frame Engineering Council Technical Activities Committee (TFEC-TAC).

Verbist, M., Branco, J. M., Poletti, E., Descamps, T., & Lourenço, P. B. (2017). Single Step Joint: Overview of European standardized approaches and experimentations. *Materials and Structures*, *50*(2), 161. https://doi.org/10.1617/s11527-017-1028-4

Villar, J. R., Guaita, M., Vidal, P., & Arriaga, F. (2007). Analysis of the Stress State at the Cogging Joint in Timber Structures. *Biosystems Engineering*, *96*(1), 79–90. https://doi.org/10.1016/j.biosystemseng.2006.09.009

Villar-García, J. R., Crespo, J., Moya, M., & Guaita, M. (2018). Experimental and numerical studies of the stress state at the reverse step joint in heavy timber trusses. *Materials and Structures*, *51*(1), 17. https://doi.org/10.1617/s11527-018-1144-9

Villarino, A., López-Rebollo, J., & Antón, N. (2020). Analysis of Mechanical Behavior through Digital Image Correlation and Reliability of Pinus Halepensis Mill. *Forests, Wood Structure and Properties*.

APPENDICES

Appendix A: Survey Results

See external document for survey results: Compression Testing of Traditional Timber Framing Truss Joinery Survey Results.

Appendix B: Production Drawings

See external document for production drawings: Compression Testing of Traditional Timber Framing Truss Joinery Production Drawings.

Appendix C: Joinery Allowable Load Calculations

The allowable loads for each joinery type were calculated using standard engineering practice and the latest applicable codes: The American Wood Council – National Design Specifications 2018 ed. (NDS, 2018) and the Timber Frame Engineering Council – Standard for Design of Timber Frame Structures and Commentary 2019 ed. (TFEC 1-19). The most conservative value between the NDS – 18 and the TFEC 1-19 was used for the allowable load calculations.

The standard practice for calculating the joint allowable loads was to calculate the allowable compressive load in the top chord (TC) and convert to the allowable point load applied to the truss at the king post (KP) using the truss geometry. The trusses used in this project have a TC pitch of 8/12 (33.7 degrees from horizontal). The geometry of the truss was calculated in-part using the Pythagorean Theorem:

$$C^2 = A^2 + B^2$$

$$C = \sqrt{A^2 + B^2}$$

Where:

$A =$ Horizontal dimension of the slope.

$B =$ Vertical dimension of the slope.

$C =$ Hypotenuse of roof pitch.

Therefore:

$$C = \sqrt{12^2 + 8^2} = 14.42$$

The truss vertical reactions, TC compression ratio, and bottom chord (BC) tension ratio were calculated symbolically with the geometry of the truss:

$$R = \frac{1}{2} * P$$

$$C_{TC} = P * \left(2 * \left(\frac{8}{14.42}\right)\right) = 0.901 * P$$

$$T_{BC} = C_{TC} * \frac{12}{14.42} = (0.901 * P) * \frac{12}{14.42} = 0.75 * P$$

Where:

$P =$ Point load applied to truss KP (lbs).

$R =$ Truss reaction on each side, lbs.

$C_{TC} =$ Relative compression in the TC, lbs.

$T_{BC} =$ Relative tension in the BC, lbs.

C.1 Material Properties

All timbers used are Douglas Fir-Larch, #1 grade. The timber design values, per the NDS – 18, differ slightly if they are classified as a Post/Timber or a Beam/Springer (Table C-1).

Table C-1: Unadjusted design stresses for Douglas Fir-Larch timbers.

Douglas Fir-Larch - No.1 (psi)	Bending F_B	Tension Parallel to Grain F_t	Shear Parallel to Grain F_v	Compression Perpendicular to Grain F_{cperp}	Compression Parallel to Grain F_c	Grading Rules Agency
Beams and Stringers	1350	675	170	625	925	WCLIB/WWPA
Posts and Timbers	1200	825	170	625	1000	WCLIB/WWPA

The listed design values are adjusted in practice with numerous adjustment factors depending on the individual situation of the timbers for their design life. For this project, all adjustment factors were set to 1.0 other than the load duration factor, C_D. The designed test

duration for this project was 10 minutes, which results in a $C_D = 1.6$ (NDS, 2018, Table 2.3.2). Final design values with the duration factor included (if applicable) are in Table C-2.

Table C-2: Adjusted design stresses for Douglas Fir-Larch timbers.

Douglas Fir-Larch - No.1 (Adjusted)	Bending F'_B	Tension Parallel to Grain F'_t	Shear Parallel to Grain F'_v	Compression Perpendicular to Grain F'_{cperp}	Compression Parallel to Grain F'_c	Grading Rules Agency
Beams and Stringers	2160	1080	272	625	1480	WCLIB/WWPA
Posts and Timbers	1920	1320	272	625	1600	WCLIB/WWPA

C.2 Designed truss failure mechanisms

It was calculated that the joinery styles would fail in one of three ways: bearing failure (i.e., crushing), block shear failure, or peg yielding (peak connection B only). The three failures are calculated using different methods depending on the joint in question but use the same core equations.

Allowable bearing stress is calculated using standard engineering analysis of bearing stress or Hankinson's equation:

$$Bearing\ Stress: P_{max} = F_x * A_b => F_x = \frac{P_{max}}{A_b}$$

$$Hankinson's\ Eqn: F'_{c\Theta} = \frac{F'_c * F'_{cperp}}{F'_c * \sin(\Theta)^2 + F'_{cperp} * \cos(\Theta)^2}\ (NDS - 18\ \text{eq. } 3.10 - 1)$$

Where:

Θ = angle between direction of load and direction of grain (longitudinal axis of member), degrees

$F'_{c\Theta}$ = allowable bearing stress at angle Θ, psi

$F'_c =$ allowable compression stress parallel to grain, psi

$F'_{cperp} =$ allowable compression stress perpendicular to grain, psi

P_{max} = maximum load acting perpendicular to bearing surface, lbs

F_x = applicable bearing stress (F_c', F_{cperp}', $F_{c\Theta}'$), psi

A_b = bearing area, in^2

Block shear is calculated using the TFEC Standard for Design of Timber Frame Structures and Commentary, 2019 (TFEC 1-19) equation 3.6-1:

$$Block\ Shear: Z' = \frac{F_v' * A_v}{2}\ (TFEC\ 1-19\ eq.3.6-1)$$

Where:

Z' = maximum load in direction of shear plane, lbs

F_v' = allowable shear stress, psi

A_v = block shear area, in^2

Peg yielding is calculated using the peg yield equations specified in TFEC 1-19 section 3.4.1 and Table 3A. The full analysis of the peg capacity using the TFEC yield equations was completed in a spreadsheet (Table C-3).

Table C-3: Peg yield equation spreadsheet input and output.

Input				
Symbol	Description	Value	Units	Code Reference
Dp	Diameter of Peg	1	in	-
L_m	Length of Main Member	2	in	-
L_s	Length of Side Member	1.75	in	-
Gp	Specific Gravity of the peg	0.73	-	NDS-18 Table 12.3.3A
Gt	Specific Gravity of the timber material	0.5	-	NDS-18 Table 12.3.3A
Θ_m	Angle of loading vs. parallel grain in main member	56.3	degrees	-
Θ_s	Angle of loading vs. parallel grain in side member	0	degrees	-

Output				
Symbol	Description	Value	Units	Code Reference
Re_double	Fe_m/Fe_s	0.855	-	TFEC 1-19 3.4-9
K_theta	General Reduction Term from loading at angle	1.156	-	TFEC 1-19 3.4-6
K_3	Reduction Term for Yield Mode III	1.891	-	TFEC 1-19 3.4-7
Fyvp	Effective yield strength of the peg in shear	2105	psi	TFEC 1-19 3.4-8
Fybp	Yield strength of the peg in bending	17413	psi	TFEC Technical Bulletin #1
Fe_parallel	Parallel dowel bearing strength	3149	psi	TFEC 1-19 3.4-10
Fe_perpendicular	Perpendicular dowel bearing strength	2529	psi	TFEC 1-19 3.4-11
Fe_m	Tenon dowel bearing strength (main member)	2692	psi	TFEC 1-19 3.4-12
Fe_s	Mortise side wall bearing strength (side member)	3149	psi	TFEC 1-19 3.4-12

Yield Limit Equations, Double Shear Only (Mortise and Tenon)			
Yield Mode	Reduction Factor	Capacity	Code Reference
Im	4.63	1164	TFEC 1-19 3.4-1
Is	4.63	2382	TFEC 1-19 3.4-2
IIIs	3.70	1687	TFEC 1-19 3.4-3
V	3.5	945	TFEC 1-19 3.4-4
Minimum Value for Design:		945 lbs	

C.3 Allowable loads for each joinery type

C.3.1 Peak Style A

The allowable compression of the TC for Peak Style A is calculated using vector analysis. The horizontal vector of the force is resolved by the bearing of the TC shoulder on the side grain of the KP. The allowable horizontal load vector will be significantly larger than the allowable vertical load vector by inspection. The vertical load vector is resolved by the bearing of the TC tenon on the KP mortise (Figure C-1), and the block shear capacity of the remaining KP material above the mortise pocket (Figure C-2).

The bearing capacity of the mortise and tenon (M&T) connection is controlled by the TC tenon material, as the KP mortise material is loaded parallel to grain and has a higher allowable bearing stress.

The bearing area of the tenon includes a 1/4” back-cut:

$$A_b = (4\frac{1}{4}" - \frac{1}{4}") * 2" = 8\ in^2$$

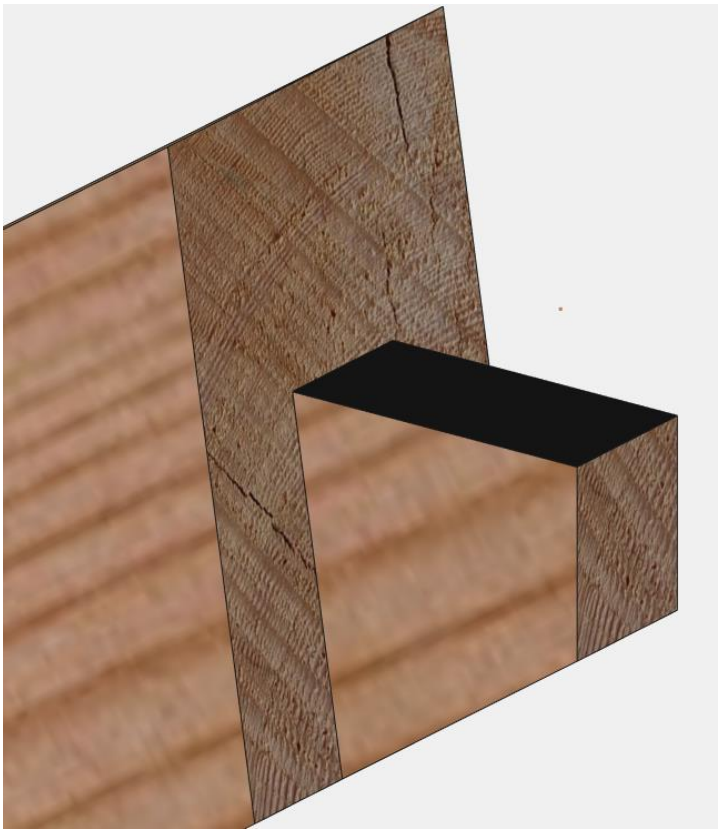

Figure C-1: Bearing surface of TC tenon in peak connection A.

The bearing stress at an angle of the TC tenon is calculated using Hankinson's equation for post/timber tenon material. The tenon is loaded 56.3 degrees relative to parallel to grain:

$$F'_{c56.3} = \frac{1600\ psi * 625\ psi}{1600\ \text{psi} * \sin(56.3)^2 + 625\ \text{psi} * \cos\ (56.3)^2} = 769\ psi$$

Therefore, the allowable vertical load vector due to tenon bearing is:

$$V = 8\ in^2 * 769\ psi = 6{,}152\ lbs$$

The block shear capacity of the KP is calculated using the block shear area (two pentagonal shear planes exist on each side of the TC tenon). The total block shear of the peak joint area was determined from the 2D model:

$$A_{v,total} = 92.7\ in^2$$

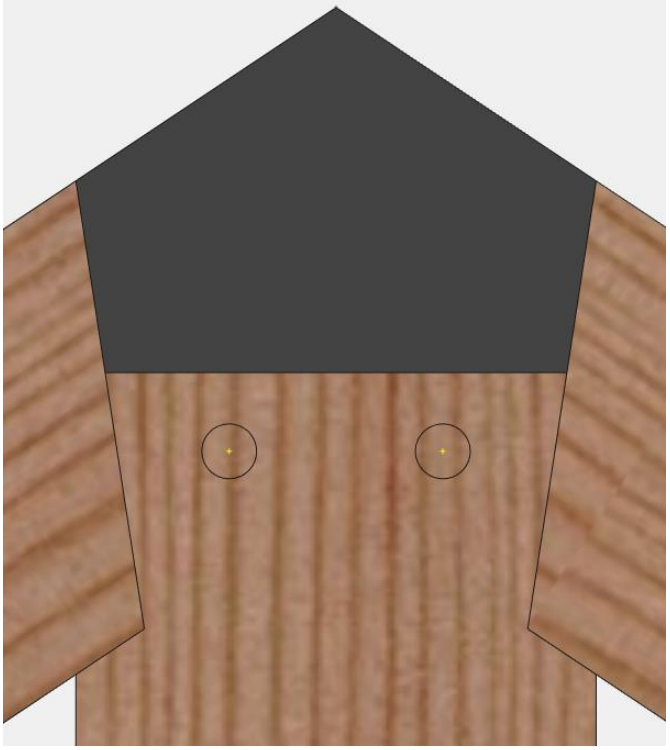

Figure C-2: Cross-section of a block shear plane in the KP of Peak Style A.

Therefore, the allowable vertical load due to the block shear capacity for a single TC is:

$$V = \frac{272\ psi * \frac{92.7\ in^2}{2}}{2} = 6{,}306\ lbs$$

The governing vertical load vector is due to the allowable bearing stress of the TC tenon, 6152 lbs.

The allowable compression in the TC was calculated using the truss geometry:

$$C_{TC} = 6152\ lbs * \frac{14.42}{8} = 11{,}089\ lbs$$

The relative point load applied to the truss to cause the TC to reach the allowable compression was calculated using the truss geometry:

$$P = \frac{11{,}089\ lbs}{0.901} = 12{,}307\ lbs$$

C.3.2 Peak Style B

The allowable compression of the TC for Peak Style B is calculated using vector analysis. The horizontal vector of the force is resolved by the bearing of the TC shoulder on the side grain of the KP. The allowable horizontal load vector will be significantly larger than the allowable vertical load vector by inspection. The vertical load vector is resolved by the (2) 1" pegs connecting the TC to the KP. Friction between the TC and KP shoulder surfaces was not relied upon for the design of this joint.

The vertical capacity of the two-pegged connection was based on the peg yield capacity discussed in Section C.2. For this thesis, a single 1" Oak peg in the Douglas Fir mortise and tenon joinery had a base capacity of:

$$Z = 945\ lbs$$

The peg yield capacity was increased with the duration factor of 1.6:

$$Z' = 945\ lbs * 1.6 = 1{,}512\ lbs$$

The total vertical load capacity of the two pegs is:

$$Z'_{Total} = 1512\ lbs * 2 = 3{,}024\ lbs$$

Due to the nature of peg yielding, the total peg capacity is the same as the vertical load capacity. Therefore, the allowable compression in the TC is:

$$C_{TC} = 3{,}024\ lbs$$

The relative point load applied to the truss to cause the TC to reach the allowable compression is the same as the allowable compression in the TC due to the nature of peg yielding:

$$P = 3{,}024\ lbs$$

C.3.3 Peak Style C

The allowable compression of the TC for Peak Style C is calculated using partial vector analysis. The bearing surface of the TC shoulder is perpendicular to the TC, so the allowable compression of the TC is directly related to the bearing capacity of the shoulder (Figure C-3). Conversely, the vertical load vector is resolved by the block shear capacity of the remaining KP material above the shoulder cut (Figure C-4).

The bearing capacity of the shoulder connection is controlled by the KP material, as the KP shoulder material is loaded at an angle to grain, and the TC shoulder material is loaded parallel to grain and has a higher allowable bearing

The bearing area of the shoulder is:

$$A_b = 5\frac{1}{2}" * 2\ \frac{11}{16}" = 14.78\ in^2$$

Figure C-3: Bearing area of TC shoulder for Peak Style C.

The bearing stress at an angle of the KP shoulder is calculated using Hankinson's equation for beam/stringer material. The shoulder is loaded 56.3 degrees relative to parallel to grain:

$$F'_{c56.3} = \frac{1480\ psi * 625\ psi}{1480\ \text{psi} * \sin(56.3)^2 + 625\ \text{psi} * \cos\ (56.3)^2} = 760\ psi$$

Therefore, the allowable compression in the TC due to shoulder bearing is:

$$C_{TC} = 14.78\ in^2 * 760\ psi = 11{,}233\ lbs$$

The block shear capacity of the KP is calculated using the block shear area (single shear plane). The block shear area was determined from the 2D model:

$$A_v = 5\frac{1}{2}" * 9" = 49.5\ in^2$$

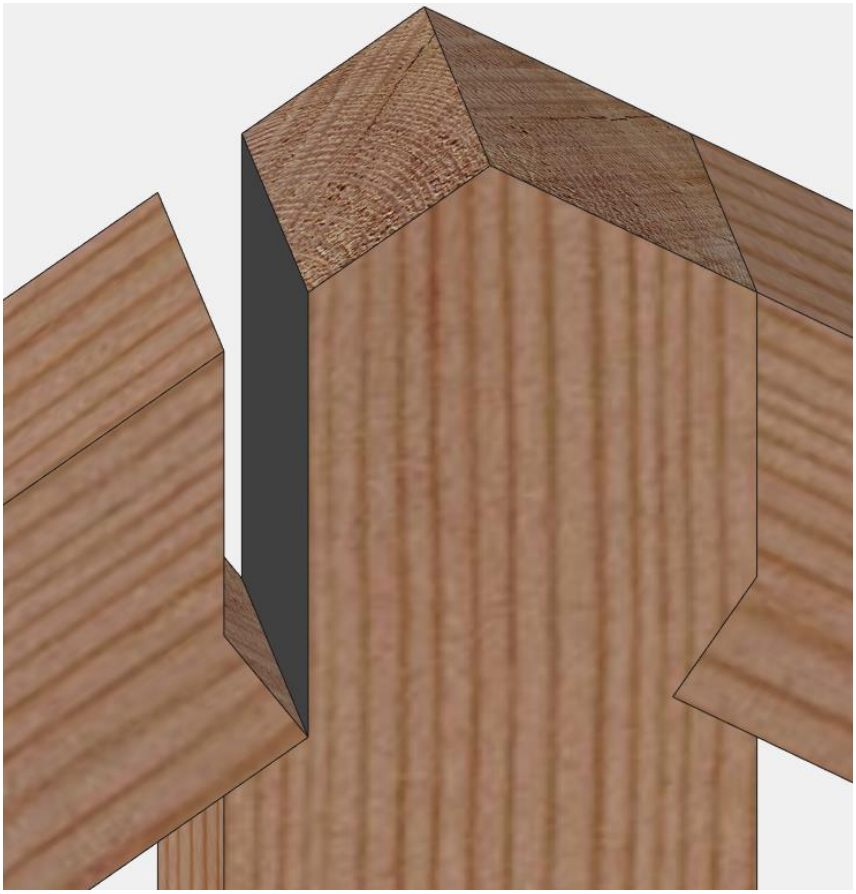

Figure C-4: Block shear plane of KP for Peak Style C.

Therefore, the allowable vertical load due to the block shear capacity for a single TC is:

$$V = \frac{272\ psi * 49.5\ in^2}{2} = 6{,}732\ lbs$$

The allowable compression due to block shear in the KP was calculated using the truss geometry:

$$C_{TC} = 6732\ lbs * \frac{14.42}{8} = 12{,}134\ lbs$$

The governing allowable compression in the TC is due to the bearing of the shoulder material. The relative point load applied to the truss to cause the TC to reach the allowable compression was calculated using the truss geometry:

$$P = \frac{11{,}233\ lbs}{0.901} = 12{,}467\ lbs$$

C.3.4 Heel Style 1

The allowable compression of the TC for Heel Style 1 is calculated using partial vector analysis. The bearing surface of the TC shoulder is perpendicular to the TC, so the allowable compression is directly related to the bearing capacity of the shoulder (Figure C-5). Conversely, the horizontal vector of the force is resolved by the block shear capacity of the remaining BC material behind the shoulder cut (Figure C-6).

The bearing capacity of the shoulder connection is controlled by the BC material, as the BC shoulder material is loaded at an angle to grain, and the TC shoulder material is loaded parallel to grain and has a higher allowable bearing stress.

The bearing area of the shoulder is:

$$A_b = 5\frac{1}{2}" * 2\ \frac{3}{8}" = 13.06\ in^2$$

Figure C-5: Bearing area of TC shoulder for Heel Style 1.

The bearing stress at an angle of the BC shoulder is calculated using Hankinson's equation for beam/stringer material. The shoulder is loaded 33.7 degrees relative to parallel to grain:

$$F'_{c33.7} = \frac{1480\ psi * 625\ psi}{1480\ \text{psi} * \sin(33.7)^2 + 625\ \text{psi} * \cos\ (33.7)^2} = 1041\ psi$$

Therefore, the allowable compression in the TC due to shoulder bearing is:

$$C_{TC} = 13.06\ in^2 * 1041\ psi = 13{,}595\ lbs$$

The block shear capacity of the BC is calculated using the block shear area (single shear plane). The block shear area was determined from the 2D model:

$$A_v = 5\frac{1}{2}" * 10\frac{1}{2}" = 57.8\ in^2$$

Figure C-6: Block shear plane of BC for Heel Style 1.

Therefore, the allowable horizontal load due to the block shear capacity for a single TC is:

$$H = \frac{272\ psi * 57.8\ in^2}{2} = 7{,}860\ lbs$$

The allowable compression due to block shear in the BC was calculated using the truss geometry:

$$C_{TC} = 7860\ lbs * \frac{14.42}{12} = 9{,}445\ lbs$$

The governing allowable compression in the TC is due to the block shear of the BC. The relative point load applied to the truss to cause the TC to reach the allowable compression was calculated using the truss geometry:

$$P = \frac{9{,}445\ lbs}{0.901} = 10{,}483\ lbs$$

C.3.5 Heel Style 2

The allowable compression of the TC for Heel Style 2 is calculated using partial vector analysis. The bearing surface of the TC tenon is perpendicular to the TC, so the allowable compression is directly related to the bearing capacity of the tenon (Figure C-7). Conversely, the

horizontal vector of the force is resolved by the block shear capacity of the remaining BC material behind the mortise (Figure C-8).

The bearing capacity of the tenon connection is controlled by the BC material, as the BC tenon material is loaded at an angle to grain, and the TC tenon material is loaded parallel to grain and has a higher allowable bearing stress.

The bearing area of the tenon is:

$$A_b = 2" * 4\ \frac{13}{16}" = 9.625\ in^2$$

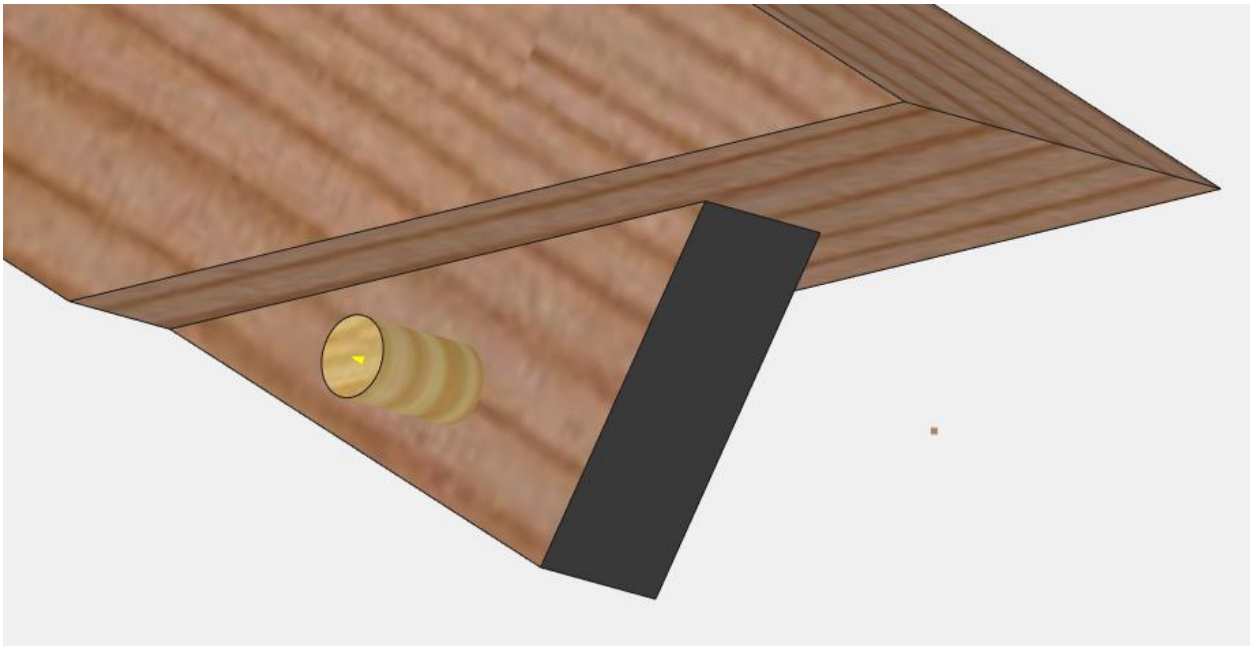

Figure C-7: Tenon bearing area of TC for Heel Style 2.

The bearing stress at an angle of the BC mortise is calculated using Hankinson's equation for beam/stringer material. The shoulder is loaded 33.7 degrees relative to parallel to grain:

$$F'_{c33.7} = \frac{1480\ psi * 625\ psi}{1480\ \text{psi} * \sin(33.7)^2 + 625\ \text{psi} * \cos\ (33.7)^2} = 1041\ psi$$

Therefore, the allowable compression in the TC due to tenon bearing is:

$$C_{TC} = 9.625\ in^2 * 1041\ psi = 10{,}019\ lbs$$

The block shear capacity of the BC is calculated using the block shear area (three quadrilateral shear planes). The block shear area was determined from the 2D model:

$$A_{v,total} = 2 * 24.8\ in^2 + 15\ in^2 = 64.5\ in^2$$

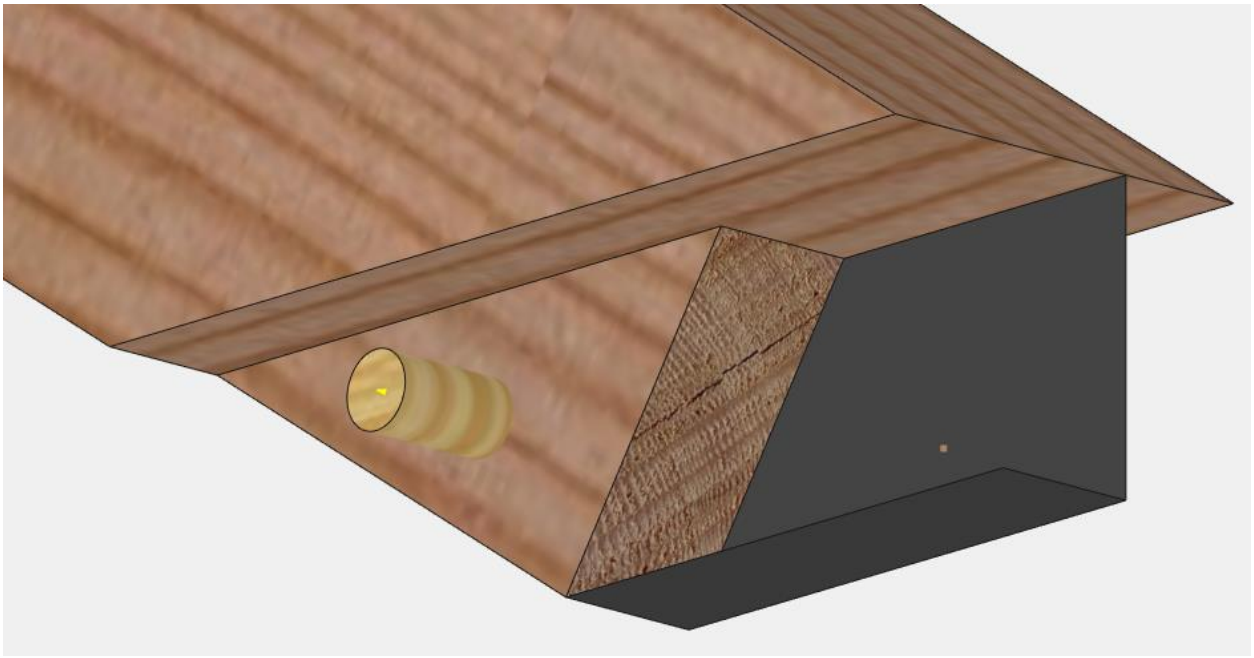

Figure C-8: Two of three shear planes in BC for Heel Style 2.

Therefore, the allowable compression in the TC due block shear in the BC is:

$$H = \frac{272\ psi * 64.5\ in^2}{2} = 8{,}772\ lbs$$

The allowable compression due to block shear in the BC was calculated using the truss geometry:

$$C_{TC} = 8{,}772\ lbs * \frac{14.42}{12} = 10{,}541\ lbs$$

The governing allowable compression in the TC is due to the bearing of the tenon material. The relative point load applied to the truss to cause the TC to reach the allowable compression was calculated using the truss geometry:

$$P = \frac{10{,}019}{0.901} = 11{,}120\ lbs$$

C.3.6 Heel Style 3

The allowable compression of the TC for Heel Style 3 is calculated using vector analysis. The vertical load vector is resolved by the bearing of the TC shoulder on the side grain of the BC. The allowable vertical load vector will be significantly larger than the allowable horizontal load vector by inspection. The horizontal load vector is resolved by the bearing of the TC tenon on the BC mortise (Figure C-9), and the block shear capacity of the remaining BC material behind the mortise pocket (Figure C-10).

The bearing capacity of the tenon/mortise connection is controlled by the TC tenon material, as the BC mortise material is loaded parallel to grain and has a higher allowable bearing stress.

The bearing area of the tenon is:

$$A_b = 4" * 2" = 8\ in^2$$

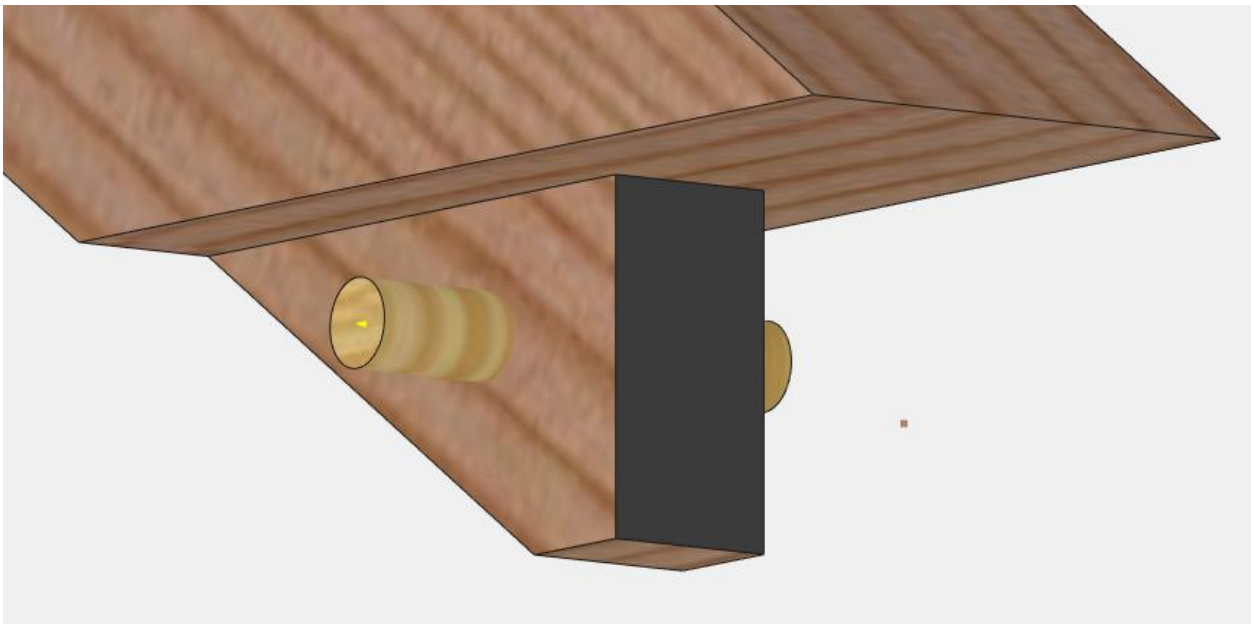

Figure C-9: Tenon bearing area of TC for Heel Style 3.

The bearing stress at an angle of the TC tenon is calculated using Hankinson's equation for post/timber tenon material. The tenon is loaded 33.7 degrees relative to parallel to grain:

$$F'_{c33.7} = \frac{1600\ psi * 625\ psi}{1600\ \text{psi} * \sin(33.7)^2 + 625\ \text{psi} * \cos\ (33.7)^2} = 1{,}081\ psi$$

Therefore, the allowable horizontal load vector due to tenon bearing is:

$$H = 8\ in^2 * 1{,}081\ psi = 8{,}648\ lbs$$

The block shear capacity of the BC is calculated using the block shear area (three rectangular shear planes). The total block shear area was determined from the 2D model:

$$A_{v,total} = 2 * 24\ in^2 + 12\ in^2 = 60\ in^2$$

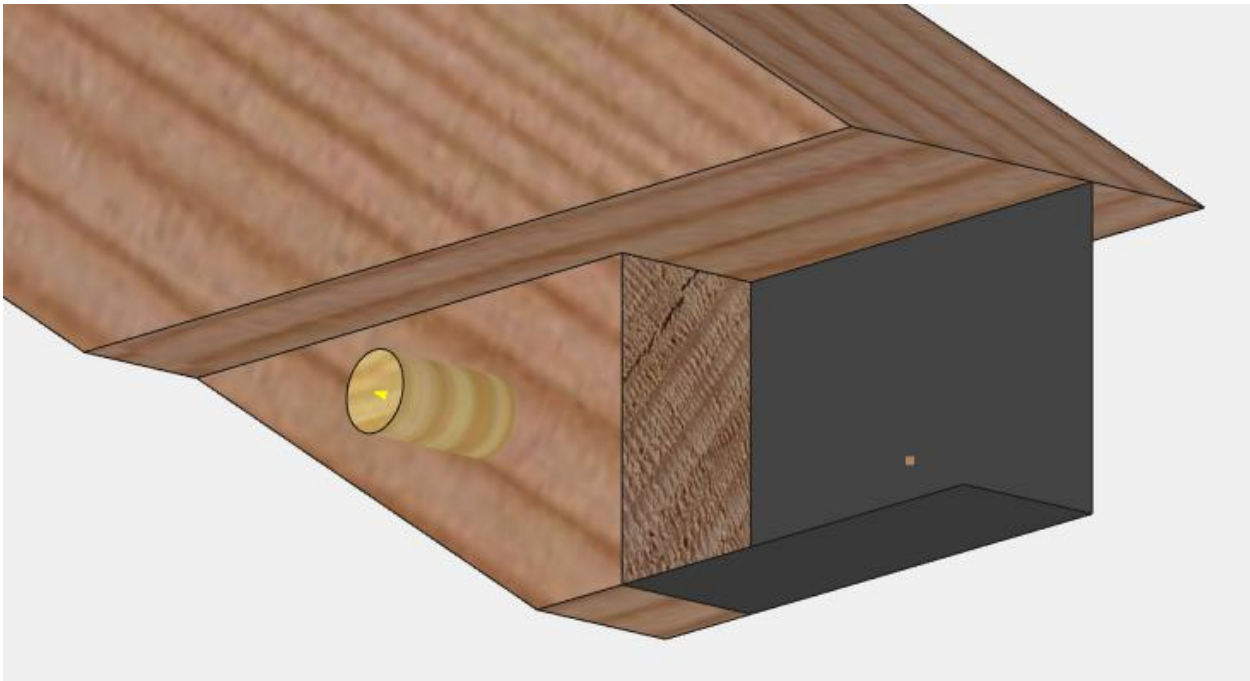

Figure C-10: Two of three shear planes in BC for Heel Style 3.

Therefore, the allowable horizontal load due to the block shear capacity for a single TC is:

$$H = \frac{272\ psi * 60\ in^2}{2} = 8{,}160\ lbs$$

The governing horizontal load vector is due to the block shear capacity of the BC, 8160 lbs. The allowable compression in the TC was calculated using the truss geometry:

$$C_{TC} = 8160\ lbs * \frac{14.42}{12} = 9{,}806\ lbs$$

The relative point load applied to the truss to cause the TC to reach the allowable compression was calculated using the truss geometry:

$$P = \frac{9{,}806\ lbs}{0.901} = 10{,}883\ lbs$$

C.4 Compiled results

Table C-4: Compiled allowable loads for each joint type.

		Limiting Failure	Allowable TC Compression (lbs)	Allowable Point Load (lbs)
Truss Peak Style	A	Tenon Bearing	11090	12310
	B	Peg Yielding	3020	3020
	C	Shoulder Bearing	11230	12470
Truss Heel Style	1	Block Shear in BC	9450	10480
	2	Tenon Bearing	10020	11120
	3	Block Shear in BC	9810	10880